The effects of a Kenyan antidiabetic plant on insulin homeostasis

by

Khairunisa Yahya Suleiman

Submitted in partial fulfilment of the requirements for the degree of

MAGISTER SCIENTIAE

in the Faculty of Science at Nelson Mandela Metropolitan University

January 2009

Supervisor: Dr. S. Roux

Co-Supervisor: Dr. T. Koekemoer

TABLE OF CONTENTS

ABSTRACT

The metabolic disorder diabetes; is a global epidemic affecting people in developed countries and increasingly in developing countries. In two decades time, 350 million people will be diabetic at the current rate of prevalence. In a preliminary study, insulin resistant rats were treated with *Prunus Africana (*plant A) for 28 days. Plasma samples obtained from *P. africana* treated rats had increased insulin levels compared to normal and untreated insulin resistant rats (Karachi, 2009). The treatment of insulin resistant rats with *P. africana* also showed increased glucose uptake in rat adipose tissue (Karachi, 2009), suggesting that *P. africana* had anti-diabetic properties.

The aim of the study was to investigate the mechanism of the anti-diabetic properties of *P africana* extract. Increased insulin secretion was confirmed by the increased C-peptide concentration in plasma samples of rats treated with *P. africana*. In order to explain the high insulin levels, several hypothesis' were investigated: (1) *P. africana* may increase insulin secretion in β cells, hence the effect of *P. africana* on insulin secretion by INS-1 cells was investigated; (2) *P. africana* may increase insulin secretion by prolonging the half-life of glucagon like peptide-1 (GLP-1) by decreasing dipeptidyl peptidase IV (DPP IV) activity; the effect of *P. africana* on DPP IV activity was determined spectrophotometrically, (3) *P. africana* may increase the half-life of insulin in the plasma by decreasing the activity of insulin degrading enzyme (IDE); the effect of *P. africana* on IDE in rat muscle and spleen samples was investigated. To explain the increased glucose uptake in adipose tissue observed in the previous study two parameters were investigated: (1) increased GLUT4 expression in *P. africana* treated rats; the effect of *P. africana* treatment on the expression of glucose transporter 4 (GLUT4) was determined using real-time polymerase chain reaction (RT-PCR), (2) *P. africana* may increase glucose utilization; the effect of *P. africana* on glucose utilization was determined in 3T3-L1 cells.

The plant extract did not significantly increase insulin secretion by INS-1 cells in the absence of glucose. *P. africana* decreased DPP IV activity in rat plasma when compared to the untreated insulin resistant rats and this could be a mechanism by which insulin secretion is increased during plant treatment. *P. africana* decreased IDE activity (however not significantly) when compared to the untreated insulin resistant

rats. *P. africana* appeared to have no effect on GLUT4 expression. The plant appeared to increase glucose utilization in 3T3-L1 cells in the absence of insulin suggesting that *P. africana* may have insulin like activity.

In summary, this study indicates that *P. africana* is indirectly involved in inhibiting DDPIV. This in turn can increase the half life of GLP-1, which in turn can enhance the secretion of insulin. *P. africana* increases glucose utilization although there was no evidence that the GLUT 4 transporter has a higher expression in the plant treated rats. Further studies should be conducted to investigate the expression of GLUT1 under the same conditions.

Keywords: *Prunus africana, Insulin secretion, INS-1 cells, GLUT4 expression, Glucose utilization, 3T3-L1 cells, DPP IV activity, IDE activity*

DECLARATION

In accordance with Rule G4.6.3, I hereby declare that the above-mentioned treatise/ dissertation/ thesis is my own work and that it has not previously been submitted for assessment to another University or for another qualification.

SIGNATURE: _____

DATE: _____

ACKNOWLEDGMENTS

All praises to God the most kind, the most merciful, for blessing me immensely time and again.

To my parents: Naima and Yahya for the encouragement, support and motivation. My brother Muhsin, thanks for the support and laughs.

My supervisors Dr. S. Roux and Dr. T. Koekemoer thank you. Dr. Roux thanks for relentlessly believing in me.

Dr. M. Mathiu and Kenya Medical Research Institute (KEMRI) for obtaining and providing the plant material. I extend my gratitude to the 'diabetes group', Department of Biochemistry & Microbiology, NMMU for setting up the insulin rat model and obtaining the tissue samples.

Dr. G. Dealtry, thanks for your much needed help in RT-PCR work and general concern. Dr. M. van de Venter thanks for the advice on cell work and RIA work. Gayle thanks for all. Brodie and Janine thanks. Jackie thanks for the help and advice. Shoni thanks for the help in protein/enzyme work as well as life lessons.

Mrs. R. Levendal and Prof. C. Frost thank you for generously donating INS-1 cells. Megan, Frank, Mary-Lou and Candace thank you for your kindness.

Mr. Lawyer Mabulu, thanks for all your help with regards to getting kits and reagents and so much more.

Last but not least, thanks Richard and Grace for the laughs, support and ideas.

LIST OF ABBREVIATIONS

cAMP	Adenosine 3',5'-cyclic monophosphate
CanX	Calnexin
CCH	Rats on a high fat diet that were insulin resistant, fed for 16 weeks
CCL	Normal rats on a chow diet fed for 16 weeks
ChREBP	Carbohydrate responsive element binding protein
Clb	B type cyclins
c-Myc	Myelocytomatosis cellular oncogene
CoA	Co enzyme A
COH	Rats on a high fat diet that were insulin resistant, fed for 12 weeks
COL	Normal rats on a chow diet fed for 12 weeks
CPT-1	Carnitine palmitoyl transferase-1
DAG	Diacylglycerol
DEX	Dexamethasone
DM2	Diabetes mellitus II
DNA	De-oxyribonucleic acid
DPAT1	Di-n-propylamino tetraline
ETC	Electron transport chain
FA	Fatty acid
FAS	Fatty acid synthase
FBS	Foetal bovine serum
G6Pase	Glucose-6-phosphatase
GDP	Guanidine diphosphate
GEFII	Guanidine nucleotide exchange factor II
GIP	Gastric inhibitory polypeptide
GK	Glucokinase
GKRP	Glucokinase regulatory protein
Glc	Glucose
GLUT2	Glucose transporter 2
GLUT4	Glucose transporter 4
GPAT	Glycerol-3-phosphate acyltransferase
GTP	Guanidine triphosphate

HFD	High fat diet
HGP	Hepatic glucose production
HSL	Hormone sensitive lipase
IBMX	Isobutylmethylxanthine
IDDM	Insulin dependent diabetes mellitus
IDE	Insulin degrading enzyme
IDF	International diabetes federation
IR	Insulin receptor
IRE	Inositol requiring kinase 1
IRS-1	Insulin substrate receptor 1
KRB	Krebs ringer buffer
LC-CoA	Long-chain acyl CoAs
LDL	Low density lipoprotein
LH	Luteinizing hormone
MAPK	Mitogen activated protein kinase
min	Minute
mRNA	Messenger ribonucleic acid
MTT	3-(4,5-Dimethylthiazol-2-yl)-2,5-diphenyltetrazolium bromide
NIDDM	Non-insulin dependent diabetes mellitus
ORO	Oil-red-O
PCR	Polymerase chain reaction
PEPCK	Phosphoenolpyruvate carboxykinase
PI-3K	Phosphoinositide-3-kinase
PI-P3	Phosphatidylinositol 3,4,5-phosphate
PKB:PKC	Protein kinase B, protein kinase C
PPAR	Peroxisomes proliferator activated receptor
qPCR	Quantitative polymerase chain reaction
ROS	Reaction oxygen species
RRP	Readily realisable pool
RXR	Retinoid X receptor
SDS	Sodium-dodecyl-sulphate
SHC	Src homologue and collagen homologue
SNARES	Snap receptors

SPT1	Serine palmitoyltransferase‑1
SREBP	Sterol regulatory element binding protein
SU	Sulphonylureas
TAG	Triacylglycerols
TBP	TATA-box binding protein
TCA	Tri-carboxylic acid cycle
TF	Transcription factor
TG	Triglyceride
t-SNARE	Syntaxin and synaptosomal associated protein 25
t-tubule	Transverse tubules
TZD	Thiazolidinedione
UN	United nations
USD	United States dollar
v-SNARE	Vesicle associated protein 2/syanaptobrevin-2
μUnits	Microunits

TABLE OF FIGURES

LIST OF TABLES

CHAPTER ONE: INTRODUCTION TO THE PRESENT STUDY

1.1 INTRODUCTION

Diabetes claims a life every 10 seconds and in two decades time, 350 million people will be diabetic, if no action is taken. The world spent an estimated 215 – 375 billion USD in 2007 to care for diabetes and the many complications that arise from the disease (IDF, 2008). Having being termed the silent epidemic, diabetes continues to ignite and sustain motivation in finding a cure.

More than 51 % of Kenyans are poor, while 10.7% South Africans live under one USD a day (www.millenniumindicators.un.org). Majority of the population in both countries are therefore depending on their governments for health services, which is a heavy burden due to the high cost of medication. Kenya spends 21 420 USD per annum, while South Africa spends an alarming 312 698 USD per annum on diabetes care (IDF, 2003). Not only is diabetes a heavy burden on the health budget, but diabetics depending on government support are often not treated optimally. Due to traditional use of medicinal plants, diabetics often know that they can improve their medication by co-treating themselves with these medicinal plants. However, the efficacy of the medicinal plants, interaction with other medication, dosage requirements and possible toxicity needs extensive further research. There is also a possibility that medicinal plants used for diabetes may reveal another way of treating the disease that may even be more efficient than current treatments.

In this study the efficacy of the medicinal plant *Prunus africana* used in Kenya for diabetes, will be investigated to elucidate its mode of action. This study will therefore contribute to the research in determining whether this plant extract can be used more effectively in treating diabetes. In addition this study will further strengthen scientific collaboration between Kenya and South Africa; the study was funded by the NRF as part of a scientific bilateral development project between South Africa and Kenya.

1.2 Diabetes

The two types of diabetes are type 1 (insulin dependent diabetes-IDDM) and type 2 (non-insulin dependent diabetes-NIDDM). Type-1 diabetes results from the autoimmune destruction of pancreatic β-cells; leading to insulin insufficiency. Type-2 diabetes is more prevalent and is caused by the inability of β-cells to secrete sufficient amounts of insulin to overcome insulin resistance established by genetic and environmental factors (Henquin, 2000).

Type-2 diabetes mellitus is a heterogeneous metabolic disorder characterized by the impairment of insulin secretion from pancreatic beta cells and insulin resistance in peripheral tissues such as liver, skeletal muscle, and adipose tissue (Zhou *et al*., 2007). Insulin resistance has been described as the combined inability of muscle and adipose tissue to facilitate glucose uptake and of the liver to suppress glucose output in response to increasing amounts of insulin. Insulin resistance is the hallmark characteristic of type-2 diabetes mellitus (DM2). The early stages of DM2 are characterized by increased blood glucose concentrations, despite the presence of normal to high insulin concentrations in the bloodstream. The later stages of DM2 are characterized by low insulin concentrations and the need for exogenous insulin due to the eventual exhaustion of insulin secretory ability by the pancreatic β cells. Blood glucose concentrations remain high over many years, clinical complications such as retinopathy, nephropathy, neuropathy and cardiovascular disease develop and thereby increase the patient's morbidity and mortality rate (Khan and Pessin, 2002).

1.3 The mystery plant *Prunus africana.*

Prunus africana is commonly known as pygeum, bitter almond, red stinkwood, bitteramandel, rooistinkhout, and nuwehout' (Simon *et al*. 2007). This evergreen tree can reach 24 m with a trunk diameter greater than 1 m. It has a dark and rugged bark, with brown and corky branches and knobby twigs. The tree has shiny simple dark green leaves, arranged in an alternate manner, and the foliage has 'an aroma of almonds when crushed' (Simon *et al*. 2007) with usually pink or red leaf stalks and white flowers arranged in clusters as indicated in figure 1.1 (Simon *et al*., 2007). The plant is restricted to afromontane forest islands in 14 mainland African countries and

4 outlying islands. It occurs mainly in the East Africa region extending through to the West, Central and Southern parts of Africa (Mukiama, 2005). *P Africana* "responds well to cultivation" (Palgrave, 1981).

Figure 1.1: A flowering *Prunus africana* plant (www.biodiversitvexplorer.org)

The use of *Prunus africana* in the pharmaceutical industry began in the 1970's. The bark extract was marketed as an effective treatment of benign prostatic hyperplasia. The plant is used traditionally in many African regions as medicine for various ailments. Some of the uses of the plant include the use of bark infusion to relieve chest pains, fever, stomach pains and malaria. Interestingly the bark was also used for urinary problems by Southern African natives. The leaves have found use in dressing wounds and infusions are drunk to enhance appetite. The plant is also used by the Maasai people for good digestion, by drinking the bark infusion (Mukiama, 2005).

P. africana extract has active constituents which include phytosterols such as b-sitosterol and b sitosterol 3-O-glucoside; these have anti-inflammatory effects by preventing the production of pro-inflammatory prostaglandins in the prostrate and aliphatic alcohols and their ferulic acid esters (such as n-tetracosanol and n-docosanol) which decrease prolactin levels and inhibit the accumulation of cholesterol in the prostrate. Bark decoctions are traditionally used in Zulu medicine, while lipid and phytosterol extracts are most commonly used in Europe (Simon *et al*., 2007). The plant also contains pentacyclic triterpenouds e.g. ursolic acid and oleonolic acid, which have anti-oedema properties (Mukiama, 2005).

Pharmacological studies have shown that *P. africana* has anti-oedema activity, increase in bladder elasticity, and stimulation of prostatic secretion. This medicinal extract is nontoxic and lowers the plasma concentrations of luteinizing hormone (LH) and testosterone; no androgenic and estrogenic action detected. Clinical trials have shown that the extract provides significant impact on nocturnal pollakuria and other symptoms of benign prostrate hypertrophy (Mukiama, 2005).

1.4 The HOMA and QUICKI indices.

There are many diseases in which insulin resistance is a key component of, such as DM2, hypertension, obesity, dyslipidemia and cardiovascular disorders. There are several methods of assessing insulin sensitivity in humans, the most common one is the euglycemic hyperinsulinemic clamp (IS) as it measures insulin action on glucose utilization under steady-state conditions. This method is laborious and is only applicable to a small number of subjects (Rabasa-Lhoret *et al*., 2003). The homeostatic model (HOMA) for the assessment of insulin was developed in 1985. It is based on feedback dependence between fasting serum concentrations of insulin and glucose in blood and is well correlated with data obtained using the isoglycemic glucose clamp (Hrebicek *et al*., 2002).

The formula for the HOMA index is;
[Insulin (in mUnits/L) **X** glucose (in mmol/L)]/22.5 (Katz *et al*., 2000).

Therefore an increase in HOMA index values indicates insulin resistance.

The quantitative insulin-sensitivity check index (QUICKI) was reported in 2000, it is a relatively new quantitative method for the assessment of insulin that correlates better than HOMA, with minimal model and clamp methods. The QUICKI has been defined as being a simple and effective quantitative method for the assessment of insulin sensitivity (Hrebicek *et al*., 2002). The QUICKI was developed so as to assess the early stages of insulin resistance. Hrebicek *et al*. (2002) stated that the QUICKI has a higher discrimination power than the HOMA index.

The formula for the QUICKI is;
1/[log fasting glucose (in mg/dL) + log fasting insulin (in μUnits/mL)] (Perseghin *et al*., 2001).

Therefore a decrease in QUICKI values indicates insulin resistance.

The QUICKI values cannot be applied universally, due to the variability in insulin determinations between different laboratories. Perhaps the biggest discrepancy of the QUICKI is that a normal range needs to be established for each laboratory with an appropriate control group because of significant inter-laboratory variations in insulin determination and/or possible differences in various populations (Rhabasa-Lhoret *et al*., 2003).

The QUICKI is a simple and effective quantitative method for the assessment of insulin sensitivity, especially for epidemiological and clinical practice where prevention and therapy of the sequelae of insulin resistance is of great importance. There is still a need to diagnose insulin resistance during the initial stages of disease in large numbers of patients, the availability of simpler, more sensitive and discriminating are desirable. There is a 'revised-QUICKI' that incorporates fasting plasma free fatty acid (FFA) and a QUICKI-glycerol that incorporates a formula including glycerol, which seem better related to the IS clamp and offer correlations similar to or higher than values obtained with log HOMA. These two 'new' QUICKI formulas provide information about insulin action on lipolysis, 'which is related to insulin action on glucose metabolism' (Rabasa-Lhoret *et al*., 2003).

1.5 Prologue and motivation of study

It is estimated that approximately 4 million deaths each year are directly related to diabetes. The disease is now the world's fourth leading cause of mortality by illness and the global epidemic shows no signs of declining (Diabetes Voice, 2007). In addition having searched extensive literature, minimal scientific experimentation has been conducted regarding the efficacy of *P. africana* as an antidiabetic plant/ treatment.

There is also an increasing demand by patients to use natural products with antidiabetic activity due to the undesirable side effects accompanied with the use of insulin and other hypoglycaemic drugs (Kaleem *et al*., 2008) as well as the exorbitant cost of some of these drugs. Further progression of DM2 can lead to a recurrence of hyperglycemia, at this point combination therapies may be initiated, involving sulphonylureas. Sulphonylureas lower blood glucose by stimulating insulin secretion from the pancreatic beta cells (Green *et al*., 2006), their molecular role is explained at a later stage in this study. The available monotherapies and combinatorial treatments are subject to secondary failure which may eventually diminish in efficacy over a period of years. Hence the need to constantly attempt to develop safer and more efficacious antidiabetic drugs (Green *et al*., 2006).

The high fat (HF) fed Wistar rats used in this study represent an insulin resistance model..As this is a follow-up study of J Karachi, frozen tissue samples were utilized in this study from rats sacrificed by J Karachi in her study in 2007 (Karachi, 2009). The rats were confirmed to be insulin resistant based on fasting glucose and insulin levels. It has been indicated that HF diets induce liver insulin resistance and that the severity of insulin resistance is increasingly dependent on the duration of the HF feeding (Clottes and Burchell, 1998). HF diets induce the pancreas to increase insulin secretion as a means to overcome insulin resistance, eventually over long term feeding of HF diets, the β cells of the pancreas become exhausted and cannot produce sufficient insulin to overcome insulin resistance; at this point the subject becomes diabetic (Terauchi *et al*., 2007). Since HF diets induce insulin resistance, a decrease in glucose uptake and hence metabolism occurs in adipose tissue.

This research is a follow up study from Karachi (2009). Table 1.1 shows the plasma insulin concentrations obtained by Karachi (2009) in a previous study. As discussed in sections 1.4, when high insulin levels are obtained the reliability of the QUICK index becomes doubtful. Table 1.1 also indicates that CCL, CCH and plant A (*P. africana* treated) rats had similar fasting glucose levels.

Table 1.1: [Insulin] in rat plasma of CCL, CCH and Plant A

Group	Insulin (ng/mL)	Glucose (mmol)
CCL	0.67	6.33
CCH	1.39	6.22
Plant A	3.92	6.21

Table 1.1 was obtained from Karachi (2009) and McKenzie (2009). Where CCL (n=5) indicate the rats on a normal diet, these were lean rats. CCH (n=5) indicate rats treated rats on a high fat diet that were insulin resistant. Plant A (n=5) indicate insulin resistant rats treated with plant A. n represents the number of rats per group. The CCL and CCH, plant A (*P. africana* treated) rats were treated with a normal chow and high fat diet for 12 weeks respectively. Thereafter plant A treatment was administered to plant A rats for an additional 4 weeks. At the same CCL and CCH rats were gavaged with water when plant A was fed to the plant A treated rats.

Table 1.2 summarize results obtained by Karachi (2009) and indicates that HF fed rats treated with an plant A extract increased glucose uptake in adipose tissue and elevated fasting plasma insulin levels. The increased glucose uptake shows a decrease in insulin resistance, however the QUICK index indicates that the rats were still insulin resistant due to the elevated insulin levels obtained during treatment. The QUICK index did not indicate this attenuation of insulin resistance by increased glucose uptake and this is a disadvantage of using the QUICKI.

Table 1.2: Glucose uptake in tissues from treated and untreated rat groups.

Group	CCL	CCH	Plant A
Liver	1305	955	1439
Muscle	1755	966	1995
Fat	2801	1089	8277

Table 1.2 was obtained from Karachi (2009). Glucose uptake in various tissues from treated and untreated rats was measured by the ^{3}H deoxy-glucose count. CCL (n=6) indicates lean rats on a normal diet. CCH (n=7) indicates rats on a high fats diet that were insulin resistant. Plant A indicates insulin resistant rats (n=5) treated with plant A. The CCL, CCH, and plant A treated rats were fed with a normal chow and high fat diet respectively for 12 weeks. Thereafter plant A treatment was administered to insulin resistant rats for an additional 4 weeks. During that 4 week period, CCL and CCH rats were gavaged with water when plant A was fed to the plant A treated rats.

1.6 Experimental approach of this study

The principle objectives of this research were to determine; (1) the best marker for insulin resistance (2) how plant A increased insulin levels in rat plasma (3) how plant A increased glucose uptake in adipose tissue.

When excessively high insulin levels are obtained the QUICKI appears unreliable in discerning whether or not the subject is insulin resistant. As according to the QUICKI equation, high insulin levels result in a low QUICKI value indicating insulin resistance, irrespective of an improvement in insulin resistance. For example in the case of the previous study (Karachi, 2009) where high insulin values were obtained in high fat rats treated with plant A, it is difficult to know whether the insulin resistant state has improved or not with the QUICKI; as the prevailing insulin levels is speculated to be due to an increment in insulin half life as opposed to insulin secretion, it is this reasoning that the QUICKI fails to accommodate. The initial stages of insulin resistance is characterised by an increase in insulin secretion so as to overcome a lack of response to normal insulin concentrations by tissues responsible for glucose maintenance such as liver, muscle, heart. Hence it is vital to use other reliable methods of determining insulin resistance. In this study, the researcher investigated whether liver glucose-6-phosphatase or glucokinase can be used as a marker for insulin resistance by measuring liver glucokinase and G6Pase activities.

To confirm whether high insulin levels were obtained by Karachi (2009) as indicated in table 1.1 in plasma from plant treated rats, the researcher determined C-peptide concentrations in plasma from plant treated rats. This is because C peptide is produced in equimolar concentrations with insulin.

I hypothesise that the high insulin levels obtained by Karachi (2009) may be attributed to:

- An increase in insulin secretion;
    - Therefore, determination of the effect of plant A on INS-1 secretion was conducted.
    - Diminished DPP IV activity: owing to an increase in GLP-1 half-life. GLP-1 stimulates insulin secretion. Hence more insulin secretion. DPP IV activity was measured in treated rat plasma as well as the direct *in*

vitro effect of plant A on human DPP IV activity, isolated from CaCO-2 cells.

- A decrease in insulin degrading enzyme (IDE) activity. The researcher investigated the effect of plant A on IDE activity in rat muscle and spleen tissues.

Table 1.2 shows that plant A increases glucose uptake in adipose tissue conducted by Karachi (2009). To confirm the results by Karachi (2009), the present study determined the effect of the plant on differentiated 3T3-L1 adipocytes. The increase in glucose uptake in plant treated adipose tissue may be attributed to an increase in GLUT4 expression and translocation and hence an improvement in insulin resistance. Hence we measured GLUT4 expression.

The high incidence of DM2 and the gravity of its complications make it crucial to understand the metabolic basis of insulin-stimulated glucose transport and insulin resistance. There are a number of hypoglycaemic drugs available for DM2, the different drugs target varied avenues within the body. However, there are certain side effects of the drugs available, this necessitates the search for a drug that can regulate blood glucose levels or induce insulin production by pancreatic β-cells, with minimal or no side effects.

CHAPTER TWO: LITERATURE REVIEW

Although most organs of the body are affected by diabetes, the primary tissues involved in diabetes are the pancreas, adipose, muscle and liver.

2.1 Pancreas

The major role of the pancreas in the body is to secrete insulin and glucagon in response to changes in blood glucose concentration. The islets of Langerhans are clusters of specialized pancreatic cells (α, β and δ cells). Glucose is the physiological regulator of glucokinase in the islets of Langerhans and the activity of glucokinase plays a crucial role in glucose induced insulin secretion (Liang *et al*., 1990). The pancreatic islets of Langerhans regulate blood glucose levels through the regulation of insulin secretion (Matschinsky, 1996). The function of pancreatic glucose sensors is to directly sense and regulate plasma glucose levels. The pancreas contains two types of glucose sensing cells, the glucagon secreting α-cells and the insulin secreting β-cells (Matschinsky and Collins, 1997). When insulin enters the bloodstream from the intestine after a rich carbohydrate meal, the resulting increase in blood glucose induces increased secretion of insulin and decreased secretion of glucagon.

The role of α- cells is to produce the hormone glucagon so as to counter act low blood glucose. When blood glucose levels slightly 'drop' due to the ongoing oxidation of glucose by the brain and other tissues, secretion of glucagon is triggered. Glucagon causes an increase in blood glucose concentration in various ways, including the net breakdown of liver glycogen, inhibiting glycolysis and stimulating gluconeogenesis (Nelson and Cox, 2005).

The role of β-cells is to produce and secrete insulin, when glucose concentrations rise. Insulin is a hormone that is involved in maintaining blood glucose, see section 3.1 for further information. The β-cells also secrete C-peptide, the role of which is explained in section 3.1.2. In addition the β-cells secrete amylin. Amylin is responsible in suppressing food intake for a shorter period, whereas insulin is responsible in suppressing food intake for a longer period (Moore and Cooper, 1991).

The δ-cells synthesize somatostatin, which is a hormone that is involved in the regulation of the endocrine system.

2.1.1 β cells

The β-cells are located in the islet of Langerhans within the pancreas. Majority of the cells in the islets are β-cells. The β-cell possesses a unique hexokinase (HK IV or glucokinase). Islet glucokinase (GK) activity appears to be governed by serum glucose levels, whereas liver glucokinase activity seems to be determined by serum insulin concentrations. The evidence to this statement is attributed to data showing an increase in pancreatic GK activity in response to increasing glucose concentration, and an increase in hepatic GK activity in response to increasing insulin concentration. An investigation was conducted where induced chronic hyperinsulinemia caused severe hypoglycaemia, the findings were that hepatic GK increased approximately up to fourfold, while islet GK decreased by about 25% of controls (Matschinsky, 2006). In the β cells, GK controls insulin secretion, this role is not played by the GK in the liver. Almost two decades ago glucokinase was proposed as the glucose sensor element of β-cells. Liang *et al.*(1990) proved that indeed glucokinase is the glucose sensor element of β-cells by using cultured pancreatic islets. The function of GK is elaborated in section 3.1.2.

In addition, the β-cell also possesses a low-affinity glucose transporter; GLUT2 (Routh *et al.*, 2007). The homeodomain protein PDX-1, referred to as IPFl/STF-l/IDX-1, is a transcriptional factor that plays a crucial role in the control of several genes expressed in the pancreatic islet. PDX-1 will further be discussed in sections 4.2.2.1. The pancreatic β-cell maintains a stable balance between insulin secretion and insulin production under normal physiological conditions. When glucose (or nutrient secretagogues) stimulates insulin release, a quick glucose induced increase in proinsulin biosynthesis at the transcriptional level occurs. This response replenishes intracellular insulin stores (Bollheimer *et al*., 1998).

The production of sufficient insulin is dependent on β cell mass and function (Maedler and Donath, 2004). Type II diabetes is characterized by a defect in insulin secretion as well as a decrease in relative β-cell volume. β-cell defects are often

poorly characterized and controversy still persists concerning the importance of abnormalities in insulin secretion in the pathogenesis of type 2 diabetes (Kjems *et al*., 2000).

2.2 Adipose and muscle tissue

One of the essential components used in maintaining glucose homeostasis is a unique glucose transport system in muscle and adipose tissue that in a matter of minutes can coordinate a 10- to 40- fold increase in glucose uptake. A disruption in this balance leads to diseases such as morbid obesity and diabetes mellitus and to cardiovascular disorders (Rea and James, 1997). Obesity and lipoatrophy induce insulin resistance and predisposition to DM2, demonstrating that adipose tissue is crucial in regulating metabolism beyond its ability to take up glucose (Saltiel and Kahn, 2001). The role of the muscle with respect to (w.r.t.) glucose is to convert surplus glucose to its storage form; glycogen and utilizing glucose for muscle contractions. On the other hand the function of adipose tissue w.r.t. glucose is converting surplus glucose to triacylglycerols.

2.2.1 Glucose transporters

Glucose transport is mediated via solute carriers known as the GLUT family of facilitative glucose transporters, each with different tissue distributions, kinetic properties and sugar specificity. Glucose transport is affected by changes in the intrinsic activity, intracellular trafficking and stability of the GLUT transporters (Khan and Pessin, 2002). The transporters present in the adipose and muscle tissues are GLUT1 and GLUT4. Glucose transporters play a central role in achieving normoglycaemia especially in the postprandial state, where glucose metabolism and storage (which occur in the adipose and muscle tissues) take place in response to elevated glucose levels by eating carbohydrates.

GLUT4 protein is mainly restricted to insulin sensitive tissues, such as cardiac, adipose and muscle tissues and is responsible for insulin-stimulated glucose uptake (Khan and Pessin, 2002). Insulin stimulates the translocation of GLUT4 from an intracellular storage compartment to the cell surface. GLUT4 has the unique property of remaining localized in intracellular vesicles in the absence of insulin. Insulin can

then recruit this transporter to the surface under metabolically appropriate conditions. The relatively low K_m value (2-5mM) of GLUT4 ensures that it operates close to its V_{max} over the normal range of blood glucose concentrations, and this ensures the rapid removal of blood glucose into the body's energy stores of glycogen and triaglycerols. In the absence of insulin (referred to as the basal state), glucose transport is rate limiting for metabolism, but insulin stimulates an increase in plasma membrane abundance of GLUT4 transporters so that insulin-stimulated transport does not limit metabolism (Gould and Holman, 1993).

The insulin stimulation of glucose uptake in adipose and muscle tissue occurs via a complex and incompletely defined signalling pathway proceeding via the insulin receptor tyrosine kinase. The main effect is to encourage movement of the GLUT4 protein from intracellular storage sites to the plasma membrane (Khan and Pessin, 2002). This transport system is used in the muscle to both sustain energy requirements during exercise and mediate glycogen storage in the postprandial state (Rea and James, 1990). The rate-limiting step at which insulin stimulates glucose uptake in muscle and adipose tissues is the translocation of GLUT4 transporters to the plasma membrane (Khan and Pessin, 2002).

In the pathogenesis of insulin resistance and DM2, adipose tissue plays a vital role. In adipocytes, the rate-limiting step in glucose utilization is glucose transport. The impairment of glucose uptake in diabetes is responsible for insulin resistance of glucose uptake. There are several factors that are attributed to this metabolic impairment, such as; 'defects in GLUT4 regulation'; alterations in GLUT4 expression and translocation, defects in the insulin signalling pathway as well as temporal and 'spatial pattern modifications of signalling molecules' (Zhou *et al*., 2007).

GLUT1 is ubiquitously found in tissues as opposed to GLUT4 which is only found in insulin sensitive tissues. GLUT1 is responsible for basal glucose uptake. GLUT1 expression is up-regulated by the activation of extracellular signal-regulated kinase (ERK), this leads to increased basal glucose uptake when acute insulin stimulation is not present (Kim *et al*., 2007). GLUT1 expression is not affected during insulin resistance (Brennan *et al*., 2004). In adipocytes, GLUT1 responds to insulin unlike in

the skeletal muscle tissue (Mueckler *et al*., 2001), where GLUT1 does not respond to insulin.

In the adipocyte, the budding of transport vesicles containing GLUT4 from intracellular compartments occurs, thereafter these vesicles fuse with the PM. The v-SNARE found in the transport vesicles facilitates this fusion, the interaction between the v-SNARE (VAMP2) and t-SNARE (syntaxin 4/SNAP23) occurs in the PM. There are approximately 3 or more different membranous compartments involved when GLUT4 transverses within the cell in response to insulin (Mueckler *et al*., 2001).

'GLUT4 translocation is compartmentalized in the muscle' (Lauritzen *et al*., 2008). The two PM domains in skeletal muscle fibres involved in glucose translocation are the transverse tubules (t-tubules) and the sarcolemma ('proper PM'), these two domains differ in protein composition. GLUT4 is found in the t-tubules and the sarcolemma. An elevated GLUT4 density is stimulated by insulin in both the t-tubules and the sarcolemma, however most of the transport stimulated by insulin occurs in the t-tubules, this explains the ability of glucose being able to permeate into 'deep muscle fibre' for use in biosynthetic reactions and production of ATP (Mueckler *et al*., 2001). During insulin resistance in the t-tubules, there is a decrease in phosphatidylinositol 3,4,5-phosphate (PI-P3) production and a decrease in GLUT4 translocation. In addition, in the t-tubules, PI-3K activation is impaired. In the sarcolemma, there is little or no change in PI-P3 production as well as GLUT4 translocation and in certain cases PI-P3 production GLUT4 translocation may be elevated. In the sarcolemma, PI-3K activity induced by insulin is increased (Lauritzen *et al*., 2008).

How is GLUT4 affected during diabetes? In the onset of insulin resistance and eventually diabetes, there is a decrease in GLUT 4 expression and translocation in the muscle, which leads to a decrease in glucose uptake, there are also defects in insulin receptor substrate -1 (IRS-1) and phosphoinositide-3-kinase (PI-3K). In the adipose tissue, there is a decrease in GLUT4 mRNA production, translocation and activation in the diabetic state (Panunti *et al*., 2004).

2.3 Liver

The liver is strategically positioned to influence glucose homeostasis through a balance between hepatic glucose uptake and utilization (HGU) and hepatic glucose production (HGP). Insulin and glucose act together to influence the fasted-to-fed transition in the liver by promoting expression of genes normally induced in the fed state, including glucokinase (GK), liver pyruvate kinase (L-PK), 6-phosphofructo-2-kinase/fructose-2,6-bisphosphatase (PFK2), acetyl-coenzyme A carboxylase, and fatty acid synthase (FAS). Conversely, genes that are activated during the fasted state, such as phosphoenolpyruvate carboxykinase (PEPCK), fructose-1,6-bisphosphatase, and carnitine palmitoyl transferase (CPT) I and II are down-regulated. This phenotypic switch requires genes to be stimulated or repressed by a coordinated process (Collier and Scott, 2004). A phenotypic switch, normally initiated by insulin or glucagon, controls the transition between the fasting and fed states, which includes transcriptional alterations that regulate metabolic enzyme abundance for multiple metabolic pathways in a coordinated manner (Collier and Scott, 2004).

The liver is therefore equipped to regulate the metabolic transitions between the fasting and fed states. The failure of the hepatocyte to undergo this metabolic reprogramming is characteristic of diabetes mellitus (Collier and Scott, 2004). Lyall *et al*. (1992) established that under diabetic conditions, the hydrolysis rate of G6P increased and hence the HGP increased (Tice and Barnett, 1962). This is attributed to the increased activity of G6Pase (Van Schaftingen and Gerin, 2002). The increase in G6Pase has also been associated with insulin resistance (Clore *et al*., 2000).

2.3.1 Liver metabolic overload

The livers of the high fat fed rats that will be tested may be overloaded. Overnutrition leads to insulin resistance and eventually DM2, hence causing changes in metabolism. These changes include lipid-derived metabolites which accumulate outside of the adipose depots (including skeletal muscle, heart and liver) in response to HF diets and the onset of obesity. It is thought that in lipid-induced insulin resistance, lipid species accumulate due to the impairment of FA oxidation, resulting in the redirection of

long-chain acyl CoAs (LC-CoAs) into ER-localized and cytosolic lipid species such as diacylglycerols (DAGs), ceramides and triacylglycerols (TAGs). This is thought to be regulated by glucose-induced increases in malonyl-CoA (Figure 2.1). Malonyl CoA serves both as an intermediate precursor *de novo* lipogenesis and as an allosteric inhibitor of CPT1. CPT1 is the rate limiting enzyme for LC-CoAs into mitochondria for β-oxidation (Muoio and Newgard, 2008). Insulin inhibits the hepatic expression of β-oxidative enzymes by antagonizing the effects of the transcription factor PPAR-γ coactivator-1 (PGC-1). This role of insulin prevails even when insulin resistance develops, although its role to suppress gluconeogenesis is attenuated. Concomitantly, hepatic steatosis develops during prolonged periods of overfeeding, leading to glucose intolerance. Ingestion of HF diets in rodents leads to the accumulation of TAGs, LC-CoAs, DAGs and ceramides. When mitochondrial levels of GPAT1 (first enzyme in TAG synthesis) or ACC2 are suppressed, FA oxidation increase, DAG levels decrease and reversal of hepatic insulin resistance occurs (Muoio and Newgard, 2008).

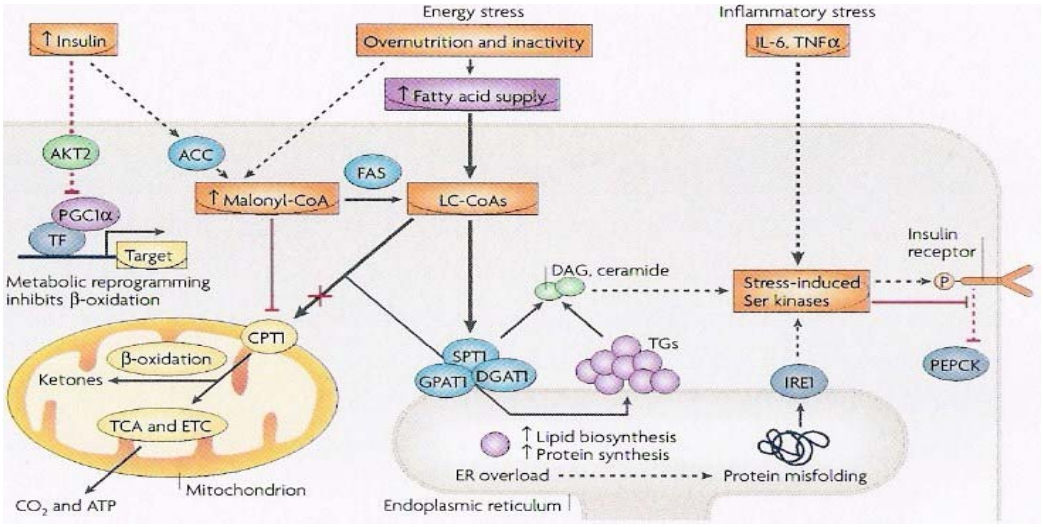

Figure 2.1: Metabolic overload in the liver. Malonyl CoA levels increase due to chronic overfeeding, which promotes fatty acid synthesis and inhibits CPT1 activity. LC-CoAs are thereafter diverted away from mitochondria oxidation (TCA cycle), towards biosynthetic enzymes (e.g. DPAT1, GPAT1 and SPT1) that produce TAGs and signalling intermediates such as DAG. Overnutrition also causes an anabolic burden on ER which results in protein misfolding and activation of IRE1. These effects activate stress induced Ser kinases which hinder insulin mediated suppression of gluconeogenesis, which allow lipid synthesis and prevent β-oxidation (Muoio and Newgard, 2008). DPAT: di-n-propylamino tetraline, ETC: electron transport chain, GPAT: glycerol-3-phosphate-O-acyltransferase, IRE1: inositol requiring kinase 1, FAS: fatty acid synthase, LC-CoA: long-chain acyl co-enzyme A, SPT1; serine palmitoyltransferase-1, TCA: tricarboxylic acid cycle.

2.4 Lipids and insulin resistance

Low density lipids (LDL) transport cholesterol and TAG from the liver to peripheral tissues as indicated in figure 2.1. Insulin resistance is associated with LDL particle size and density, as well as the oxidation state of the LDL. Normal (non-insulin resistant) subjects are observed to have large and less dense LDL particles. During insulin resistance the LDL diameter and density change to smaller, denser LDL particles. Lipoprotein lipase catalyzes the removal of a triglyceride from very low density lipids (VLDL) to form LDL making the LDL denser, hence containing more cholesterol. These smaller, denser particles are easily oxidized. Insulin resistance is associated with increased numbers of partially oxidized LDL particles (Carantoni *et al*., 1998).

Obesity leads to insulin resistance and contributes to the development of DM2. Insulin's ability to inhibit lipolysis and reduce the plasma FFA concentration is impaired in DM2. Resulting in an increase in plasma FFA concentrations, which fail to suppress normally after ingestion of glucose. Elevated plasma FFA inhibit insulin-stimulated glucose uptake at the level of glucose transport. Acute elevations in FFA concentrations induce an increase in muscle FA-CoA and DAG concentrations. They activate protein kinase C θ (PKCθ), which increases serine phosphorylation with subsequent inhibition of the IRS-1 tyrosine phosphorylation, the association of p85 subunit of PI-3K with IRS-1 and activation of PI-3K. The suppressed PI-3K activity decreases GLUT4 translocation and eventually decreases glucose transport (Panunti *et al*., 2004).

Short-term exposure to increases in FFA stimulates insulin secretion from the β cell. In the β cells, FA-CoA directly stimulates insulin exocytosis and augments secretion by increasing intracellular calcium. Its derivatives activate PKC, which stimulates exocytosis of insulin. Chronic exposure of the β cell to elevated free FA-CoA levels inhibits insulin secretion. This increases β oxidation and increases acetyl-CoA, resulting in an inhibition of pyruvate dehydrogenase and elevated citrate levels, inhibiting phosphofructokinase and subsequently glycolysis. The decrease in glucose metabolism results in decreased malonyl CoA (similar to liver metabolic overload)

which increases CPT-1 activity and decreases the ATP generation, which is vital for glucose-stimulated insulin secretion (Panunti *et al*., 2004).

Increased FFA is a key abnormality in peripheral and hepatic insulin resistance and hence a therapeutic target. Increased FFA may also contribute to direct vascular abnormalities and β cell dysfunction. The overall effects of increased plasma FFA are; (i) β cell dysfunction and apoptosis may occur (ii) increase in inflammatory cytokines (iii) inhibition of insulin secretion (iv) reduction in glucose transport (v) decrease in GLUT4 translocation (vi) inhibition of PI-3K activation (vii) inhibition of IRS-1 tyrosine phosphorylation (Panunti *et al*., 2004).

2.5 Muscle metabolic overload

Similar to the liver, intramuscular levels of lipid signalling molecules (e.g. LC-CoAs DAG and ceramides) positively correlate with TAG content and negatively correlate with insulin resistance. Transgenic overexpression of DGAT1 in skeletal muscle was shown to increase TAG content and prevent diet-induced insulin resistance, in association with 20-30% reductions in muscle DAG and ceramide levels (Muoio and Newgard, 2008). Mitochondrially derived by-products of lipid oxidation (rather than diversion of lipid metabolites into biosynthetic pathways) may have a pivotal role in the development of insulin resistance in skeletal muscle. Chronic exposure of muscle to increased lipids induces an increase as opposed to a decrease in expression of genes (e.g. PPAR α/δ) of the fatty acid β-oxidative pathway (Figure 2.2). Lipid-induced upregulation for the enzymatic machinery for β-oxidation in muscle is not co-ordinated with upregulation of downstream metabolic pathways such as the TCA cycle and electron transport chain. This could result in incomplete metabolism of FAs in the β-oxidation pathway and accumulation of lipid-derived metabolites in the mitochondria (Muoio and Newgard, 2008).

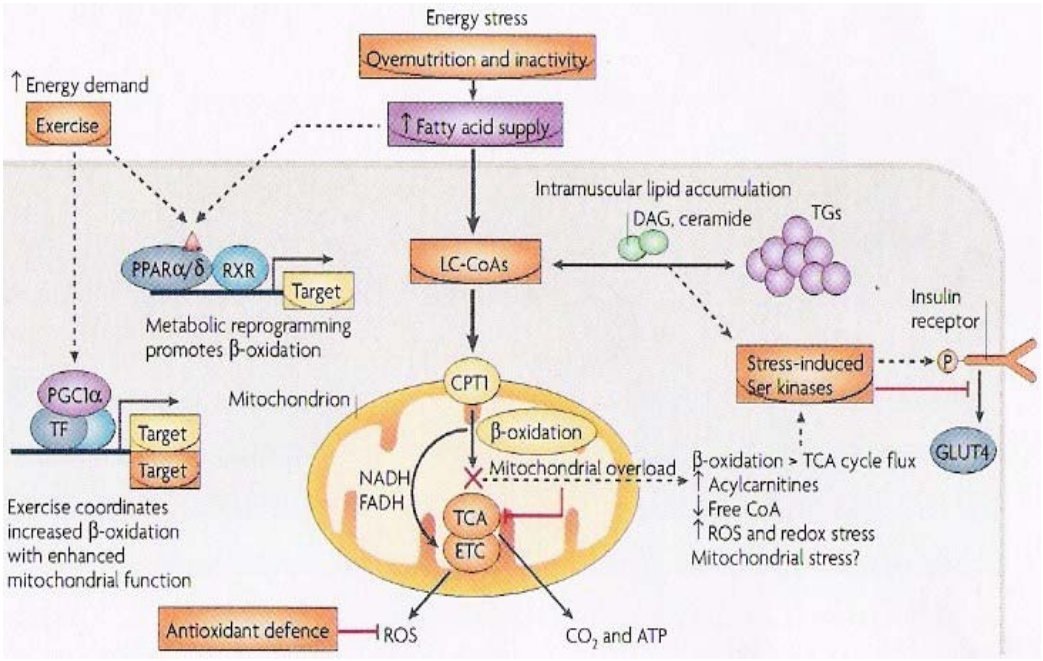

Figure 2.2: Metabolic overload in the skeletal muscle. During overnutrition, fatty acid influx and PPARα/δ-mediated activation of target genes promote β oxidation without a coordinated increase in TCA cycle. As a result, metabolic by-products of incomplete fat oxidation (acylcarnitines and ROS) accumulate in the mitochondria. These stresses might activate Ser kinases that hinder insulin signalling and GLUT4 translocation. (Muoio and Newgard, 2008). CPT: carnitine palmitoyl transferase, DAG: diacylglycerol, ETC: electron transport chain, LC-CoA: long-chain acyl co-enzyme A, PGC1: PPAR-γ coactivator-1, PPAR: peroxisomes proliferating activated receptor, ROS: reactive oxygen species, RXR: retinoid X receptor, TCA: tricarboxylic acid cycle, TF: transcription factor, TG: triglycerides.

Thus far, the definition, metabolic changes and effects that occur during diabetes mellitus 2 have been discussed. The effect of insulin resistance on hepatic enzymes is covered in the next chapter.

CHAPTER THREE: HEPATIC ENZYMES AND INSULIN RESISTANCE

3.1 INTRODUCTION

Certain hepatic enzymes have elevated activities associated with diabetes; these enzymes include PEPCK, G6Pase, PGC-1α and GFAT. Other proteins have elevated activities which prevent diabetes, these include GK, GK regulatory protein (GKRP), Glycogen Targeting Subunits, PFK2, Sterol regulatory element binding protein-1c (SREBP-1c), Myelocytomatosis cellular oncogene (c-Myc) and carbohydrate responsive element-binding protein (ChREBP) (Collier and Scott, 2004).

3.1.1 Glucose-6-phosphatase (G6Pase)

G6Pase is vital in glucose production. This enzyme catalyzes the dephosphorylation of glucose-6-phosphate (G6P) to free glucose, this is the last step in gluconeogenesis and glycogenolysis. This process is carried out in the lumen of the endoplasmic reticulum and necessitates several other proteins in addition to the catalytic subunit. These include transporters for G6P, glucose, and inorganic phosphate. The terminal result of this reaction allows glucose to be transported out of the hepatocyte and into circulation. G6Pase is a hydrophobic protein that is embedded within the endoplasmic reticulum (ER) membrane (Mithieux *et al*., 2004) as indicated in figure 3.1, it is uniquely membrane bound with its catalytic site positioned towards the lumen of the ER (Bouche *et al*., 2004). G6Pase is a nonspecific phosphohydrolase. The gene encoding the G6Pase catalytic subunit is stimulated by cAMP and glucose and repressed by insulin (Collier and Scott, 2004).

The G6Pase gene is stimulated by glucose. If the balance involving glucose phosphorylation and glucose 6-phosphate hydrolysis is disturbed, producing a high G6Pase to GK ratio, irregular hepatic glucose metabolism results and is marked physiologically as a metabolic disturbance resembling DM2. Thus, a delicate balance exists where GK and G6Pase compete to control the direction of glucose flux and ultimately the metabolic signalling system that encourages the fasting-to-fed transition of the liver (Collier and Scott, 2004). In an intact G6Pase catalytic subunit there are three integral proteins (i) a G6P specific translocase, T1, mediates penetration of G6P

through the membrane (ii) a relatively nonspecific phosphohydrolase situated with its active site facing the luminal cavity and (iii) a second translocase, T2, mediating efflux of Pi (Arion *et al*., 1998). It is vital to measure G6Pase activity in an intact G6Pase subunit so as to measure the actual dephosphorylation of G6P and not other sugar phosphates such as mannose-6-phosphate, since G6Pase is a non-specific phosphohydrolase.

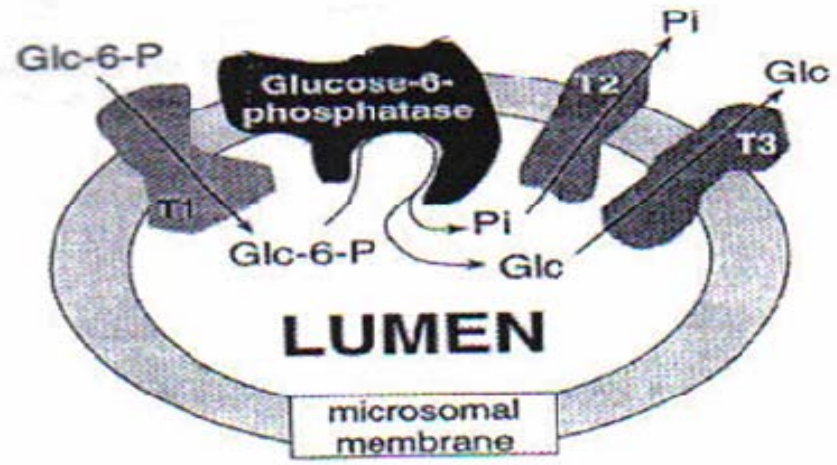

Figure 3.1: The Arion model of the G6Pase system. T1 is a specific G6P transporter that transports only G6P into the lumen. Glucose-6-Phosphatase in intact microsomes catalyzes only the hydrolysis of G6P into glucose and Pi due to the presence of the specific transporter T1. G6Pase is however observed to be a non-specific catalytic. In intact microsomes G6Pase can only catalyze G6P because T1 allows the entry of G6P only. In disrupted microsomes, G6Pase is observed to be non-specific due to the uncoupling of T1. T2 is a phosphate transporter that transports Pi out of the lumen. T3 is a glucose transporter that transports glucose out of the lumen (Burchell and Clottes, 1998). Glc-6-P: Glucose 6 phosphate, Glc: Glucose, Pi: Inorganic phosphate.

During insulin resistance there is increased hepatic glucose production as well as a significant increase in G6Pase and PEPCK activities (Panunti *et al*., 2004). The determination of whether G6Pase can be used as an insulin resistance marker was conducted in this study.

3.1.2 Glucokinase (GK)

The liver removes a considerable portion of glucose from the blood and thus is specially suited to metabolize large quantities of carbohydrates. The four hexokinases involved in the first of glycolysis step are Hexokinase I, II, III and IV. Hexokinase IV otherwise known as glucokinase (GK) is about half the molecular mass of the of the other hexokinases (I,II and III) (Postic *et al*., 2001). GK is the chief glucose-

phosphorylating enzyme in the liver; its abundance is regulated at a variety of levels, including transcriptionally by insulin and glucagon, and post-translationally by the GKRP. Hence GK initiates glycolysis unlike hexokinase (Collier and Scott, 2004). GK displays sigmoidal kinetics and its activity is not altered significantly by physiological concentrations of G6P (Potstic *et al*., 2001) therefore GK has a low affinity for glucose (Collier and Scott, 2004), however small changes in GK concentration are significant as they have an impact on the rate of glucose stimulated insulin secretion as well as the rate of glucose metabolism. GK also has a significant role in glucose utilization and glycogen synthesis (Postic *et al*., 2001) and GK activity increases and decreases parallel to changes in blood glucose levels within the physiological range. Glucose metabolism proceeds with phosphorylation of the hexose and its subsequent metabolism via various pathways (Collier and Scott, 2004).

GK plays a vital role in glucose disposal (Agius L, 2008) and GK activity is highly correlated with blood glucose concentration and is thus considered to be a hepatic "glucose-sensor"(Collier and Scott, 2004) for insulin secretion in the β cells of the pancreas (Matschinsky *et al*., 2006). The inhibitory protein; glucokinase regulatory protein (GKRP) regulates GK. At basal glucose concentrations (5 mmol/l) GKRP binds to GK with high affinity, blood glucose homeostasis is maintained by the liver by glucose production (red arrows) via glycogenolysis from glycogen and via gluconeogenesis from lactate and other gluconeogenic substrates. During the postprandial state, hyperglycemia (glucose concentrations >5 mmol/l) causes dissociation of GK from GKRP and translocation of GK into the cytoplasm; this results in increased glucose phosphorylation to G6P and conversion to glycogen, lactate, and triglyceride (TG). If TG production via glycolysis to pyruvate and synthesis of fatty acids exceeds the very low density lipids (VLDL) secretion capacity, TG accumulates in the hepatocyte (Agius, 2009).

In high fat fed rats with hepatic insulin resistance, the activities of G6Pase and GK are dramatically increased and decreased respectively. During insulin resistance, the increased G6Pase activity contributes to increased hepatic glucose production (Minaissian *et al*., 1998). GK activators can alleviate the hyperglycaemia associated with DM2 by increasing hepatic glycogen synthesis and glucose stimulated pancreatic insulin release (Castelhano *et al*., 2005).

3.4 MATERIALS AND METHODS

In this study, unless otherwise stated the T-test analysis; two-sample assuming equal variance was used for data analysis.

3.4.1 Measurement of G6Pase and GK activities

Glucose-6-phosphatase is a non-specific phosphorylase tightly associated with the endoplasmic reticulum and nuclear membranes of liver and kidney cells. *In vitro* via microsomes (small endoplasmic reticulum vesicles), G6Pase exhibits a phenomenon termed latency, with part of its activity expressed only when the membrane is disrupted, increasing both activity and affinity (Van Schaftingen and Gerin, 2002).

3.4.2 Tissue preparation

For the G6Pase assay (Diagram I) 0.1 grams of frozen liver tissue (from insulin resistant and non insulin resistant rats) was cut up into about 5 mm pieces and homogenized in 0.5ml of homogenization buffer (250 mM sucrose, 1 mM EDTA, 20 mM Tris-HCl, 1 mM DTT and 0.1 mM PMSF) at pH 6.8. A Potter-Elvehejm homogenizer was used to homogenize the liver at 700 rpm for 10 strokes. The homogenate was collected and centrifuged at 14000 x g for 20 minutes. The supernatant (S1) was discarded and the pellet (P1) was resuspended in Triton buffer (2% Triton X-100, 25 mM HEPES and 250 mM sucrose at pH 6.8) and centrifuged at 10000 rpm for 20 minutes, thereafter supernatant (S2) was assayed as described before (Van Schaftingen and Gerin 2002).

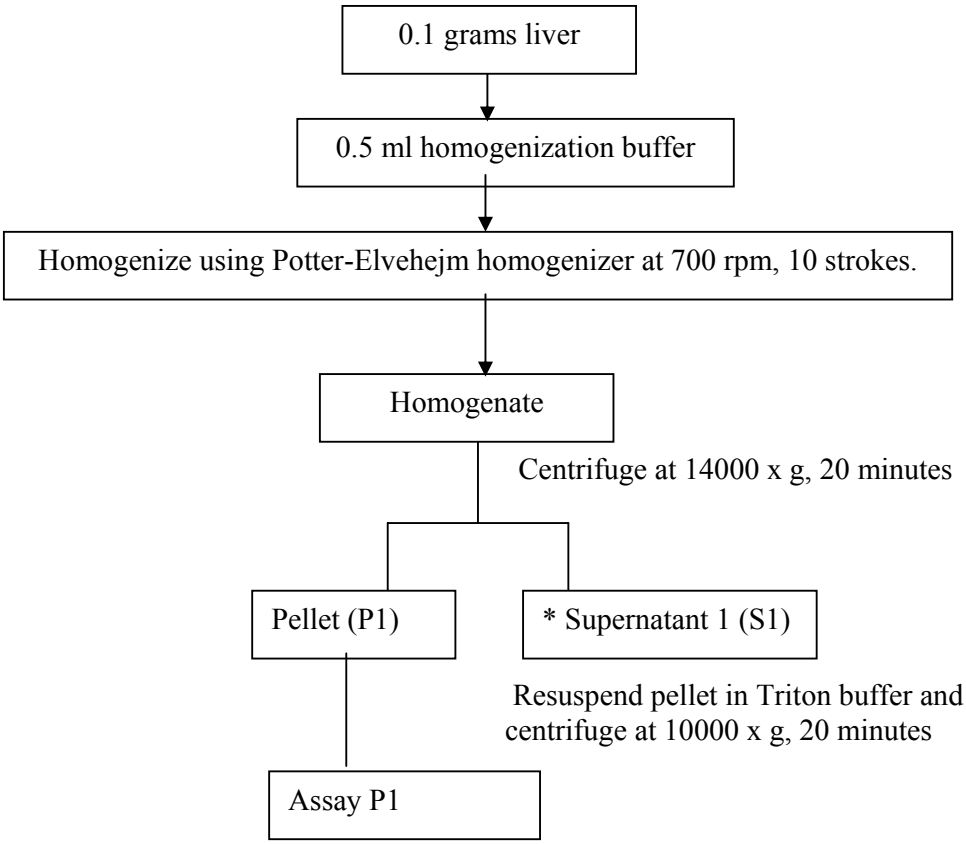

Diagram I: Procedure used to isolate liver microsomes.

For the GK assay (Diagram II), the homogenate was obtained in the same manner as the G6Pase assay from frozen liver tissue (using insulin resistant rats and normal rats), however the homogenate was centrifuged at 12000 x g for 10 minutes. The supernatant (S1) obtained was then assayed according to a modification of the Sigma protocol to suit a microtiter plate assay. Briefly, 140 µl reaction cocktail (75 mM Tris Buffer, 600 mM Magnesium chloride, 120 mM ATP, 360 mM glucose, 27 mM β-NADP) was added to the required wells in a microtiter plate, 5 µl of G6PDH was added to all wells. To the test wells 5 µl test sample was added. To the blank designated wells 5 µl enzyme diluent (50 mM Tris HCl buffer) was added.

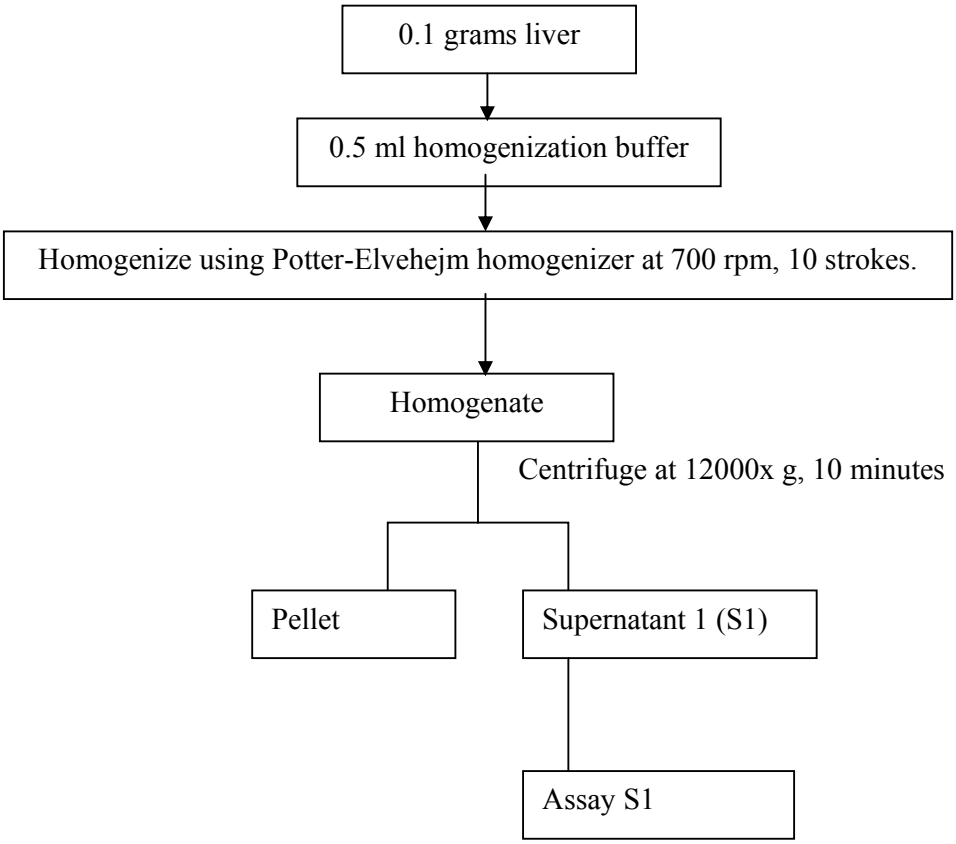

Diagram II: **Procedure used to obtain liver cytosol.**

3.4.3 Determination of G6Pase activity of using ascorbic assay

As indicated in the equation below, G6Pase hydrolyses G6P into glucose and phosphate. The phosphate is then quantified using colorimetric determination of inorganic phosphate.

$$G6P \xrightarrow{G6Pase} Glucose + Pi$$

Inorganic phosphate reacts with ammonium molybdate in an acidic solution forming phosphomolybdic acid. In the ascorbic assay, phosphate and molybdate combine to form a heteropoly complex. The phosphomolybdate complex is colourless, but can be converted to a coloured complex, by reduction of the phosphomolybdate complex (Cogan *et al*., 1999). For example, ascorbic acid is used to reduce the phosphomolybdate complex (Gawronski and Benson, 2004) in the assay used in this

study. This method achieves increased colour development, linearity, and sensitivity. Sodium citrate is added to stabilize the colour of the assay, by complexing excess molybdate and stopping further colour development. The phosphomolybdate complex (Figure 3.2) is then measured by a spectrophotometer at 815 nm, the molar extinction coefficient of the phosphomolybdate complex at 815 nm is 26 319 M^{-1} cm^{-1} (Cogan *et al*., 1999).

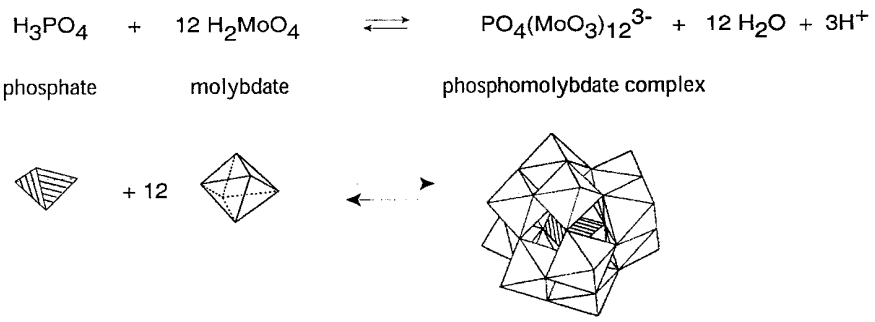

Figure 3.2: **Phosphomolybdate complex formation (Cogan *et al*., 1999).**

Briefly, a standard curve was set up on a 96 well plate, using different dilutions of phosphate solution as a standard. 5 µl of Triton X-100 treated sample (different dilutions of sample) was added to assigned wells on a 96 well plate. 45 µl assay mixture containing 10 mM βGP was added to designated wells (to distinguish between alkaline phosphatases and G6Pase) and 45 µl assay mixture containing 10 mM G6P was added to other designated wells. The plate was then incubated for 20 minutes at 37°C. The reaction was stopped by adding 150 µl of solution C (2:1 ratio of 12% ascorbic acid and 2% ammonium molybdate) to all wells and the plate was incubated for 5 min at room temperature. 150 µl solution D (2% citrate, 2% acetic acid and 2% SDS) was thereafter added to each well (Van Schaftingen and Gerin, 2002).

3.4.4 *In vitro* GK assay optimization

The principle of the GK assay is indicated in the equation below. Hexokinase phosphorylates glucose to G6P. G6P in the presence of β-NADP is then oxidized by G6PDH to form 6-Phospho-D-gluconate, while β-NADP is reduced to form β-NADPH. The increase of β-NADPH is monitored spectrophotometrically at 340 nm.

$$\beta\text{-D(+) Glucose} + \text{ATP} \xrightarrow{\text{GK}} \text{Glucose-6-phosphate} + \text{ADP}$$

$$\text{D-Glucose-6-Phosphate} + \beta\text{-NADP} \xrightarrow{\text{G6PDH}} \text{6-Phospho-D-gluconate} + \beta\text{-NADPH}$$

(SPGLUC09).

The method was modified from the Sigma enzymatic assay of glucokinase (SPGLUC09). Briefly, the reaction cocktail (75 mM Tris HCl buffer, 600 mM $MgCl_2$, 120 mM ATP, 360 mM glucose, 27 mM β-NADP) was incubated for 10 min in a water bath, the pH was thereafter adjusted to pH 9.0, 280 µl reaction cocktail was added to all wells in a microtiter plate. 10 µl of G6PDH (100 units/ml) was added to all the wells containing the reaction cocktail. The effect of G6PDH on the hexokinase assay, isolated from *Leuconostoc mesenteroides* (Sigma-Aldrich G-8404, EC 1.1.1.49) and *Saccharomyces cerevisiae* were tested. Hexokinase activity was tested to prove that the assay was time and concentration dependent. The plate was thereafter equilibrated at 30°C in a microtiter plate reader and the absorbance (at 340 nm) was monitored for 15 min to determine the stability of the enzyme. For the blank, 10 µl of the enzyme diluent (50mM Tris-HCl at pH 8.5) was added to the wells assigned for the blank. For the test wells 10 µl of varying concentrations of liver samples diluted in enzyme diluent was added to the respective wells.

3.4.5 Protein determination (BCA and Bradford)

The BCA method is based on the conversion of Cu^{2+} to Cu^{+} under alkaline conditions, like the Lowry assay. Although previously the Lowry method had been used extensively in protein determination the Folin-Ciocalteau reagent in alkaline medium

is unstable, non-ionic detergents as well as some buffer salts may also interfere with the reaction (Smith *et al*., 1985). Hence the BCA method has gained more popularity. The Cu^{+} is detected by reaction with BCA to give an intense purple colour with an absorbance maximum at 562 nm. This method is more sensitive than the Lowry method, capable of detecting down to 0.5 µg/ml. The most advantageous point of BCA is that it is more tolerant of the presence of compounds that interfere with the Lowry assay (Walker and Wilson, 2005).

The BCA assay was done according to Smith *et al*., 1985. Briefly, reagent A (1% bicinchoninic powder, 2% sodium carbonate, 0.16% sodium tartate, 0.4% sodium hydroxide, 0.95% sodium bicarbonate), was prepared. Reagent B was also prepared for the assay which consisted of 4% copper sulphate. A working solution C, was prepared on the day of the assay which consisted of 50 parts reagent A and 1 part reagent B. To the assigned wells 10 µl of each standard, blank or unknown sample was pipetted into a microtiter plate. 200 µl solution C was added to each well. The samples were mixed for 30 seconds at intensity 2 on a plate shaker. The microtiter plate was thereafter incubated at 37°C for 20 min. The absorbance was read at 570 nm after the incubation period. BSA was used to set up a standard curve as indicated in Appendix I.

The Bradford method is based on Coumassie brilliant blue (a dye) binding to protein. The free dye at low pH has absorbance maxima at 470 nm and 650 nm, but when bound to protein, it has an absorbance maximum at 595 nm. The advantages of this method include simplicity in preparing the reagent and the speed at which the colour develops as well as stability of the reagent. A disadvantage is that it is not as sensitive as the BCA method (20 µg/ml). It is also a relative method, because the quantity of dye binding differs with the content of the basic amino acids; arginine and lysine in the protein. Hence the choice of a standard is difficult. Furthermore, many proteins will not dissolve adequately in the acidic reaction medium (Walker and Wilson, 2005). Initially the Bradford assay was used to determine protein in the samples that were used for the G6Pase assay, it was found that the Triton X-100 present in the buffer in these samples affected the Bradford assay. After reading more literature it was confirmed that indeed Triton X-100 and other detergents such as SDS affect the Bradford assay (Andrews and Shultz, 1995). However, the Bradford assay used in this

was modified to avoid influence from detergents. The BCA assay was used to determine protein content in the G6Pase samples. The Bradford assay was used for the determination of protein from the samples used in the GK assay.

For the Bradford dye reagent, 0.05 g Serva Blue G dye (CBBG) was dissolved in 50 ml of 88% (v/v) phosphoric acid solution and 23.5 ml absolute ethanol. The solution was made to 500 ml with double distilled water (dd.H_20) and stirred for 30 min at room temperature. The solution was thereafter filtered through Whatman No. 1 filter paper and was stored in a container covered with foil.

For the standard BSA solution (1 mg/ml), 0.1 g of BSA was dissolved and made up to 100 ml with PBS. 1 ml aliquots were stored at -20°C. a working solution of 0.2 µg/ml was prepared by diluting 200 µl of the 1 mg/ml solution with 800 µl with dd.H_20.

50 µl of diluted unknown samples was added to assigned wells in a 96 well plate. 200 µl of Bradford reagent was then added to all wells containing standard or sample and incubated for 10 min at room temperature. The absorbance was then read at 595 nm and 460 nm. Protein concentration estimations were calculated form the equation generated by linear regression analysis by plotting the absorbance ratio 595/460 versus BSA concentration (Zor and Selinger, 1996).

3.5 RESULTS AND DISCUSSION

It should be noted that the identity of the plant (*Prunus africana*) was revealed to the author towards the end of this study. Hence the plant will still be referred to as plant A or C4 (in figures and tables).

CCL: denotes rats fed a normal diet; lean control rats that were gavaged with water for 4 weeks before being sacrificed at 16 weeks. CCH: denotes rats that were fed a HF diet that were insulin resistant that were gavaged with water for 4 weeks before being sacrificed and at 16 weeks. Plant A/C4: denotes rats that were fed a HF diet and were insulin resistant and were treated with *P. africana* for 4 weeks prior to being sacrificed at 16 weeks. In 1959 the first description of a 'high fat diet' was used to induce obesity (Masek and Fabry, 1959). Following studies by numerous researchers showed that high fat diets cause hyperglycemia and insulin resistance (Buettner *et al*., 2006). It is accepted that high fat diets can be used to generate a rat model for the metabolic syndrome and insulin resistance with compromised β cell function (Oakes *et al.* 1997, Ahren *et al.* 1999, Lingohr *et al.* 2002). The metabolic syndrome is described as the coincidence of obesity, hypertension, dyslipidemia and insulin resistance (Laaksonen *et al.* 2004) that occurs in humans.

3.5.1 *In vivo* effect of plant A on G6Pase in liver

The increase in hepatic glucose production (HGP) in the diabetic (Clore *et al*., 2000) and the insulin resistant states (Minassian *et al*., 1998) is mainly attributed to an increase in G6Pase and a decrease in GK activity in these two mentioned states. Figure 3.3 shows that there is no significant difference in total G6Pase activities between CCH and CCL, although CCH (0.01 nmol/min/mg) had slightly lower (17 % decrease) G6Pase activity compared to CCL (0.02 nmol/min/mg). These data show total G6Pase activity (G6Pase catalytic subunit measured) and not actual G6Pase activity, since an intact G6Pase system was not obtained because intact microsomes were not isolated. In an intact G6Pase system (where transportation rate of G6P is the limiting factor; due to the presence of T1), insulin resistance increases G6Pase activity (Van Schaftingen and Gerin, 2002). As previously stated, insulin suppresses catalytic G6Pase activity, as observed in table 1.1, CCH samples had higher insulin

concentration than the CCL samples. Thus I speculate that the higher insulin levels suppressed catalytic G6Pase activity as is evident in literature.

There was a 58% decrease in total G6Pase activity in plant A (0.006 nmol/min/mg) treated rat samples compared to CCL rat samples ($p<0.001$). Significantly higher G6Pase activity was expected in the insulin resistant rats, however as mentioned the G6Pase activity measured was not in an intact G6Pase system. These data are in accordance with the decrease in G6Pase catalytic activity in the presence of insulin (Collier and Scott, 2004), as treatment with plant A caused an increase in insulin levels in rat plasma (Karachi, 2009), observed in table 1.1. However taking into account that the G6Pase system was not intact, I conclude that the treatment of plant A reduces G6Pase activity by other mechanisms other than insulin suppression of G6Pase gene expression and activity. Thus plant A is expected to decrease G6Pase activity and the data shows that plant A decreased G6Pase activity (Figure 3.3). In disrupted microsomes only the catalytic component of the enzyme complex can be measured. In contrast the intact microsomes represent transport activity; hence the rate limiting step of G6P accumulation (Savage *et al*., 2005) is glucose transportation. There was a significant difference between CCH and plant A ($p<0.04$); where CCH had higher catalytic G6Pase activity as compared to plant A; this is again attributed to the higher insulin levels in plant A treated rats when compared to the CCH rats. It is clear from the results that intact microsomes were not obtained and this may be attributed to the homogenization process, hence only the catalytic activity of G6Pase was measured. The buffer may also cause disruption of the microsomes hence I suggest changing the buffer when homogenizing liver samples. I suggest that intact microsomes should be isolated from fresh liver as opposed to frozen liver (to avoid microsomal disruption due to the freeze and thaw process) so that the G6Pase activity can be determined in intact microsomes to give an accurate impression of actual G6Pase activity in the rat, alternatively other methods can be used to isolate microsomes such as lyophilisation, $CaCl_2$ precipitation and sucrose gradient centrifugation. One cannot use G6Pase as a marker for insulin resistance if the G6Pase system is not intact; as the glucose transporter (T1) is absent in a G6Pase that is not intact. The glucose transporter; T1 is the rate limiting step towards G6P dephoshophorylation as previously mentioned. Therefore, I opted to determine whether GK activity can be used as a marker for insulin resistance.

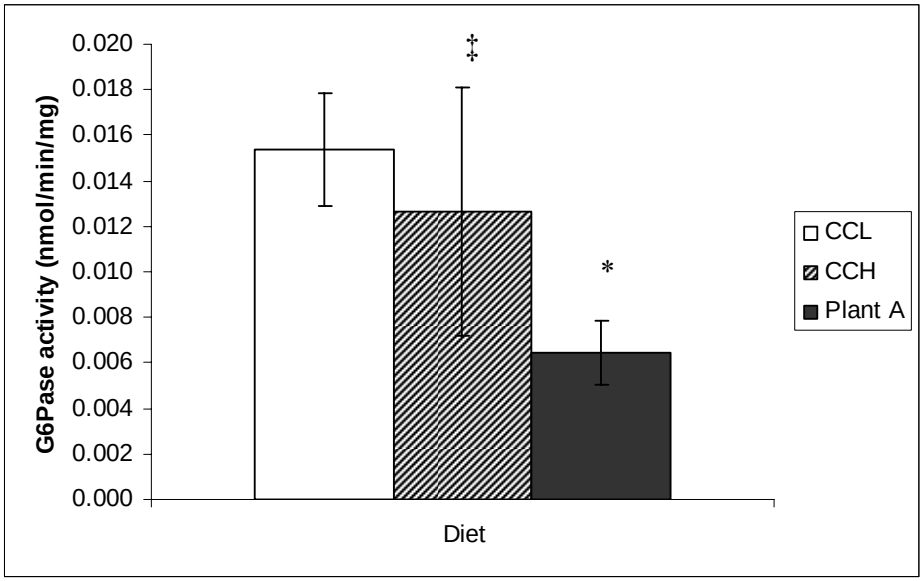

Figure 3.3: Catalytic glucose-6-phosphatase activity in disrupted microsomes. The microsomes were disrupted in 10% Triton X-100. Each value represents means ± S.D (n= 5). CCL represents low fat fed normal rats and CCH represents high fat fed rats that were insulin resistant, both groups were treated with water for 28 days. Plant A represents HF fed (insulin resistant) rats that were treated with plant A for 28 days. *P<0.001 represents significant difference when compared to CCL and ‡P<0.04 represents significant difference when compared to plant A.

3.5.2 *In vivo* effect of plant A on GK in liver

The main motivation in measuring glucokinase activity was so as to determine if GK can be used as an alternative marker for insulin resistance. Since a previous study showed an increase in insulin levels in the plasma from the plant A treated rats. It was decided to measure glucokinase activity. As it is from the glucose metabolism (in which glucokinase is involved in) that produces ATP which stimulates insulin secretion. This contrasts the role of GK in the liver. I decided to measure glucokinase activity in the liver, since during insulin resistance, hepatic GK is drastically altered. Further on, in this study, GK expression was to be determined in adipose tissue.

Figure 3.4 indicates the standard curves obtained from the GK assay using G6PDH from *Leuconostoc mesenteroides* and *Saccharomyces cerevisiae* respectively.

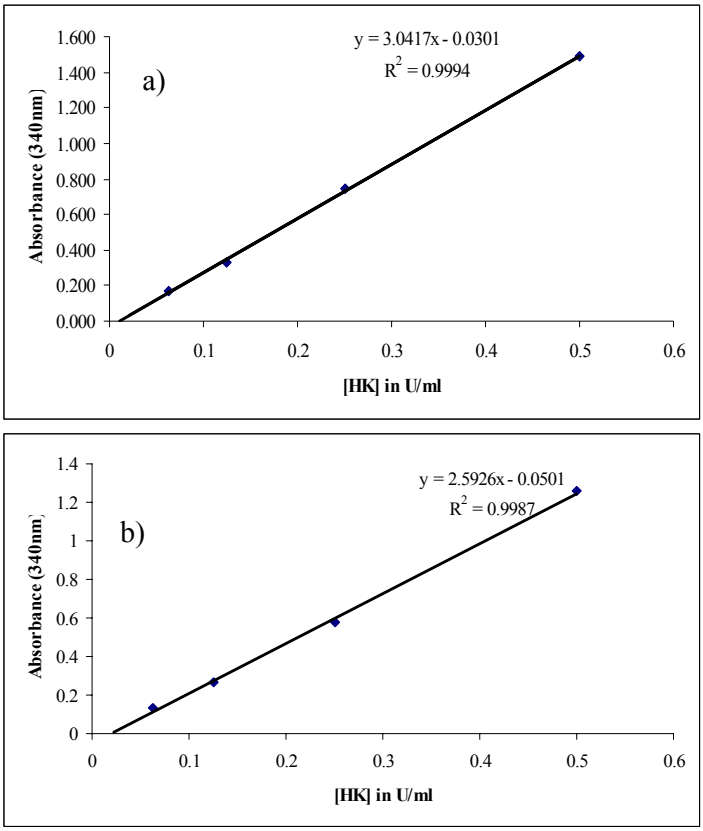

Figure 3.4: **Standard curve of glucokinase assay. In a 300 µl assay system the glucokinase concentration in units/ml was obtained by measuring the absorbance at 340 nm at the end of 10 minutes. The G6PDH used in the assay is from a) *Leuconostoc mesenteroides* and b) *Saccharomyces cerevisiae*. The equations obtained from linear regression and r2 values and are shown in the graphs.**

A better R^2 value was obtained when using G6PDH from *Leuconostoc mesenteroides* than when using G6PDH from *Saccharomyces cerevisiae*, with these data, it was decided to use G6PDH from *Leuconostoc mesenteroides* for subsequent GK assays.

Figure 3.5 a) and 3.5 b), show that as there is a linear increase in absorbance with time for 0.0625-0.5 U/ml hexokinase concentration.

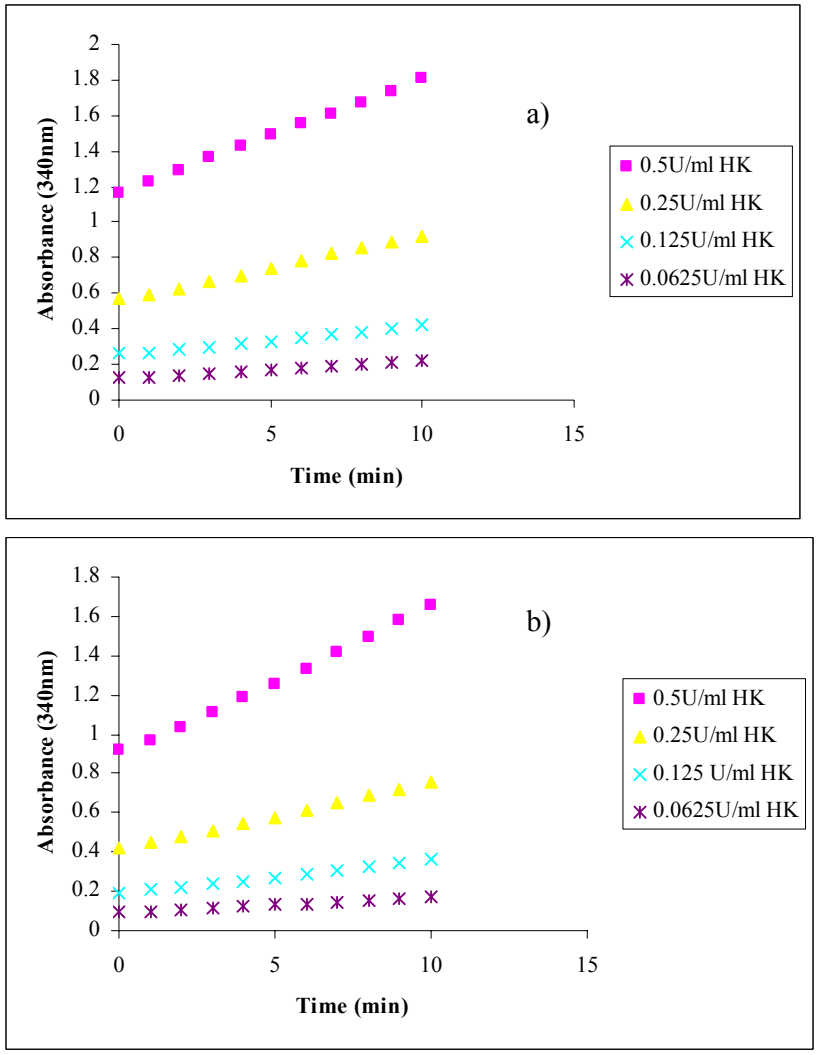

Figure 3.5: **Progress curve for Hexokinase activity. The assay was conducted in a period of 10 min, using G6PDH from a) *Leuconostoc mesenteroides* and b) *Saccharomyces cerevisiae*.**

The hexokinase concentration used as a control would be 0.25 U/ml. Figure 3.5 a) and 3.5 b) indicates that the absorbance values obtained from using G6PDH from *Leuconostoc mesenteroides* were higher than those obtained from *Saccharomyces cerevisiae*. The suggested assay time by the Sigma protocol was 5 minutes.

Figure 3.6 indicates that no significant data was found in GK activity between the normal (CCL), insulin resistant rats (CCH) and plant A treated rats. The GK activity is slightly lower (but not significant) in the insulin resistant rats compared to the normal rats ($p<0.29$). These data are expected as glucokinase (a hexokinase isomer; hexokinase IV or hexokinase D) is markedly decreased in the insulin resistant and

diabetic states (Minassian *et al*., 1998, Lam *et al*., 2003) as the GK gene is induced by insulin and a decrease in GK activity is attributed to insulin resistance (Minassian *et al*., 1998). The lack of significant data in GK activity between the normal and insulin resistant states is attributed to the method used to measure GK activity. The insulin resistant rats on a high fat diet (CCH) had a lower (but not significant) GK activity compared to plant A treated rats ($p<0.25$). A slightly higher (but not significant) GK activity was noted in rats treated with plant A when compared to normal rats ($p<0.64$). It follows that the trend of having GK activity Plant A >CCH (not significant) and Plant A>CCL (not significant) is similar to the plasma insulin levels whereby Plant A>CCH and Plant A>CCL (see Table 1.1) respectively, is in agreement with the fact that hepatic GK activity is induced by insulin (Matschinsky, 2002) and not glucose unlike pancreatic GK activity. These studies warrant further study on the influence of plant A treatment for a longer time period on glucokinase. These studies also warrant further studies on the effect of insulin resistance stage on glucokinase activity.

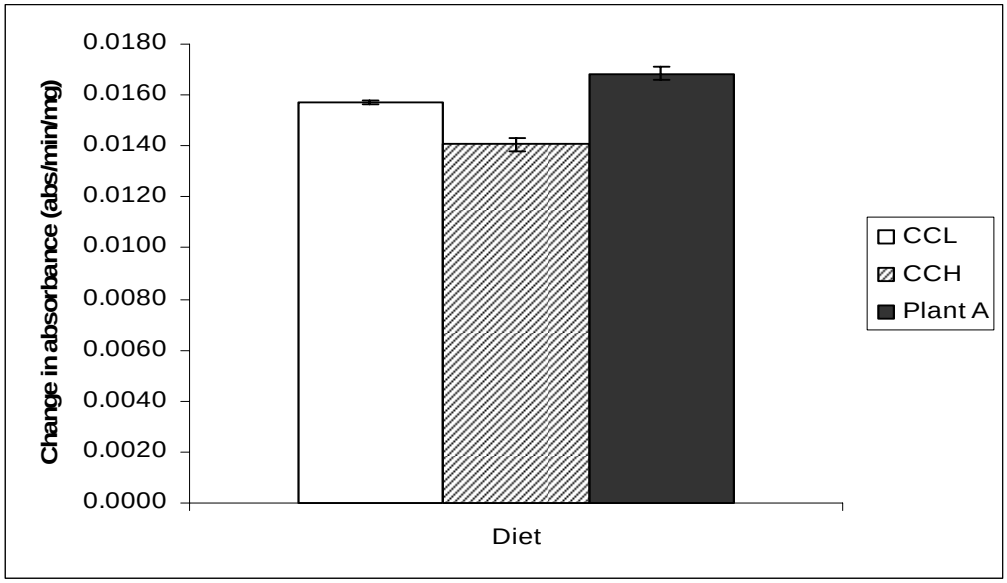

Figure 3.6: The change in absorbance representing Glucokinase activity in liver cytosol. Each value represents means ± S.D (n= 3). CCL represents low fat fed normal rats and CCH represents high fat fed rats that were insulin resistant, both groups were treated with water for 28 days. Plant A represent HF fed (insulin resistant) rats that were treated with plant A for 28 days.

During insulin resistance, decreased G6Pase gene expression may represent a vital adaptive mechanism to decreased GK gene expression (Minassian *et al*., 1998) and

this speculation could explain the data obtained in figures 3.3 and 3.6. In addition in the insulin resistant state, 'glucose effectiveness' is decreased; whereby either GK expression is decreased or an impaired regulation of GK by GKRP (Agius, 2009).

CHAPTER FOUR: INSULIN RELEASE

4.1 Introduction

Insulin is a small protein with a molecular weight of 5800, with 2 polypeptide chains, A and B, joined by two disulphide bonds, observed in figure 4.1. It is a key polypeptide hormone regulating the control of metabolism and the maintenance of normoglycaemia and normolipidaemia (Pirola *et al*., 2004). Insulin has a short plasma half life (4-6 min), as would be expected from the necessity to respond rapidly to changes in blood glucose. The actions of insulin can be divided into (i) short-term (glucose uptake and metabolism), (ii) intermediate-term (protein and lipid turnover) and (iii) long-term (cell growth and mitogenesis) effects (Duckworth *et al*., 1998). Insulin has anabolic functions which include the promotion of glycogen, triglyceride and protein synthesis.

4.1.1 Insulin transcription

The pancreatic β cells are the only cells that express insulin, whilst the insulin promoter controls insulin transcription. PDX-1 (pancreatic/duodenal homebox-1) is the most critical insulin transcription factor: it is only expressed in the pancreatic β cells and is vital for glucose-stimulated insulin gene transcription. PDX-1 is also vital for the maintenance of the β cell phenotype and pancreatic development (Ren *et al*., 2007). PDX-1 gene expression has been shown to be decreased in cultured β cell lines chronically exposed to high glucose concentrations. Waeber *et al*.(1996) proposed the likelihood that PDX-1 contributes to the β cell-specific activity of the GLUT2 promoter. The GLUT2 gene is regulated in a positive manner by glucose but ironically decreases in the β cell in many experimental models of diabetes. As GLUT2 disappearance during diabetes is cell-specific, PDX-1 is one of the cell-specific regulators of GLUT2 gene expression; (1) because GLUT2 expression is not altered in the liver and the kidney of diabetic animals and (2) because PDX-1 expression is restricted to the β and δ pancreatic cells and absent in the liver and kidney cells. The identification of islet-specific transcriptional factors such as PDX-1 is of great importance as several genes are abnormally regulated only in the β cells during diabetes but may be normally expressed in non-islet tissues such as the liver or the kidney in the case of GLUT2 (Waeber *et al*., 1996).

4.1.2 Insulin biosynthesis

When insulin mRNA is translated, preproinsulin is synthesized in the pancreatic β cell. Insulin is produced as part of a larger protein (Figure 4.1), to ensure adequate or proper folding of insulin. This preproinsulin is an inactive single-chain precursor with an amino-terminal "signal sequence" that directs its passage into secretory vesicles. The signal sequence is also needed to direct the preproinsulin into the endoplasmic reticulum (ER) for post translational processing. About 30-60 seconds after preproinsulin is produced, the signal sequence is removed enzymatically upon entering the ER and the formation of three disulphide bonds produces proinsulin. Proinsulin is then transported along the microtubule network system in transport vesicles to the cis part of the Golgi apparatus. The proinsulin is first packaged into clathrin-coated granules, where proinsulin is further converted to insulin and C-peptide; via cleavage of 2 peptide bonds. The clathrin-coated granules then become mature granules, where the insulin crystals are formed; hence insulin is stored in mature secretory granules until release or degradation by crinophagy (Ren *et al*., 2007).

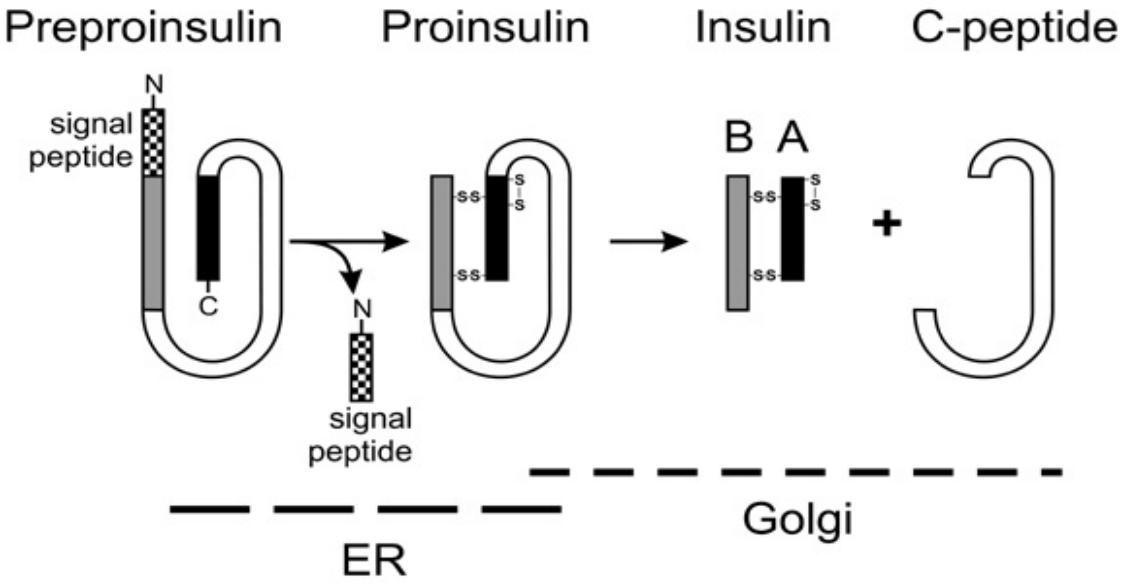

Figure 4.1: Formation of mature insulin. Upon translation of insulin mRNA, preproinsulin (inactive) is produced in the pancreas, signal peptide is then cleaved off from the preproinsulin forming proinsulin in the ER, proinsulin is further processed by removal of C-peptide in the Golgi into A and B chains of insulin linked by disulphide bonds to form active insulin (Morrissey, 2006).

With highly developed ER specialized for insulin synthesis, β-cells can control the rate of insulin production by regulating insulin synthesis in the ER in response to glucose stimulation.

4.1.2.1 C-peptide

C-peptide is a single chain of 31 amino acids with a molecular weight of 3020. C-peptide or 'connecting' peptide plays a critical role in the synthesis of insulin as it links the A chain and B chain in a fashion that allows correct folding and inter-chain disulphide bond formation. When C-peptide is removed from proinsulin by proteolytic processing, the COOH-terminal part of insulin's B chain becomes exposed and free to assume an appropriate conformation for effective interaction with the insulin receptor. Figure 4.2 shows the linear representation of human proinsulin indicating amino acid sequence of C-peptide and indicates the position of the COOH-terminal pentapeptide (Wahren *et al*., 2000).

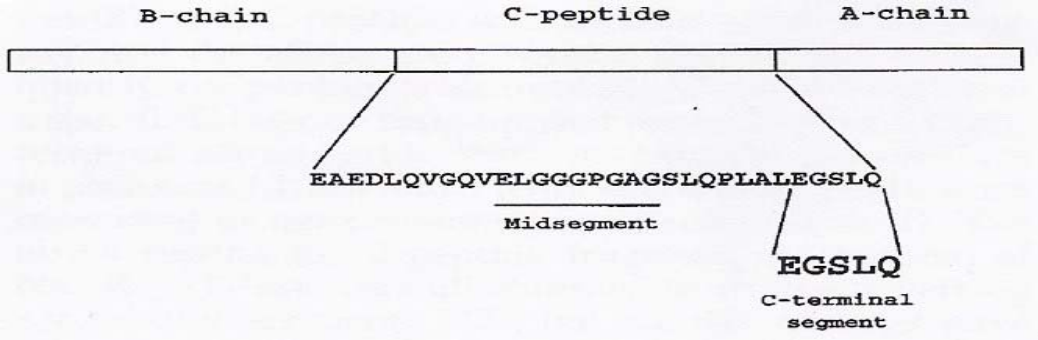

Figure 4.2: **Amino acid sequence of C-peptide in human proinsulin with COOH-terminal indicated (Wahren *et al*., 2000).**

Further research on C-peptide has shed light that 'connecting' peptide is a belittling term for the peptide, as it has recently been disproved that C-peptide is biological inert. Observations confirm that C-peptide has biological function (Henriksson *et al*., 2006).

C-peptide has been shown to bind to a G- protein coupled receptor. C-peptide is also involved in non-chiral membrane interactions and has insulinomimetic interactions (Henriksson *et al*., 2006). Wahren *et al*.(2000) observed that when patients with DM1 who lack C-peptide receive C-peptide administration the following occur; augmented blood flow in skeletal muscle and skin, diminished glomerular hyperfiltration,

reduced urinary albumin excretion and improved nerve function. There is a possibility that C-peptide replacement together with insulin administration, may prevent the development or retard the progression of long-term complications in DM1 (Wahren *et al*., 2000).

The measurement of C-peptide is used as an indication of insulin secretion or reflection of β-cell function, because C-peptide has a longer half-life than insulin; 30 minutes versus 4-6 minutes respectively. Insulin undergoes a large and variable hepatic extraction from the portal vein as well as peripheral clearance that may vary under different physiological circumstances; including insulin levels, disease state and nutrient administration (Kjems *et al*., 2000). As a result, the peripheral concentration of insulin cannot be assumed to reflect direct changes in pancreatic secretion. To avoid these limitations inherent in measurements of serum insulin levels, many investigators, have used plasma C-peptide levels as a measure of β-cell function. The basis of this approach is that C-peptide is co-secreted with insulin in an (i) equimolar ratio, (ii) is not extracted by the liver, and (iii) has a constant peripheral clearance (Van Cauter *et al*., 1992). The limitation with measuring peripheral C-peptide levels is that one may not be able to evaluate rapid changes in insulin secretion, because of the 'long' half-life of C-peptide (Van Cauter *et al*., 1992).

4.2 Insulin release

What stimulates or regulates insulin release? Blood levels of glucose, amino acids and gastrointestinal hormones, such as glucagon like peptide-1 (GLP-1). Insulin secretion is affected by metabolic signals and transcription factors that are required for suitable differentiation and growth of various types of pancreatic islet cells. Insulin secretion is the result of changes in the β cell's membrane potential and calcium-dependent action potentials (Ren *et al*., 2007) as observed in figure 4.3.

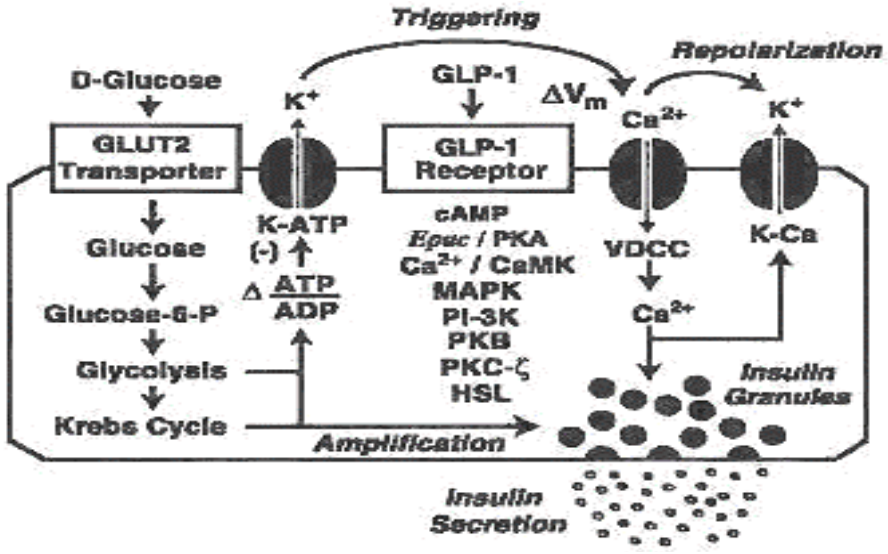

Figure 4.3: Factors influencing insulin secretion. Some of the actions of the cAMP-linked hormones are independent of protein kinases. cAMP has been demonstrated to bind to cAMP receptor proteins known as Epac1 and Epac2, also known as cAMPGEFs. The cAMP-activated Epacs stimulate exchange of GDP for GTP on Rap1, hence activating GTP binding protein. Intracellular calcium levels are partially controlled by Epacs as they regulate release of calcium from intracellular stores (Holtz *et al*., 2004). cAMP: adenosine 3',5'-cyclic monophosphate GLP-1: glucagon-like-peptide-1, HSL: hormone sensitive lipase, KATP: potassium dependent ATP channels, MAPK: mitogen activated protein kinases, PI-3K:phosphatidylinositol-3 kinase, PKB: protein kinase B, PKC: protein kinase C, VDCC: voltage dependent calcium channels.

Most of the insulin released by β cells is from insulin secretory granules. For insulin to be released, the granules must be recruited from the cytoplasm, translocated to the plasma membrane (PM) where they dock, fuse with the plasma membrane and release their contents into the extracellular space. Snap receptors (SNARES) are the group of proteins responsible for directing the insulin vesicles to the PM. Docking of the vesicle with the PM involves the linking of the PM proteins syntaxin and synaptosomal-associated protein 25 (SNAP-25) with the vesicle-associated protein 2 (VAMP-2 or synaptobrevin-2). Syntaxin and SNAP-25 are referred to as t-SNARE and VAMP-2 is referred to as v-SNARE (Ren *et al*., 2007).

When insulin granule secretion responds to glucose stimulation, insulin is released in two phases as shown in figure 4.3. The two characteristic phases are; the rapid but transient first phase of insulin release and a sustained second phase. β cells contain 2 pools of insulin containing secretory granules that have distinct release processes. A limited pool of granules (<5%) is available for immediate release and is known as the readily releasable pool (RRP). Most of the insulin though (>95%) belongs to the reserve pool and must undergo mobilization before they can gain release competence.

The first phase of insulin release is attributed to granules in the RRP and the depletion of this pool marks the end of the phase. The re-supplication or mobilization from a reserve pool of granules and release of these mobilized granules is responsible for the second phase of insulin secretion (Ren *et al*., 2007). In DM2 there are defects in the first and second phases of insulin responses (Panunti *et al*., 2004).

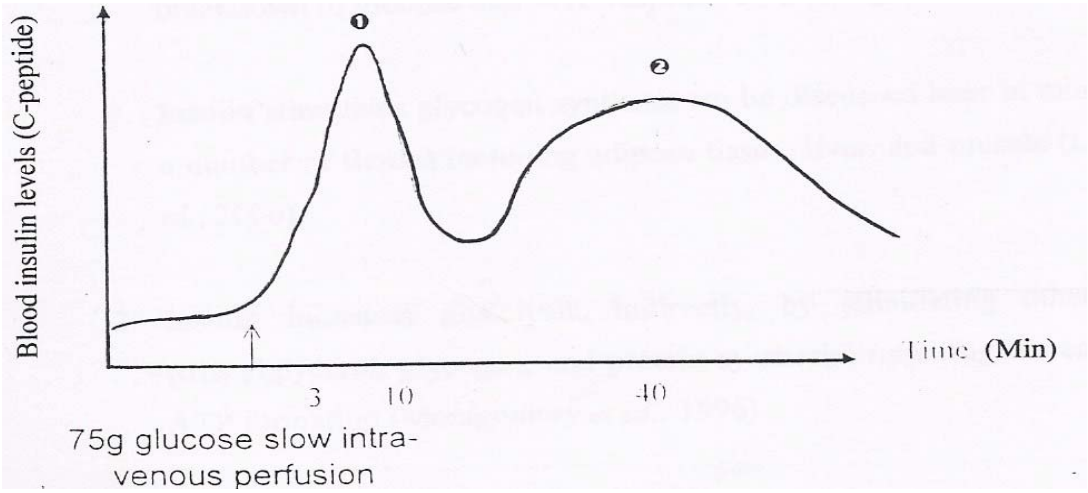

Figure 4.3: Biphasic release of insulin. Upon glucose stimulation, insulin is released in 2 phases; the first phase is rapid and short lived, whereas the second phase is slow and longer (Servier *et al*., 2001).

4.2.1 Regulation of insulin secretion by glucose

The main intracellular signals for insulin secretion are derived from glucose metabolism. Glucose affects insulin at all levels, including transcription, translation and release.

The β cells do not release insulin in response to glucose itself, but to glucose metabolism. GLUT2 facilitates entry of glucose into the β-cells once blood glucose concentration rises. Intracellular glucose is then metabolized to generate ATP, resulting in an increase in the cytosolic ATP: ADP (Yeom *et al*., 2006) which results in the closure of the K_{ATP} channels, membrane depolarization and initiation of electric activity. The resting membrane potential of about -60mV found in cells arises from the loss of K^+ ions to the extracellular space. In β cells, the dominant K^+ channel is of the Kir6.2 variety that is also found in many other types of cells (Ren *et al*., 2007).

Intracellular Ca^{2+} plays a crucial role in the regulation of glucose-mediated insulin secretion. The depolarization of the plasma membrane (PM) by the closure of the K_{ATP}- channels permits the opening of the L-type voltage dependent Ca^{2+} channels (L-VDCC) which results in an increase in the influx of calcium and an increase in the intracellular Ca^{2+} concentration; this event causes exocytosis of the insulin granules. This ATP sensitive potassium K_{ATP} insulin releasing pathway is referred to as the triggering pathway (Ren *et al*., 2007).

SNARE proteins play a vital role in insulin granule secretion. The granule protein v-SNARE and the β cell PM protein t-SNARE, bring insulin granules in close proximity to the PM and PM Ca^{2+} channels. Glucose excitation leads to the closure of the K_{ATP} channels and the opening of the Ca^{2+} channels. Thereafter, the RRP granules located just beneath the inner mouth of the Ca^{2+} channels become exposed to high levels of Ca^{2+} causing RRP granule release or exocytosis. The release of the RRP granules depends on whether the Ca^{2+} channels are open or closed (Ren *et al*., 2007).

Glucose also affects Ca^{2+} influx through Cdk5. Cdk5 phosphorylates the subunit of L-VDCC which decreases its activity by hindering the binding of L-VDCC to the SNARE proteins. The activity of cyclin dependent kinase 5 (Cdk5) is dependent on glucose. High glucose concentrations inhibit Cdk5 activity which in turn increases the inward whole-cell Ca^{2+} channel current and increases Ca^{2+} influx, resulting in enhanced insulin secretion. Epinephrine inhibits insulin release and may even override glucose-stimulated insulin release (Ren *et al*., 2007).

Thus, glucose triggers insulin secretion and amplification. The amplifying effect of glucose on insulin release is referred to as the augmentative pathway. This pathway does not cause insulin secretion, but enhances Ca^{2+} mediated secretion. The augmentation pathway is independent of K_{ATP} channel inhibition (Ren *et al*., 2007).

Priming or acidification of insulin secretory granules must first occur prior to release of the insulin granules. The priming of an insulin granule depends on the simultaneous process of a V-type H^+-ATPase and ClC-3 Cl^- channels as shown in figure 4.4. The uptake of Cl^- ion establishes the extent of granular acidification as it offers a counter-ion needed to allow continuous H^+ pumping. The ClC-3 Cl^- channels

activity is prevented by high concentrations of ADP. Glucose metabolism results in a decrease of ADP level and an increase in ATP level, resulting in granular acidification. Acidification must first occur before insulin secretion occurs. Insulin granules can undergo exocytosis only after acidification. The exocytosis of granules occurs when Ca^{2+} influx increases to 'exocytotic levels' and therefore amplifying insulin secretion (Ren *et al*., 2007).

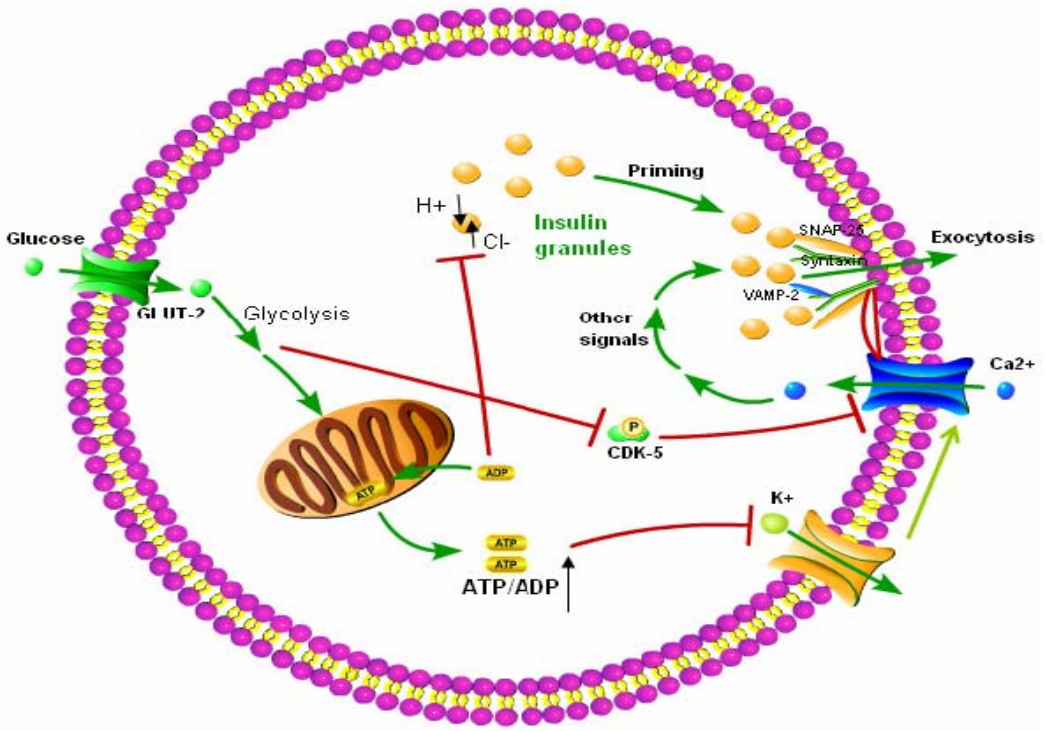

Figure 4.4: Insulin secretion by glucose control. The triggering pathway and the amplifying pathway are the two mechanisms by which glucose metabolism stimulates insulin secretion. (1) GLUT-2 facilitates the entry of glucose into the β cells, where glucose undergoes glycolysis. An increase in the ATP:ADP ratio results due to glucose metabolism, this inhibits the ATP sensitive K_{ATP}-channels, resulting in membrane depolarization, as well as the opening of VDCC, leading to the significant increase in cytosolic calcium, and this triggers exocytosis. When SNAP 25 and syntaxin link with VAMP-2, the docking of the vesicle occurs, this brings the insulin granules in close proximity to the PM and calcium channels. The opening of the calcium channels exposes the RRP granules to high levels of Ca2+, leading to exocytosis of the RRP granule. Inhibition of VDCC occurs when CDK5 phosphorylates the VDCC subunit, although the presence of high glucose concentrations inhibits Cdk5 kinase, resulting in elevated calcium influx and increased insulin secretion. (2) For secretion to occur, the insulin granules in the reserve pool must be acidified. The concurrent operation of the V-type H+-ATPase and ClC-3 Cl- channels is the key factor in the priming or mobilization of the insulin granules. The extent of granular acidification is dependent on Cl- uptake as it provides a counter-ion needed to permit H+ pumping that is continuous. Cl- activity can be inhibited by ADP, although the metabolism of glucose decreases the level of ADP, so that insulin secretion is enhanced due to acidification of insulin secretory granules (Ren *et al*., 2007). Cdk5: cyclin dependent kinase 5 kinase, RRP: readily realisable pool, SNAP-25: synaptosomal associated protein 25, VAMP-2: vesicle associated protein 2, VDCC: voltage dependent calcium channels,

Several plants have been shown to enhance insulin secretion. *Ocimum sanctum* (holy basil) leaf extracts for example stimulates insulin secretion from perfused pancreas, isolated islets and clonal rat pancreatic β-cells (BRIN-BD11 cells glucose-responsive clonal insulin-secreting cell line) (Hannan *et al*., 2006). *Viscum album* (mistle toe) and *Coriandrum sativum* (coriander) have also been documented to stimulate insulin secretion form clonal pancreatic β-cells (Gray and Flatt, 1999).

4.2.2 The effects of glucose on insulin transcription and translation

Glucose controls all aspects of insulin regulation. Glucose is the main physiological regulator of insulin transcription, translational regulation of insulin biosynthesis and insulin secretion. The response of β cells to glucose is complex. The large stores of insulin in granules are found in cells. As previously mentioned, insulin is immediately released from a small proportion of these stores in response to glucose. These stores need to be replenished and the immediate start of insulin biosynthesis ensures this renewal. Glucose-induced insulin biosynthesis is regulated mainly at the translational level. During this duration, glucose metabolism may be coupled to the transcriptional activation of immediate-early response factors. During periods of extended glucose stimulation (more than 12 hours), glucose increases insulin biosynthesis by hastening insulin gene transcription while simultaneously increasing preproinsulin mRNA stability and protein translation (Ren *et al*., 2007).

4.2.2.1 Insulin transcription by glucose control

A large of pool of cytoplasmic insulin mRNA (10-15% of all the β cells' mRNA) is contained in the β cells. At low glucose concentrations large quantities of insulin mRNA are present. The insulin mRNA reservoirs found at low plasma glucose concentrations (less than 3mM) is attributable to basal insulin gene transcription. There is an increase in glucose transcription at higher glucose concentrations. Regulating insulin mRNA synthesis is an intricate process. No single factor completely controls insulin gene expression and transcription continues even when components involved in the stimulus-dependent up-regulation of insulin gene transcription are blocked or even knocked out (Ren *et al*., 2007).

Figure 4.5 shows that there are several factors contributing to glucose-induced insulin transcription, including MafA, PDX-1, a heterodimer which constitutes of E12/E47 and E2/5 and BETA2/Neuro D. A3, C1 and E1 boxes are glucose responsive elements found on the insulin promoter which are also involved in glucose-induced insulin transcription. The activation of these mentioned factors regulate insulin gene transcription. Glucose metabolism in the β cell initiates the regulation of the upstream signalling of these factors. PDX-1 mediates the most vital effects of glucose on insulin translation. Glucose affects PDX-1 function in various ways including (i) a shift in the cellular distribution of PDX-1 from the cytoplasm to the nucleus (ii) increases the potential of the PDX-1 activation domain and (iii) increases PDX-1 binding to A3 (insulin promoter). The effects of glucose on PDX-1 are partly due to phosphorylation of PDX-1 via the activation of PI3-K. PI3-K kinase pathway is considered a central regulator of PDX-1 and of glucose-induced insulin gene transcription. Since PI3-K is a key molecule in the insulin receptor pathway, the activation of insulin gene transcription has been suggested to be a result of a feed forward mechanism involving the binding of secreted insulin to its receptor on the β-cell surface (Ren *et al*., 2007). Glucose and PDX-1 influence histones and this influence also modulates insulin transcription. When glucose levels are low, PDX-1 interacts with histone deacetylases (Hdac-1 and Hdac-2), recruiting them to the insulin gene promoter where they deacetylate histones and thereby down-regulate insulin gene expression (Ren *et al*., 2007).

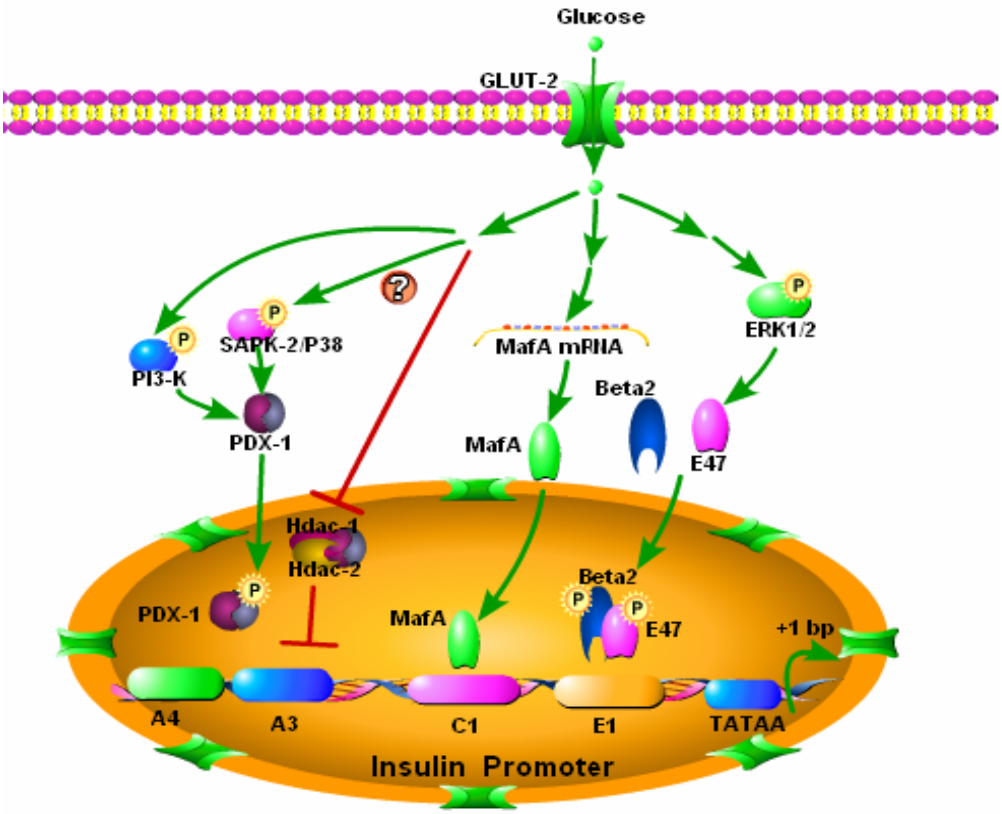

Figure 4.5: Insulin gene transcription is controlled by glucose. For insulin transcription to occur, insulin transcription factors must be activated, the upstream signals of these factors are generated by glucose metabolism in β cells. (1) The translocation of PDX-1 from the cytoplasm to the nucleus, its activation and binding to A3 element is induced by glucose metabolism. This process also involves PI3-K and perhaps SAPK2/P38. Alternatively the route may involve histones and PDX-1. During low glucose levels, histone deacetylases Hdac-1 and Hdac-2 interact with PDX-1. Hdac-1 and Hdac-2 are then recruited to the insulin gene promoter by PDX-1, this induces the down regulation of insulin gene expression by deacetylating histone H4. During high glucose concentrations, the inhibition of insulin gene expression decreases. ERK1/2 is activated by stimulatory glucose concentrations, ERK1/2 enhance BETA2 and E47 heterodimerization as well as their binding to the sites of the E-box. (3) MafA is affected at the mRNA level by glucose. Increased MafA transcription and hence an increase in MafA protein is enhanced by stimulatory glucose concentrations (Ren *et al.*, 2007). ERK: extracellular signal-regulated kinase, PDX-1: pancreas-duodenum homeobox-1, PI-3K: phosphatidylinositol-3-kinase, SAPK-2: stress-activated protein kinase-2.

Prolonged glucose stimulation results in an increase in insulin transcription, which is complementary to the glucose-induced translational control of proinsulin biosynthesis. Under conditions of sustained secretory drive, stimulation of proinsulin gene transcription by glucose appears to be vital for maintaining preproinsulin biosynthesis and hence conserving pancreatic insulin stores (Ren *et al.*, 2007).

4.2.3 Insulin translation by glucose control

When insulin is secreted in response to glucose stimulation, renewed insulin biosynthesis commences immediately to replenish the insulin stores. Insulin biosynthesis is mainly regulated at the translational level after short term (less than 2 hours) glucose stimulation (Ren *et al*., 2007).

The mechanism of how glucose regulates proinsulin synthesis in β cells is unclear. eIF2 is a vital factor in the regulation of protein biosynthesis. The eIF2 factor participates in the formation of translational ternary complex (eIF2-GTP.Met-tRNA) recruiting charged initiator methionyl-tRNA to the 40S ribosomal subunit. This complex assembles only if eIF2 is in its GTP bound state. After the formation of the 80S ribosome, the GTP bound to eIF2 is then hydrolyzed to GDP. The recycling of the inactive eIF2-GDP complex to the active eIF2-GTP is catalyzed by the guanine nucleotide exchange factor, eIF2B. The state of phosphorylation determines the activity of the eIF2 complex. PKR-like ER kinase (PERK) is a vital regulator of insulin translation in β cells. PERK phosphorylates eIF2 complex and hence lowers insulin translation. PERK activity is sensitive to glucose levels, hence PERK signalling is critical to normal β cell function. eIF4F is an initiation complex which initiates 40S ribosome recruitment to mRNA in insulin synthesis. Hypophosphorylated 4E-BPs inhibits eIF4F complex formation, but phosphorylation of 4E-BP1 counters this inhibition and induces an increase in mRNA translation (Ren *et al*., 2007).

In primary islets and pancreatic β cell lines, glucose increases 4E-BP1 phosphorylation, indicating the importance of eIF4F assembly in glucose stimulated protein synthesis (Ren *et al*., 2007).

4.2.4 Other genes and proteins affected by glucose

Delayed long term responses is induced by glucose through inducing the expression of other genes involved in β cell function such as GLUT2, pyruvate kinase and acetyl-coA carboxylase. The expression of these genes is vital so as to meet the elevated metabolic and secretory demands during prolonged or repeated periods of hyperglycemia (Ren *et al*., 2007).

4.2.5 Other factors that stimulate insulin secretion

Incretins (peptides associated with food intake-stimulation of insulin secretion from the pancreas) such as GLP (glucagon-like peptide) and GIP (gastric inhibitory peptide) induce insulin secretion via cAMP signalling (Panunti *et al*., 2004). Certain amino acids; namely alanine, glycine and arginine stimulate insulin secretion.

4.2.6 Insulin secretion stimulated by GLP

GLP-1 (glucagon-like-peptide-1) is an incretin hormone secreted from the L-cells of the small intestine and released by the gastrointestinal system following nutrient ingestion and controls blood glucose through pleiotropic effects on the pancreatic islets, central nervous system, and the gastrointestinal tract. It is a naturally occurring hormone that markedly augments glucose-stimulated insulin secretion through sensitizing the β cell action of glucose. GLP-1 regulates energy intake, gastrointestinal motility, and nutrient disposal. In addition to potentiating insulin release, GLP-1 is involved in the regulation of β cell development, growth and survival (Li *et al*., 2005).

The effects of GLP-1 on the β cell are mediated via the GLP receptor. GLP-1 and GIP attach to G-protein coupled receptors, activating adenylate cyclase to increase cAMP, which activate PKA (protein kinase A). They also act directly on insulin exocytotic machinery through a binding protein called the cAMP sensor (cAMP guanine nucleotide exchange factor II; GEFII) (Panunti *et al*., 2004).

Wang *et al*.(1999) showed that GLP-1 enhanced the expression of PDX-1 in insulinoma cells. In the adult pancreas, PDX-1 regulates genes associated with pancreatic cell differentiation and maturation. These include the insulin, glucokinase, GLUT2 and amyloid precursor protein genes (Perfetti *et al*., 2000). Thus it suffices to state that GLP-1 indirectly stimulates insulin transcription through enhancing PDX-1 transcription.

GLP-1 has also been documented to reduce postprandial and fasting glycaemia in subjects with DM1 and DM2. GLP-1 is quickly degraded in plasma by the enzyme dipeptidyl peptidase IV (DPP IV), resulting in the short circulating half-life of intact GLP-1 of about 1 min (Cheon *et al*., 2005).

In the diabetic state, GLP-1 secretion is impaired but potency is still retained in DM2 (Kim *et al*., 2005). The short half-life of GLP-1 encouraged the development of alternate strategies to exploit the potent antidiabetic activity of GLP-1. One approach is to hinder DPP IV activity (see figure 4.6), thereby prolonging the circulating half-life of endogenous GLP-1. DPP IV/CD26) is an enzyme that is found throughout the body in both plasma and the endothelial lining of several organs, such as the kidney, liver, and intestine. It alters biological levels of several peptide hormones, chemokines and neuropeptides, by specifically cleaving penultimate amino acids of alanine or proline residues, and thereby modulating their activities (Cheon *et al*., 2005). Mentlein *et al.*(1993) established that DPP IV removed the N-terminal dipeptide from GLP-1. It cleaves a number of biologically active peptides, including GLP-1, which is degraded from the active form of GLP-1, i.e., GLP-$1_{7–36}$amide, yielding GLP-$1_{9–36}$amide. GLP-$1_{9–36}$ amide, has been shown to exhibit GLP-1 receptor antagonistic properties. It was demonstrated that glucose tolerance was improved in animals lacking DPP IV following glucose treatment. In addition increased GLP-1 levels and insulin secretions were achieved. It seems that DPP IV directly alters bioactive GLP-1 levels *in vivo*, thus significantly influencing glucose tolerance and insulin secretion. In patients with DM2, intravenous infusion of GLP-1 resulted in the plasma glucose lowering effect. Because it is rapidly eliminated from the circulation, active GLP-1 itself is unsuitable for curing DM2. Therefore, DPP IV inhibition may be a more viable alternative in DM2 treatment, acting instead through the preservation of active GLP-1 levels. Demonstration of the potential use of oral DPP IV inhibitors for the treatment of diabetes has been shown by the results of several inhibitors in clinical trials (Cheon *et al*., 2005).

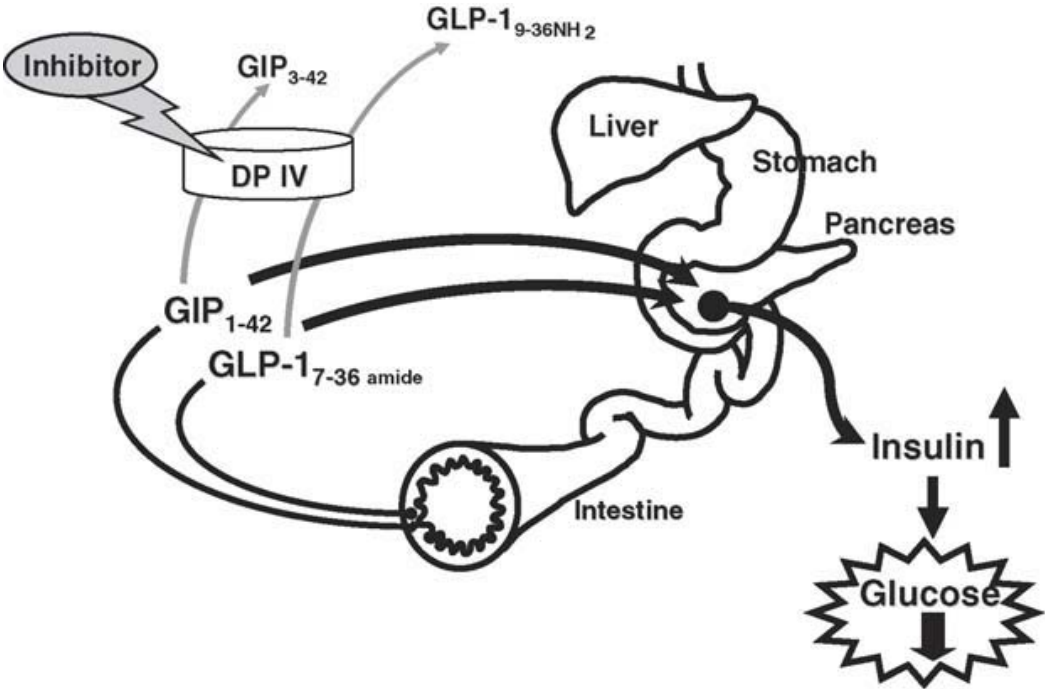

Figure 4.6: Mechanism of action of DPP IV inhibitors. In the DM2 state, DPP IV inhibitors improve glucose tolerance. DPP IV inhibitors have been implicated in suppressing β cell apoptosis. It is by potentiating neurotransmitter-mediating actions and gastric emptying that DDPIV inhibitors suppress appetite, glucagon secretion (McIntosh *et al*., 2006).

The potential side effects of DPP IV inhibition include neurogenic inflammation, increase in blood pressure, enhanced general inflammation, and allergic reactions. The most common side effects of the common DPP IV inhibitor Januvia are upper respiratory tract infection, stuffy/runny nose, sore throat, and headache. However, the effects of longer-term (more than a year) treatment with DPP IV inhibitors are not known. Long-lasting DPP IV inhibitors such as vildagliptin, sitagliptin and saxagliptin all significantly reduce plasma DPP IV activity throughout a 24-h period (Deacon and Holst, 2006).

4.2.7 Insulin secretion stimulated by amino acids.

Alanine, arginine and glycine are the only three amino acids that stimulate insulin secretion. They achieve this via the same fundamental mechanism as glucose. Their entry into the β cell leads to ionic changes that depolarize the β cell, trigger Ca^{2+} uptake and stimulate exocytosis of insulin-containing granules. But the K_{ATP} channel is not involved in this process. Alanine and glycine share a symport that also transports Na^{+} into the β cell (Figure 4.7). The influx of Na^{+} is sufficient to depolarize

the cell, activating the Ca^{2+} channel with ensuing Ca^{2+} uptake and insulin release. An exclusive arginine transport protein is also present in the β cell PM. Arginine is a cation at physiological pH and can directly depolarize the β cell. Arginine, is the strongest insulin secretagogue, measured on a mole for mole basis. It is often used to initiate insulin secretion in the clinical testing of β cell capacity (Gopel *et al*., 2000).

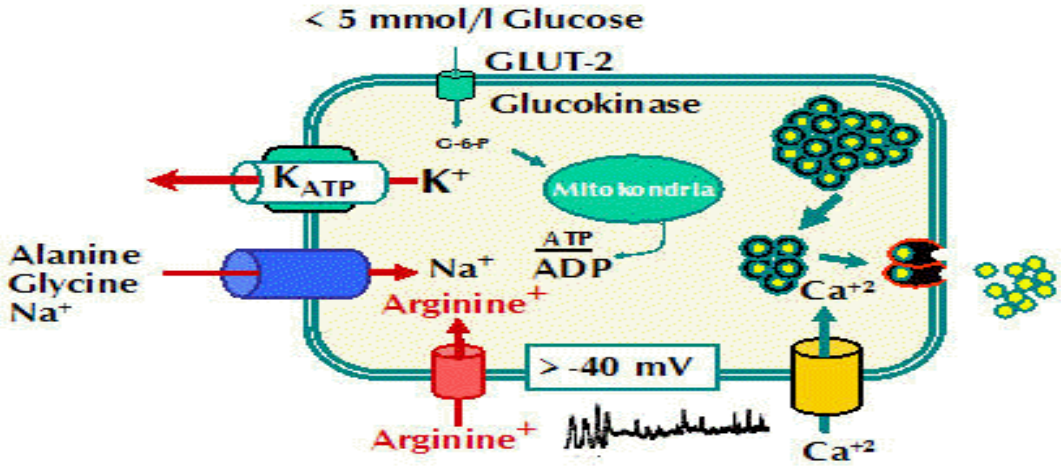

Figure 4.7: Insulin secretion by glycine, alanine. Alanine and glycine share the same symport with Na^+ into the β cells. The Na^+ influx is sufficient to depolarize the cell and activate the Ca2+ channels, with subsequent Ca^{2+} uptake and insulin release (Gopel *et al*., 2000).

4.2.8 Insulin secretion: specific targets by drugs and potential targets for plant A

Thus far, the therapeutic diabetic targets in the pancreas to increase insulin release have been discussed. These targets include; (i) DPP IV inhibitors; so that DPP IV does not break down GLP quickly (ii) increasing GK activity by using GK activators (iii) increasing ATP concentration and or concomitantly decreasing ADP concentration this will in turn activate the ClC-3 Cl^- channels and increase the acidification rate of the insulin granules so that insulin is released faster (iv) closing K_{ATP} channels by increasing the expression/activity of PKA or reducing the concentration of ADP, whilst increasing the concentration of ATP (v) opening Ca^{2+} channels inducing membrane depolarization (Panunti *et al*., 2000).

4.3 Metabolic effects of insulin.

Insulin has vital metabolic effects, such as; (i) stimulating glucose uptake in the muscle and adipose tissues (ii) stimulating glycolysis in the liver, muscle and adipose tissues (iii) stimulating glycogen synthesis in the liver and muscle tissues (iv)

inhibiting glycogenolysis in the liver and muscle tissues (v) stimulating amino acid uptake in the liver and muscle tissues (vi) stimulating protein synthesis in the liver, muscle and adipose tissues (vii) stimulating FA and TAG synthesis in the liver and adipose tissues (viii) inhibiting lipolysis in the liver and adipose tissues.

4.3.1 Carbohydrate metabolism

The overall effect of insulin is to decrease plasma glucose concentration. Insulin achieves this by several ways; (1) Glycogen synthesis; in the muscle and liver, insulin activates glycogen synthase and inactivates glycogen phosphorylation, so that G6P is channelled into glycogen. (2) Inhibition of glycogen breakdown and gluconeogenesis, this primarily occurs in the liver. (3) Promotion of glucose uptake by increasing the number of glucose transporters in the cell membrane, this occurs in the adipose, muscle and other tissues.

4.3.2 Insulin clearance and degradation

What is the biological function of insulin clearance and degradation? It is to remove and inactivate circulating insulin. Hormonal control of metabolism requires delivery and removal of the hormone for cellular regulation. Insulin removal and degradation are regulated processes and abnormalities in insulin clearance are integral to diseases such as type II diabetes (Duckworth *et al*., 1998). Insulin degradation is inextricably linked to insulin action. All insulin sensitive tissues degrade insulin; the first step to insulin degradation is binding to the receptor (similar to insulin action).

Insulin has a short plasma half life of 4-6 minutes, because of the need to respond rapidly to changes in blood glucose (Duckworth *et al*., 1998).

DPP IV is a multifunctional protein expressed on the surface of several cell types including epithelial, endothelial, and lymphoid cells. It is identical to the T cell activation antigen CD26 and the adenosine deaminase binding protein. DPP IV is also released as a soluble form in plasma. As mentioned previously DPP IV is a therapeutic target for type II diabetes due to its role as a serum protease that cleaves incretin hormones of the glucagon family of peptides, thus regulating glucose homeostasis. Studies indicate that a DPP IV inhibitor improves impaired glucose

tolerance (O'Brien, 2006). Moreover, DPP-IV is not only a protease for substrates relevant to energy homeostasis, but it also has a range of additional functions such as its involvement in immunity (Michel *et al*., 2008). Therefore, it is considered to be a moonlighting protein. As a protease, it has several other substrates, and it also acts as a receptor and co-stimulatory protein in the immune system. In this regard, CD26 is considered to be an important regulator of T-cell function. These pleiotropic effects of DPP-IV or CD26 lead to numerous potential uses of its inhibitors other than type 2 diabetes including inflammatory diseases (Michel *et al*., 2008). Monitoring serum levels of DPP IV activity and the inhibition of that activity will be of increasing importance as several potential DPP IV inhibitors move through clinical trials as therapeutics for type II diabetes (O'Brien, 2006).

As previously mentioned DPP IV is a serine protease that cleaves N-terminal dipeptides from polypeptides with L-proline or L-alanine at the penultimate position. This enzyme is a member of the prolyl oligopeptidase (POP) family, a subfamily of serine proteases which includes DPP IV, POP, DPPII, DPPVIII, DPPIX and fibloblast activation protein. The unique property of the POP family is that they are highly selective toward peptides that have a proline residue at the penultimate position (O'Brien, 2006).

4.3.3 Liver and insulin clearance

The liver is the primary site for insulin clearance. About 50% of portal insulin is removed during first pass transit, but this percentage varies widely under different conditions. Hepatic uptake is not a static process; it is influenced by both physiological and pathophysiological factors. Most insulin uptake is receptor mediated hence very high concentrations of insulin (500-2000 μU/ml) result in a decrease in the fractional uptake although total uptake is increased. Prolonged increases in portal insulin levels also result in reduced clearance due to receptor down-regulation. Removal of insulin from the circulation does not imply immediate destruction of the hormone. A considerable amount of receptor-bound insulin is released from the cell and re-enters the circulation (Duckworth *et al*., 1998).

Generally, glucose ingestion increases hepatic insulin uptake. Clearance rates are decreased in obesity, diabetes and liver disease. The reduced hepatic clearance is also associated with reduced insulin sensitivity, supporting the relationship of insulin degradation and insulin action. Clearance rates elevate when hormones such as catecholamine and GH increase (Duckworth *et al*., 1998).

The primary cellular mechanism for hepatic uptake and degradation of insulin is a receptor-mediated process (Figure 4.8). Most hepatic uptake is due to hepatocytes, with Kupfer cells contributing about 15% to the total. Pinocytosis may be a significant factor in hepatocyte insulin uptake at high insulin concentrations. Pinocytosis, a non-receptor-mediated insulin uptake, may also be involved in some insulin actions (Duckworth *et al*., 1998).

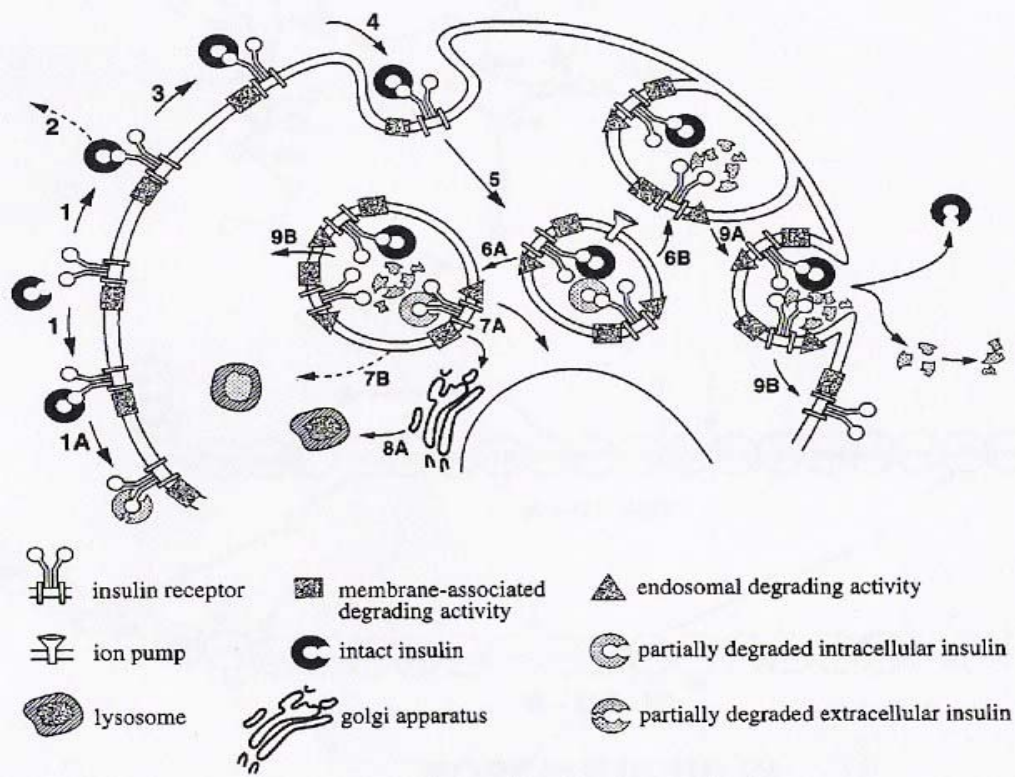

Figure 4.8: **Cellular handling and degradation of insulin model**. **1A; Insulin first binds to its receptor, 2; and then intact insulin is released. 3; Co-localization 'capping' in plasma membrane. 4; Formation of coated pits and then 5; endocytosis. 6; Initiation of insulin degradation; 6A further intracellular processing of insulin and degradation products, 6B; diacytosis of intact insulin and degradation products.7; Distribution of insulin or its degradation products; 7A Cytoplasm, nucleus and Golgi, 7B; lysosomes. 8; Delivery of insulin to lysosomes from organelles other than endosomes 9; Recycling of the insulin receptor; 9A; delivery to the plasma membrane by diacytosis, 9B; return to original function state (Duckworth *et al*., 1998).**

4.3.4 Kidney and insulin clearance

The kidney is the main site of insulin clearance from the systemic circulation, removing about 50% of peripheral insulin. The kidney also removes 50% of circulating proinsulin and 70% of C-peptide by glomerular filtration. Insulin clearance by the kidney occurs by two mechanisms (i) glomerular filtration and (ii) proximal tubular reabsorption and degradation. Glomerular clearance of insulin may occur both by non-specific diffusion and by specific receptor-mediated transport. On entering the tubule lumen, more than 99% of the filtered insulin is reabsorbed by proximal tubule cells, mainly by endocytosis. Little insulin is ultimately excreted in urine. The kidney also clears insulin from the postglomerular, peritubular circulation, also via receptor-mediated processes. In man, about one-third of the total renal clearance is via this route (Duckworth *et al*., 1998).

In contrast to the liver, lysosomes play a larger and earlier role in kidney insulin degradation, with most of the endosomal insulin and partially degraded insulin fragments delivered directly to lysosomes where degradation is completed. Intracellular and endosomal products of insulin degradation in kidney are identical to hepatic products and consistent with the action of IDE (Duckworth *et al*., 1998).

The kidney plays a larger role in insulin clearance in insulin-treated patients with diabetes than in normal subjects. Since insulin administered by subcutaneous injections escapes first-pass removal by the liver, the kidney has increased importance in insulin removal in these patients. Renal patients may reduce insulin requirements considerably and increase the potential for hypoglycaemia in insulin treated patients (Duckworth *et al*., 1998).

4.3.5 Other tissues and insulin clearance

Insulin not cleared by the liver and kidney is eventually removed by other tissues. All insulin-sensitive cells remove and degrade insulin. The muscle plays a significant role in insulin removal after the liver and kidney. Like in other tissues, in the muscle, insulin binds to its receptor, it is internalized and degradation occurs (Duckworth *et al*., 1998).

Adipocytes, fibroblasts, monocytes, lymphocyte, gastrointestinal cells and many other cells take up insulin and degrade the hormone. All cells that contain insulin receptors and internalization mechanisms can degrade insulin. Insulin action in adipocytes correlates better with degradation than with delivery (Duckworth *et al*., 1998).

4.3.6 Degradation

Significant amounts of insulin may be cleared and degraded extracellularly in wounds. This degradation appears to be mainly due to IDE and may play a role in the wound-healing activity of insulin. Insulin degradation ensures that insulin levels are modulated and that blood glucose concentrations do not get dangerously low (Duckworth *et al*., 1998).

4.3.7 Insulin Degrading Enzyme (IDE)

IDE (Figure 11) is a 110 000 mol weight thiol metalloendopeptidase located in cytosol, peroxisomes, endosomes, and on the cell surface, cleaves small proteins of diverse sequence, several of which share a tendency to form-pleated sheet-rich amyloid fibrils, including insulin ,amylin, atrial natriuretic factor, and calcitonin (Farris *et al*., 2004). IDE has multiple cellular functions in addition to degradation, including binding and regulatory functions. Typical IDE is sensitive to chelators. Cellular insulin degradation occurs in a sequential fashion with several identified steps. The initial degradative step occurs in endosomes with two or more cleavages in the B chain. This is followed by reduction of the disulfide bonds by PDI, yielding an intact A chain and several B chain fragments. The insulin fragments are then further cleaved, probably by multiple proteolytic systems, including lysosomes. Intracellular degradation is initiated in endosomes, which contain IDE. Internalized insulin interacts with IDE and monoclonal antibodies to IDE microinjected into cells inhibit cellular insulin degradation. Overexpression of IDE increases the rate of insulin degradation by cells. Insulin degradation is a complex and multicomponent process (Duckworth *et al*., 1998).

IDE requires a sulfhydryl group, perhaps vital for protein conformation rather than for catalytic activity. Insulin has the highest affinity for IDE (K_m = 20 nM), although the

enzyme degrades other substrates such as IGF-II (Insulin like growth factor II), ANP (atrial natriuretic peptide), TAGF-α (transforming growth factor α), amyloid, insulin B chain, oxidized haemoglobin and β-endorphin. Peptides including EGF and IGF-I are hydrolyzed slowly by IDE, making them competitive inhibitors. Noteworthy is that proinsulin intermediates are degraded by IDE proportionally to their insulin-like activities (Duckworth *et al*., 1998).

Although liver, kidney, and muscle are major tissues involved in insulin metabolism, the highest level of rIDE transcripts is in testes, tongue, and brain. The tissue distribution and developmental regulation of rIDE strongly suggest that IDE may have other functions besides degrading insulin, and we should expand our systems used for IDE studies (Kuo *et al*., 1993). There are many other proposed roles of IDE including, regulation of certain cytosolic organelles, specifically proteasomes, androgen and glucocorticoid receptors and possibly peroxisomes (Duckworth *et al*., 1998).

What is the role of IDE in diabetes? In mice, IDE hypofunction induced by IDE gene disruption leads to hyperinsulinemia (Gu *et al*., 2004). The IDE region of chromosome 10q has also been genetically linked to type 2 diabetes mellitus and to fasting glucose levels. In this regard, it was shown that transferring a 3.7-cM chromosomal region containing the IDE gene from an inbred rat model of DM2 to a normoglycemic rat reiterated several features of the diabetic phenotype, including hyperinsulinemia and postprandial hyperglycemia (Farris *et al*., 2004).

The attenuation of IDE activity (by using IDE inhibitors) so that the half life of insulin in the plasma is increased, may be a potential therapeutic target. Plant A may have molecules that inhibit IDE activity or expression and we propose that this may be the reason why plasma insulin levels were high. Hence the quantification of IDE in the rat samples is paramount to investigate this suggestion.

4.4 MATERIALS AND METHODS

To determine whether the increased serum insulin described by Karachi (2009) was due to an increased insulin secretion or due to less insulin degradation experiments were done to determine both.

Increased insulin secretion:

- Quantify plasma C peptide (section 4.4.1)
- Insulin secretion by pancreatic cell line (section 4.4.2)
- Insulin secretion stimulated by GLP (determine DPPIV inhibition (section 4.4.3)

Decreased insulin degradation

- Quantify plasma IDE (section 4.5.1)

4.4.1 C-peptide quantification

In the radioimmunoassay (RIA) protocol, a known concentration of labelled tracer antigen is incubated with a constant dilution of antiserum so that the concentration of the antigen binding sites on the antibody is limited. If unlabeled antigen is added to this reaction, there is competition between labelled tracer and unlabeled antigen for the limited and constant number of binding sites on the antibody. Therefore, as the concentration of the unlabeled antigen increases, the amount of tracer bound to antibody decreases. This is measured after separating antibody-bound from free tracer and counting either one or the other or both fractions. A standard curve is set up with increasing concentrations of standard unlabeled antigen and the amount of antigen in unknown samples is calculated from this standard curve. The four major components of the RIA reaction are (i) a specific antiserum to the antigen to be measured (ii) the availability of a radioactive labelled form of the antigen (iii) a method to separate antibody bound tracer from bound tracer (iv) an instrument to count radioactivity; in this study a liquid scintillation counter was used (Linco Research, 2008).

C-peptide was quantified in rat plasma samples using the rat C-peptide RIA kit from LINCO Research (RCP-21K) according to the manufacturer's instructions. In brief, on day one, 100 µl of assay buffer was added to marked eppendorf tubes, except the controls that contain

(i) total count tubes – 100 µl of rat c-peptide antibody and no assay buffer

(ii) non specific binding tubes- no standard (purified recombinant rat C-peptide) + no rat C-peptide antibody (300 µl assay buffer) and
(iii) reference tubes- no standard but with 100 µl of rat C-peptide antibody (200 µl assay buffer).
100 µl of unknown sample or standard or quality control sample was added to the respective eppendorf tubes. On day two, 100 µl of rat C-peptide antibody was added to all tubes except the control tubes (ii). Each assay included (in duplicate), a standard curve with purified recombinant rat C-peptide concentrations ranging from 25-1600 pM, three controls as mentioned above and quality control 1 and quality control 2. The samples were thereafter vortexed, covered and incubated for 22 hours at 4°C. 100 µl of I^{-125} rat C-peptide tracer was added to all the samples. The samples were again vortexed, covered and incubated for 24 hours at 4°C. On day three, 1 ml of precipitating reagent (goat anti-guinea pig IgG serum) was added to all tubes except the control tubes. The samples were then incubated for 20 min at 4°C, centrifuged at 3000 x g for 20 min at 4°C. The supernatant was then decanted carefully so as not to dislodge the pellet. 1 ml of liquid scintillation cocktail (Perkin Elmer Life Analytical sciences-6013327) was added to each tube. Each pellet was re-suspended in 1ml of scintillation liquid and counted using a liquid scintillation analyzer for 15 minutes/tube.

4.4.2 INS-1 cell culturing

INS-1 cell line is a rat insulinoma cell line isolated from rat pancreatic islets. INS-1 cells are used in β cell biology studies. Although the cell line is dedifferentiated, it shares vital characteristics akin to normal β cells. INS-1 cells synthesize and release insulin in a glucose responsive manner (Huotari *et al*., 1998); hence the motivation of using INS-1 cells in this study is to determine the effect of plant A on insulin release in INS-1 cells. Cells were maintained with INS-1 media consisting of 1x RPMI 1640+Glutamax (Gibco Invitrogen, USA), 10% Fetal bovine serum (FBS), 100 mM sodium pyruvate (Gibco Invitrogen, USA), 1 M HEPES in 0.85% NaCl (BioWhittaker, USA), 50 µl 2-mercaptoethanol (50 mM) (Gibco Invitrogen, USA). Cells were maintained in sterile 100 x 20 mm tissue culture dishes (Greiner bio-one, Germany) at 37°C in an atmosphere of 5% CO_2 using a direct heat incubator (Thermo Forma, USA). Cells were seeded into 96 well plates at a density of 3 x 10^5 cells/well

for insulin quantification, cytotoxicity and proliferation studies. Passage numbers between 60 and 100 were used for the experiments.

4.4.2.1 Plant cytotoxicity studies in INS-1 cells

The importance of testing the toxicity of the plant is to ensure that the results obtained from the insulin secretion study is not as a result of cell death induced by plant toxicity. The assay used to determine cell cytotoxicity is the MTT (3-(4,5-Dimethylthiazol-2-yl)-2,5-diphenyltetrazolium bromide) assay. MTT is yellow in colour and is a water soluble dye that is reduced by metabolically active cells (but not dead cells) to a purple formazan product that is insoluble in aqueous solutions. Hence DMSO is used to solubilise the purple formazan crystals (Freshney, 1994) before determining the absorbance spectrophotometrically at 570 nm.

1 mg of plant A was weighed and suspended in 2.5% DMSO in INS-1 media, a final concentration of 1 mg/ml of plant A was prepared. 1 mg/ml of Plant A was then vortexed for 1 min and sonicated for 15 min before the following dilutions were made; 0.0025 mg/ml, 0.00625 mg/ml, 0.0125 mg/ml, 0.025 mg/ml, 0.05 mg/ml, 0.1 mg/ml and 0.2 mg/ml these dilutions were used to treat the INS-1 cells. Cells were seeded at density of 3 x 10^5 cells/well in a 96 well microtiter plate for 24 hours. The control wells were treated with 2.5% DMSO made up in INS-1 media. Each assigned well was treated with its respective plant A concentration and incubated for 48 hours. Thereafter, all media/treatment was removed from the wells. A stock solution of 5 mg/ml MTT in PBS was made and a 10 X dilution of this stock solution was made up in fresh media (hence 0.5 mg/ml MTT). 200 µl of 0.05mg/ml MTT was added to all treated wells and incubated at 37°C for 3 hours, all the media was aspirated. 200 µl of DMSO was added to all the wells and the absorbance was read at 570 nm in a microtiter plate reader (Holst-Hansen and Brunner, 1998). The experiment was conducted in triplicate. The results were expressed as a percentage of the control.

4.4.2.2 Insulin secretion by INS-1 cells

INS-1 cells were treated with varying glucose concentrations to determine the optimal glucose concentration to induce the maximum insulin secretion. Cells were seeded at

a density of 3 x 10^4 cells/well in a 96 well microtiter plate and were incubated at 37°C for 48 hours in a direct heat incubator (Thermo Forma, USA). Each well was washed once with 50 µl Krebs-Ringer-bicarbonate-HEPES buffer (KRB) consisting of 118.4 mM NaCl, 4.75 mM KCl, 1.192 mM MgSO4, 2.54mM $CaCl_2$, 10 mM HEPES, 2 mM NaHCO3, 0.1% BSA (Janjic *et al*., 1999) at pH 7.4. All the media was removed from the wells and the cells were exposed to 50 µl pre-incubation KRB media for 30 min at 37°C. KRB was also used as a diluent for glucose, glibenclamide and plant A. Thereafter assigned wells were treated with 100 µl of their respective treatment; media (untreated control) or glucose, 1 µM glibenclamide (Zydus Cadila, India) or plant A and incubated for 10 min respectively at 37°C. Glibenclamide was used as a positive control. The supernatant from each well was collected after 10 min had elapsed and stored at -20°C until required for insulin determination by the RIA (Wilson, 2006). Total insulin content was determined in the INS-1 cells by adding 100 µl of 0.18 M HCl in 70% ethanol to the cells in the plate and covering the plate with a plate sealer to avoid evaporation. The plate was incubated overnight and stored at -20°C until required for insulin determination. Assay buffer from the RIA kit (Linco, USA) was used as the diluant for the sample dilutions required in the experiments.

4.4.3 DPP IV quantification

The substrate Gly-Pro-*p*-nitroanilide was used to measure DPP IV activity. DPP IV has post-proline dipeptidyl aminopeptidase activity that hydrolyzes N-terminal dipeptides from the unsubstituted N-terminus of peptides with the sequence of X-Pro-Z and X-Ala-Z, figure 4.9 below shows the reaction.

$$\text{Gly-Pro-}p\text{-nitroanilide} \xrightarrow{\text{DPP IV}} \text{Gly-Pro} + p\text{-nitroaniline}$$

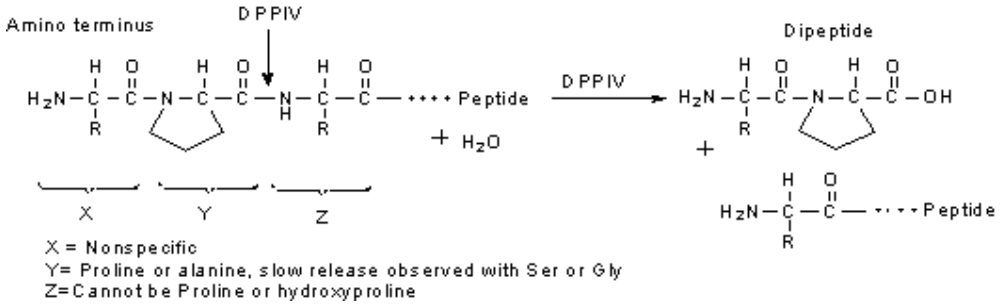

Figure 4.9: DPP IV has post-proline dipeptidyl aminopeptidase activity that hydrolyzes N-terminal dipeptides from the unsubstituted N-terminus of peptides with the sequence of X-Pro-Z and X-Ala-Z (Sigma, 2008).

4.4.3.1 CaCo-2 cell culturing and DPP IV activity

CaCo-2 cells are human carcinoma colon cells that provide a rich source of membrane bound DPP IV. CaCo-2 cells were cultured in RPMI media with 10% Fetal calf serum and grown in an atmosphere of 5% CO_2 at 37°C using a direct heat incubator (Thermo Forma, USA). Cells from passage number 21 were grown in 100 x 20 mm tissue culture dishes (Greiner bio-one, Germany). Medium was changed every two days until confluence (5 days) was reached. Thereafter media was changed everyday after confluence. Cells were harvested 14 days past confluence. On the harvesting day, the cells were washed with PBS and solubilised in a harvesting solution (10mM NaCl, 50mM Tris-HCl, 0.5% NP-40, 0.3 µg aprotinin-pH 8.0), 2ml of harvesting solution per plate. The cells were centrifuged at 10000 x g for 30 minutes at 4°C. The supernatant which contains the enzyme was assayed. An assay buffer (50mM Tris-HCl, 0.05 % Triton X-100-pH 8.0) was used to dilute the supernatant. 10 µl of plant extract and 10 µl of metformin (5 mM) were added to designated wells respectively in a 96 well microtiter plate. 90 µl enzyme was added to all the wells. 10 µl of substrate (19.4 mM gly-pro-pNA) in assay buffer was added to all wells. The plate was then incubated for 5 min at 37°C and the absorbance was read at 410 nm using a spectrophotometer for 20 min to obtain progress curves.

4.4.3.2 Determination of DPP IV activity in rat serum samples

Plant A may need to be metabolized in order to be inhibit DPP IV activity, hence the necessity in determining DPP IV activity in the serum samples of plant A treated rats. Hence the importance of determining DPP IV activity in the plant treated and

untreated samples. Metformin was used as positive control as Metformin has been implicated in decreasing DPP IV activity (Mannucci *et al*., 2001).

90 µl of plasma was added to the 96 well microtiter plate. The reaction was initiated by adding 10 µl of 19.4 mM Gly-Pro-*p*-nitroaniline (Gly-Pro-*p*NA) to all wells. The plate was then incubated for 5 min at 37°C and the absorbance was read at 410 nm using a spectrophotometer for 20 min to obtain progress curves.

4.4.4 Rat skeletal muscle IDE quantification

Quantification of IDE was performed with a Calbiochem Innozyme Insulysin/IDE Immunocapture Activity Assay kit (Calbiochem, USA). The kit uses an affinity purified polyclonal antibody that recognizes human, mouse and rat IDE immobilised on a 96 microtiter well plate to capture the enzyme. A FRET substrate, Mca-GGFLRKHGQ-EDDnp measures the activity of captured IDE. The fluorophore is released from the quenching molecule Dnp once the cleavage of the scissile amid bond between R and K is released. This results in an increase in fluorescence. The increase in fluorescence is measured using an excitation wavelength of 320 nm and an emission wavelength of 405 nm (Calbiochem instruction manual).

IDE was extracted from frozen rat muscle and spleen samples. 0.2 g tissue was homogenized in 1 ml homogenization buffer (50 mM HEPES, 10% glycerol, 1 % Triton X-100, 0.05 ml/g protease inhibitor cocktail-pH 7.5). The homogenate was then centrifuged at 10000 x g for 10 min at 4°C. The protein content in the supernatant was quantified using BCA assay. After confirming that the protein content was greater than 5 mg/mL, the IDE in the supernatant was assayed.

The method was adhered to as per the manufacturer's instructions. Briefly, the desired number of strips from the 96 well plate were removed. The strips were washed by pipetting 350 µl of sample buffer (1X) into each well. The contents were then emptied into the sink. The strips were washed once more to make a total of two washes. After the final wash, the plate was tapped gently on to paper towels to remove excess sample buffer (1X). 100 µl of control and undiluted samples were added to the assigned wells. A plate sealer was then used to cover the plate and the plate was

incubated for 1 hour at room temperature with gentle shaking. 350 µl sample buffer (1X) was added to each well so as to wash the plate. After washing, the contents were discarded. Thereafter the plate was gently tapped on to a paper towel to remove residual liquid. The plate was washed for a total of 5 washes. 100 µl substrate (1X) was added to the plate. The plate was then covered with a plate sealer and foil (to protect from light) and incubated for 3 hours at 37°C. The fluorescence was read at an excitation wavelength of 320 nm and an emission wavelength of 405 nm.

4.5 RESULTS AND DISCUSSION

4.5.1 Effect of plant A on C-peptide concentration in rat plasma

Figure 4.10 shows the C-peptide concentration in rat plasma samples determined using a radioimmunoassay kit. Figure 4.10 indicates that firstly, plant A treated rats were observed to have significantly higher C-peptide (2.3 ± 1.07 nM) concentrations when compared to normal non-insulin resistant (1.22 ± 0.3 nM). Plant A treated rats were observed to have higher C-peptide concentrations however not significant compared to insulin resistant (1.55 ± 0.47 nM) rats. Secondly, plant A treated rats had higher insulin (0.75 ± 0.33 nM) concentrations when compared to normal (0.11 ± 0.05 ng/ml) and insulin resistant (0.17 ± 0.1 nM) rats. Thirdly, the plasma samples from the normal rats had a lower (1.22 ± 0.3 nM) concentration of C-peptide compared to the plasma samples of the insulin resistant (1.55 ± 0.47 nM) rats. The trend in C-peptide levels between the different groups correlate with the insulin levels obtained from a previous study (Karachi, 2009), who found low insulin values (Table 1.1) in CCL (normal) rat samples compared to the CCH and plant A treated rats. In this study low C-peptide values in CCL rat samples compared to CCH and plant A treated rats were obtained. In that study, plant A treated rats were observed to have higher insulin concentrations when compared to normal (CCL) and insulin resistant (CCH) rats respectively (Karachi, 2009). In addition, plasma samples from the normal rats had a lower concentration of insulin compared to the plasma samples of the insulin resistant rats. As previously, C-peptide level has been interpreted as an indicator of insulin secretion because it is co-secreted on an equimolar basis with insulin from the β-cell and is not extracted or metabolized by the liver (Chen *et al*., 2003). To overcome insulin resistance, the β cells of an insulin resistant subject produce more insulin, this explains the high C-peptide concentrations in the insulin resistant rats induced by a high fat diet obtained in figure 4.10. The markedly higher C-peptide levels obtained from the rats treated with plant A, suggests that the plant may stimulate insulin secretion.

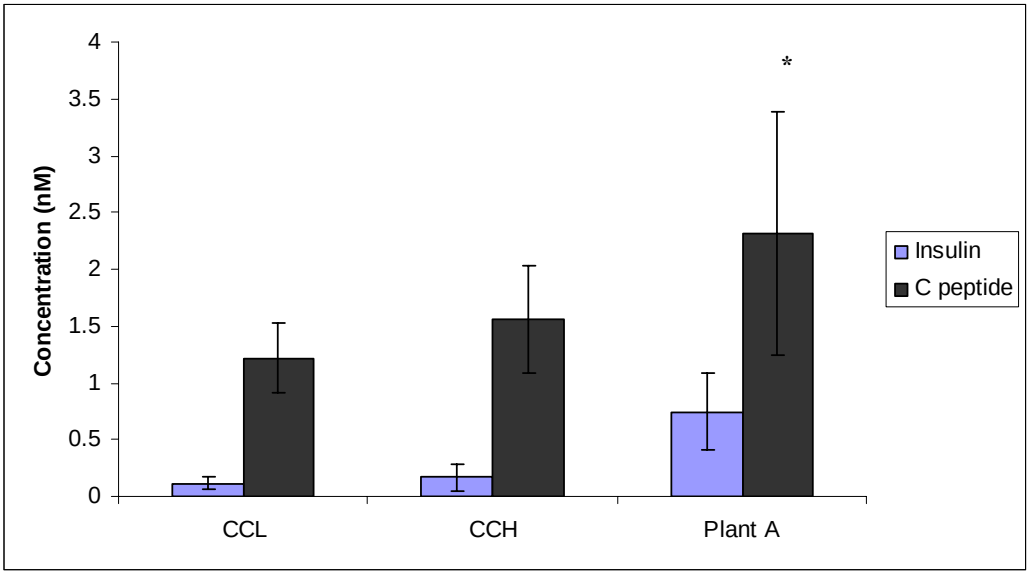

Figure 4.10: C-peptide concentration in rat plasma samples. The rat plasma was snap frozen at -80°C. Each value represents means ± S.D (n=6). CCL represents low fat fed rat controls and CCH represents of high fat fed rat control, both groups were treated with water for 28 days. Plant A represent HF fed rats that were treated with plant A for 28 days. * is $p \leq 0.05$ when plant A was compared to CCL. The insulin concentrations were determined in rat plasma samples by Karachi 2009, in a previous study.

It is evident from figure 4.10 that C-peptide levels for each particular sample compared to the insulin levels of the same samples are higher. This can be attributed to the fact that C-peptide has a longer half life than insulin. According to Hills and Brunskill (2008) C-peptide *in vitro* seems more potent on a molar basis than insulin. Characteristically C-peptide signalling effects are apparent at mid-high pM concentrations, maximal at ~1–5 nM and thereafter decline. In contrast, insulin responses generally become evident at ~10 nM increasing up to 100–1000 nM where they plateau (Hills and Brunskill, 2008).

C-peptide is not an inert peptide as previously mentioned, it exerts critical physiological effects. C-peptide binds to cell membranes, stimulates the Na,K-ATPase and the endothelial nitric oxide (NO) synthase. Furthermore, there is evidence that C-peptide decreases glomerular hyperfiltration and increases glucose utilisation. A main proportion of the C-peptide stimulation of glucose utilisation is mediated by nitric oxide. C-terminal fragments, but not fragments from the middle segment of C-peptide, are as effective as the full-length peptide in stimulating whole-body glucose turnover in streptozotocin-induced diabetes rats (Wilhem *et al*., 2008).

Zierath *et al*. (1991) demonstrated that physiological concentrations of human C-peptide increased glucose transport in human skeletal muscle in a dose-dependent fashion. They further demonstrated that C-peptide partly shares a common pathway with insulin in stimulating skeletal muscle glucose transportation as simultaneous exposure of maximal concentrations of insulin and C-peptide did not result in an additive effect of 3-o-methylglucose transport. C-peptide did not alter the binding of insulin to the insulin receptor. C-peptide stimulates glucose transport by a mechanism independent of the insulin receptor and tyrosine kinase activity and in contrast to insulin, catecholamines did not reveal a counter-regulatory effect on the C-peptide mediated glucose transport. *In vitro* studies with isolated mouse muscle showed that C-peptide did not stimulate glycogen synthesis in isolated mouse muscle (Wilhem *et al*., 2008).

It was demonstrated in 1983 that in alloxan-treated rats, supra-physiological concentrations of C-peptide increased and prolonged the hypoglygemic effect of exogenous insulin on whole body glucose uptake (Zierath *et al*., 1991).

4.5.2 Studies with INS-1 cells

4.5.2.1 Plant A cytotoxicity on INS-1 cells

It was vital to determine at which concentration if at all plant A was toxic to the cells, so as to attribute insulin obtained from the media to insulin secretion by INS-1 cells and not from β cell death of the INS-1 cells. Figure 4.11 shows the cytotoxic effect of plant A on INS-1 cells. The general rule is that a plant concentration causing less than 80% cell survival when compared to the control is too toxic to the cells.

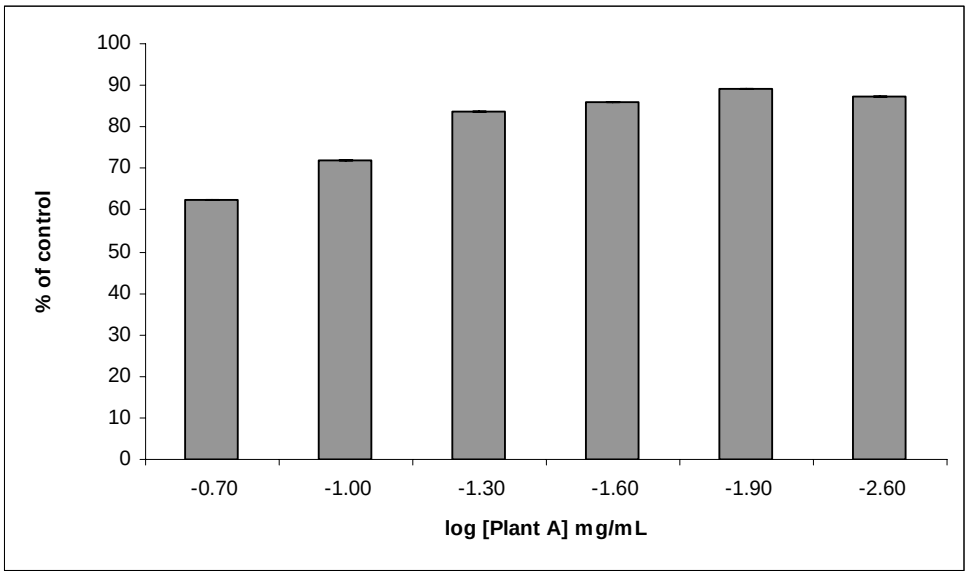

Figure 4.11: **Plant A cytotoxicity study on INS-1 cells using the MTT assay. Cells were seeded in a 96 well microtiter plate at a density of 3 x 10^4 cells/well and incubated for a 24-h period. The cells were treated with plant A extract and incubated for a 48-h period. Plant A concentrations ranged between 0.0025 and 0.2 mg/ml. Data points represent the mean ± SD (n=3) from a single experiment.**

4.5.2.2 The effect of glucose and plant A on INS-1 secretion

The glucose sensitive insulin secreting INS-1 rat insulinoma cell line is widely used as a satisfactory model system for studying the regulation of insulin secretion (Fulceri *et al*., 2000).

Impaired glucose intolerance (during insulin resistance) is accompanied with a decrease in acute insulin secretory response and a decrease in insulin stimulated glucose disposal (Weyer *et al*., 1999).The ideal plant would be able to reverse this decline in acute insulin secretory response. Post-prandial hyperglycaemia is caused by this first phase insulin response (see figure 4.3 showing biphasic phase of insulin) (Panunti *et al*., 2004). Figure 4.12 shows the effects of varying treatments on insulin secretion by INS-1 cells under acute conditions in 10 minutes.

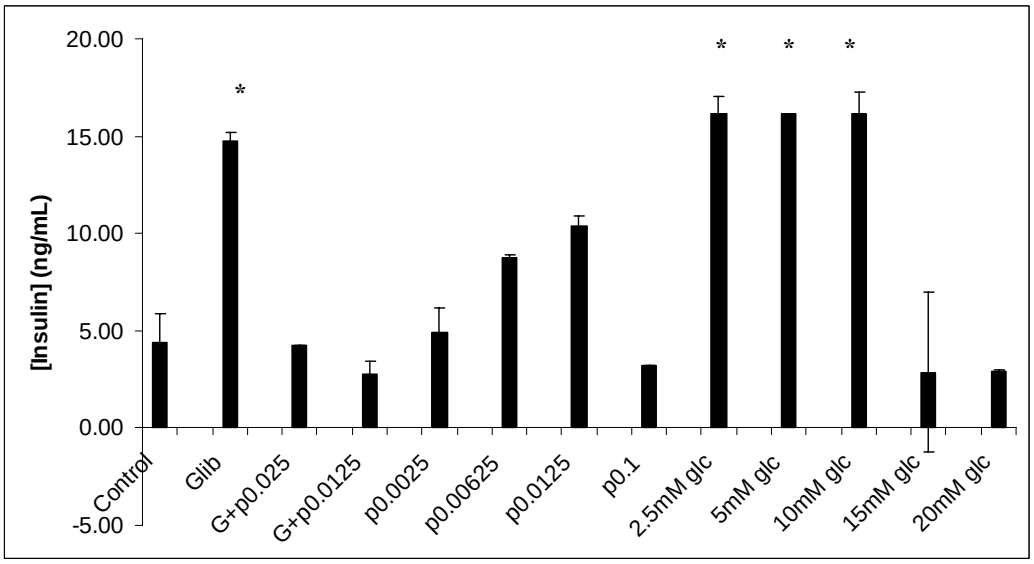

Figure 4.12: **Effect of varying plant and glucose concentrations and 1 µM glibenclamide plus plant on insulin secretion by INS-1 cells after 10 minutes of stimulation under basal conditions. A RIA kit was used to determine insulin using scintillation counting. Cells were seeded in a 96 well plate at a density of 3 x 10^5 cells/well and incubated for a 24-h period. The control represents INS-1 media. Glib represents 1 µM glibenclamide, G+P represents 1 µM glibenclamide and plant treatment in mg/mL. Plant concentrations are denoted as p in mg/mL. Glc represents glucose. Insulin concentration was determined using a RIA kit. Each value represents means ± SD (n=3) of insulin (ng/mL) in duplicate per experiment. * p<0.05 when compared to the control. The experiment was performed 3 independent times with similar results.**

Glibenclamide, a sulphonylurea, was used as a positive control. According to Gibbon (2005), glibenclamide is a type II diabetes drug with a T_{max} of 4 hours and a $T_{1/2}$ of 10 hours. The duration of its action is 24 hours. A low initial dose of 1.25 mg daily is

recommended. The drug is metabolised in the liver to weakly active metabolites and removed equally through biliary and renal routes (Gibbon, 2005). When INS-1 cells were treated with 1 μM glibenclamide 14.75 ± 0.41 ng/mL of insulin was secreted. The motivation of treating the INS-1 cells with a glibenclamide and plant A combination is so as to determine whether a combination therapy has a synergistic effect on insulin secretion in the INS-1 cells, as often people use medicinal plant and conventional drugs during treatment. The effect of 1 μM glibenclamide combined with 0.025 mg/mL plant A slightly increased insulin secretion when compared to the control, however not significantly. The effect of 1 μM glibenclamide combined with 0.0125 mg/mL plant A slightly decreased insulin secretion when compared to the control, however not significantly. It is concluded that there is no synergistic effect on insulin secretion when glibenclamide is combined with plant A treatment. Therapies to overcome defects in insulin secretion include sulfonylurea (SU) and non sulfonylurea secretagogues. The SU drugs bind to a specific SU receptor on the pancreatic β cell (see figure 4.13). This closes the K_{ATP} channels and helps cell membrane depolarization and calcium entry (Panunti *et al*., 2004). The whole channel consists of a core of four Kir6.2 subunits surrounded by four SUR1 subunits. The SUR1 complex acts as a regulator of the K^+ channel, binding ATP as well as SU compounds (Gopel *et al*., 2000).

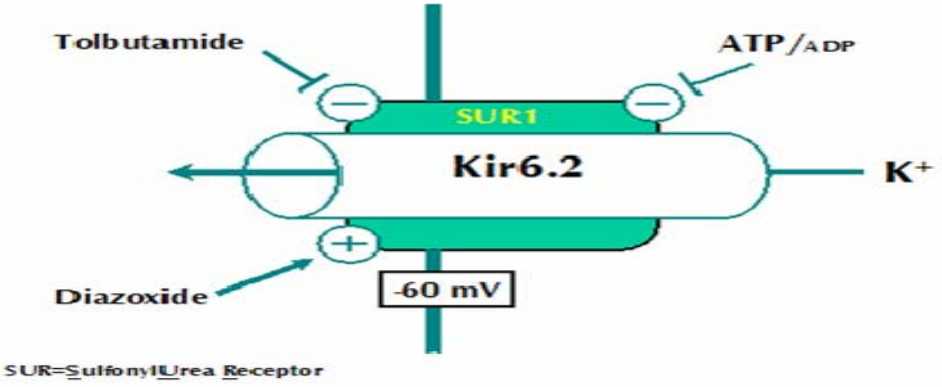

Figure 4.13: **K_{ATP} Channel in pancreatic cells. Tolbutamide is a SU compound used to treat DM2. Diazoxide stimulates the K_{ATP} channel and promotes K^+ efflux, membrane polarization and inhibition of insulin secretion (Gopel *et al*., 2000).**

ATP and tolbutamide have inhibitory actions on the K_{ATP} channel; hence they inhibit K^+ efflux. This results in depolarization of the β cell, Ca^{2+} influx and insulin secretion. Interestingly, there is evidence that SU's trigger β cell apoptosis, since

prolonged exposure of β cell lines and islets to the SU's; glibenclamide and tolbutamide induced apoptotic β cell death (Maedler and Donath, 2004). It was suggested that the process is Ca^{2+} dependent, because blocking the voltage-gated L-type Ca^{2+} channel or opening K_{ATP} channels using diazoxide blocked glucose-and tolbutamide- induced Ca^{2+} concentration increase and inhibited apoptosis (Maedler and Donath, 2004).

The plant A concentrations of 0.0025 mg/mL, 0.00625 mg/mL and 0.0125 mg/mL, increased insulin secretion by the INS-1 cells at basal levels although not significantly to 4.92 ± 1.27 ng/mL, 8.75 0.16 ng/mL, 10.39 ± 0.48 ng/mL respectively when compared to the control. An increase in plant A concentration from 0.0025 mg/mL to 0.0125 mg/mL stimulated an increase in insulin secretion by the INS-1 cells, although significant a difference to the control was not observed upon plant A treatment. Interestingly, 0.1 mg/mL stimulated low insulin secretion to 3.23 ± 0.001 ng/mL although not significantly when compared to control and the other plant A concentrations tested. It is speculated that 0.1 mg/mL is toxic to the INS-1 cells.

INS-1 cells secrete insulin in a glucose dependent way (Hugl and Merger, 2007). Thus it was expected for the INS-1 cells to secrete more insulin with response to increasing glucose concentrations (from 2 – 10 mM). However as observed in figure 4.12, insulin was not secreted by the INS-1 cells in response to increasing glucose concentrations. The most insulin (16.14 ± 0.87 ng/mL) secreted by the INS-1 cells was stimulated by 2.5 mM glucose and 5 mM glucose. These results vastly contrast those found by Wilson (2006) Department of Biochemistry and Microbiology NMMU, with another batch of cells. They found that 10 mM glucose stimulated more insulin secretion (42 ng/mL of insulin) by INS-1 cells than 2 mM glucose (17 ng/mL of insulin) (Wilson, 2006). In this study, using a different batch of INS-1 cells from Wilson (2006) 2.5 mM glucose induced the INS-1 cells to secrete 16 ng/mL of insulin per well of cells. A factor that may contribute to the anomalous data is that there was a variation in the number of cells/well. Inevitably a lower number of cells will contribute to less amount of insulin reported irrespective of treatment. Thus in future the number of cells should be incorporated in calculating insulin concentration.

Pancreatic cells assist in maintaining physiological glucose concentrations (5 mmol/L glucose) by producing more insulin. The INS-1 cells used (in this study) may produce the same amount of insulin irrespective of prevailing glucose concentrations during acute conditions and hence do not respond to prevailing glucose concentrations, if the seeding factor were ruled out. Fulceri stated that the limitations of using INS-1 cells as a model include; (i) possible loss of the glucose responsiveness in INS-1 cells during culturing and (ii) limited capacity in response to glucose during acute challenge (Fulceri *et al*., 2000).

The least insulin was secreted when stimulated by 15 and 20 mM glucose; 2.85 ± 4.11 and 2.9 ± 0.11 ng/mL respectively. Glucotoxicity may have occurred in INS-1 cells treated with very high glucose concentrations of 15 mM and 20 mM glucose. More insulin was secreted when stimulated by 2.5 mM glucose than at 20 mM glucose. Hence more insulin was secreted at lower glucose concentrations than at higher glucose concentrations.

Pertaining to the issue of glucotoxicity in INS-1 cells, rat and human islets have a difference in glucose sensitivity. In rat islets, an increase in glucose concentration to 11 mM promotes β cell survival. In contrast to rat islets, human islets show a dose-dependent increase in proliferation when islets are chronically exposed to increasing glucose concentrations from 5.5 to 33 mM (Maedler and Donath, 2004).

Insulin secretion and insulin releasing effects of other secretagogues in pancreatic β cells is controlled by changes in blood glucose levels. Increases in blood glucose levels also control insulin gene transcription by modulating the function of three β cell specific transcription factors; PDX-1, MafA and NeuroD1. Defects in these mentioned transcription factors have been associated with decreased insulin secretion and hyperglycemia (Muniappan and Ozcan, 2007).

4.5.2.3 The effect of plant A on total insulin content

Insulin content is a reflection of insulin stores in the β cells (Ling *et al*., 2006). The effect of various treatments on insulin content is indicated in figure 4.14. 1 μM glibenclamide (3.49 ± 0.24 ng/mL) slightly but not significantly increased the total

insulin content when compared to the effect of control (2.8 ± 0.47 ng/mL). The effect of 1 μM glibenclamide combined with 0.025 mg/mL plant A increased the total insulin content (3.4 ± 0.2 ng/mL) but not significantly when compared to the effect of the control.

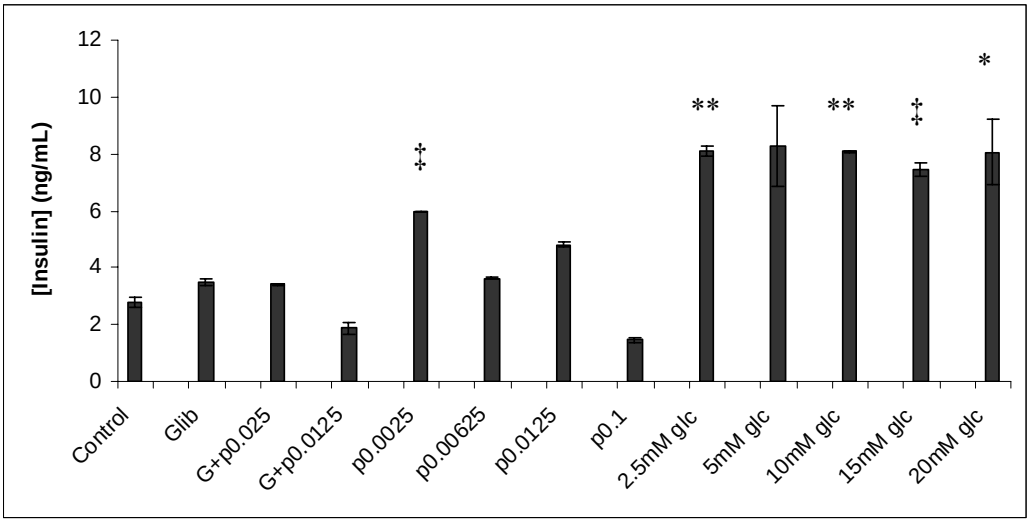

Figure 4.14: Effect of varying plant concentrations glucose on total insulin content in INS-1 cells. G+P represents 1 μM glibenclamide and plant treatment in mg/mL. Plant concentrations are denoted as p in mg/mL. Glc represents glucose. A RIA kit was used to determine insulin concentration using scintillation counting. The control represents INS-1 media. Glib represents 1 μM glibenclamide. Each value represents means ± SD (n=3) of a duplicate. **P<0.005, ‡P<0.02, *P<0.05 when compared to the control. The experiment was performed 3 independent times with similar results.

The effect of 1 μM glibenclamide combined with 0.0125 mg/mL plant A decreased the total insulin content (1.87 ± 0.95 ng/mL) but not significantly when compared to the effect of the control. The effect of 0.0025 mg/mL plant A significantly increased insulin content when compared to the control as indicated in figure 4.14. The effect of 0.00625 mg/mL and 0.0125 mg/mL plant A increased insulin content to 3.63 ± 0.02 ng/mL and 4.81 ± 1.12 ng/mL respectively, however not significantly when compared to the control. 0.1 mg/mL of plant A (1.46 ± 0.98 ng/mL) decreases insulin content as this concentration is cytotoxic to the INS-1 cells.

There is a significant increase in insulin content on treatment with 2.5 mM glucose (8.09 ± 0.18 ng/mL), 5 mM glucose (8.27 ± 1.43 ng/mL), 10 mM glucose (8.07 ± 0.02 ng/mL), 15 mM glucose (7.44 ± 0.22 ng/mL) and 20 mM glucose (8.07 ± 1.18 ng/mL) when compared to the control. Chronic treatment of INS-1 cells with high glucose levels or glucotoxic levels induces a deficiency in the late stages of insulin

exocytosis, therefore reducing insulin content as well as reducing glucose stimulated insulin secretion (Dubois *et al*., 2007). Glucose is known to stimulate insulin transcription and hence the high total insulin content data obtained from treating the INS-1 cells with glucose. The lower total insulin content obtained from treatment of glibenclamide can be attributed to the fact that glibenclamide does not stimulate insulin transcription.

4.5.2.4 The effect of plant A, diazoxide and verapamil on insulin secretion in INS-1 cells

Diazoxide is a K_{ATP} channel opener, therefore the drug inhibits insulin secretion (Hannan *et al*., 2006). The effect of diazoxide in the presence of plant A extract was determined. The motivation of testing plant A and diazoxide was to establish whether these conditions inhibit the insulin-releasing effects of plant A extract, if this was so then the closure of K_{ATP} channels participates in overall mechanism of plant A action. Verapamil is a calcium channel blocker thereby inhibiting insulin secretion in β cells. It is a drug that is used in the management of some supraventricular arrhythmias, which is also used in the management of hypertension, ischemic heart disease and the treatment of prophylaxes of angina pectoris (Gibbon, 2005). The motivation of testing verapamil in the presence of plant A on INS-1 cells was to establish whether the insulin releasing effects of plant A were inhibited by verapamil, if this was so then the opening of the VDCC participates in the mechanism of plant A action (Hannan *et al*., 2006). The motivation as to using the drug concentrations are that they have been tested in those concentrations in a previous study (Hannan *et al*., 2006). The effect of two drugs (verapamil and diazoxide) and drug and plant combination treatments on insulin secretion in INS-1 cells after 10 min of insulin stimulation is shown in figure 4.15.

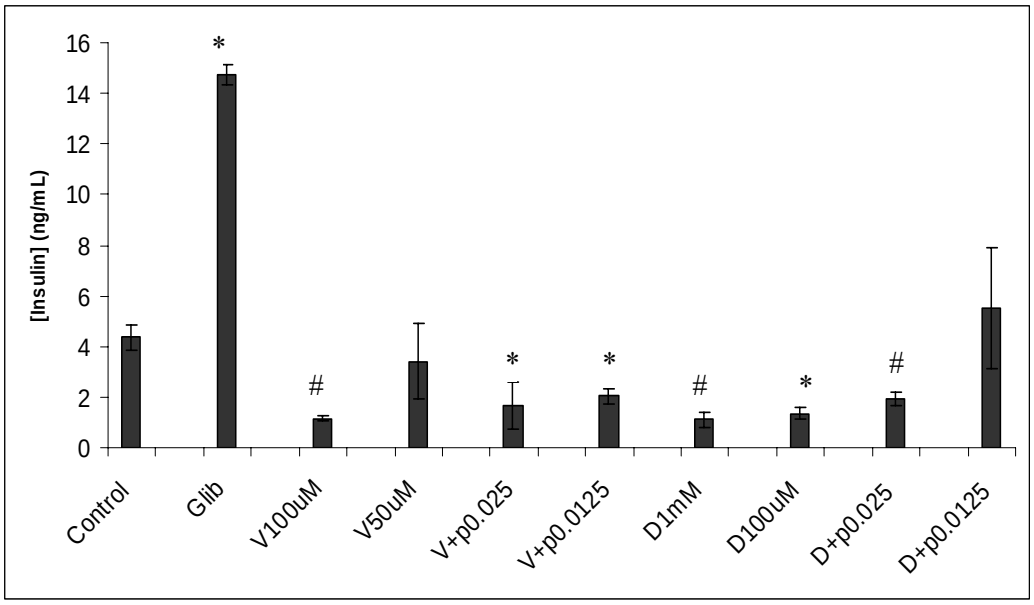

Figure 4.15 (a): **Effect of varying drug concentrations and 1 µM glibenclamide as well as drug combined with plant treatments on insulin secretion by INS-1 cells under acute conditions (10 minutes). A RIA kit was used to determine insulin concentration using scintillation counting. Cells were seeded in a 96 well plate at a density of 3 x10^4 cells/well and incubated for a 24-h period. KRB media and the respective treatment (in KRB media) was used to stimulate insulin secretion for 10 min. The control represents INS-1 media. Glib represents 1 µM glibenclamide. V denotes verapamil, D denotes diazoxide. 50 µM verapamil was combined with the respective plant concentration. 100 µM diazoxide was combined with the respective plant concentration. Each value represents means ± SD (n=3) of a duplicate. * P<0.05, # P<0.01 when compared to the untreated control.**

As indicated in figure 4.15 the control (INS-1 media treated cells) stimulated the INS-1 cells to produce 4.35 ± 0.5 ng/mL of insulin. 1 µM glibenclamide significantly increased the ability of INS-1 cells to secrete insulin to 14.80 ± 0.4 ng/mL of insulin, when compared to the control.

100 µM verapamil decreased insulin secretion by 73% to 1.16 ± 0.1 ng/mL insulin when compared to the control. 50 µM verapamil decreased insulin secretion by only 22% to 3.39 ± 1.49 ng/mL insulin therefore 50 µM verapamil was not as effective in inhibiting insulin secretion as 100 µM verapamil. The effect of 50 µM verapamil combined with 0.025 mg/mL plant A further decreased insulin secretion by 53 % in comparison to the control to 1.68 ± 0.93 ng/mL although the effect of 50 µM verapamil combined with 0.0125 ng/mL plant A slightly increased insulin secretion (2.03 ± 0.32 ng/mL) but not sufficiently back to the control (4.35 ± 0.4 ng/mL).

1 mM diazoxide significantly decreased insulin secretion by 75% to 1.1 ± 0.31 ng/mL when compared to the control. 100 μM diazoxide significantly decreased insulin secretion by INS-1 cells to 1.35 ± 0.24 ng/mL when compared to the control. Figure 4.16 indicates that the higher drug concentrations of both verapamil and diazoxide had a greater effect in inhibiting insulin secretion by the INS-1 cells. 100 μM diazoxide combined with 0.025 mg/mL plant A slightly increased insulin secretion by INS-1 cells (1.92 ± 0.25 ng/mL) when compared to the effect of 1 mM diazoxide (1.1 ± 0.31 ng/mL) and 100 μM diazoxide (1.35 ± 0.24 ng/mL). When 100 μM diazoxide combined with 0.0125 mg/mL plant A was administered to the INS-1 cells, insulin secretion increased to 5.5 ± 2.4 ng/mL when compared to the control. This is a 27% increase in insulin secretion when compared to the control. I suggest that plant A may influence the closing of the K_{ATP} channel, thereby stimulating insulin secretion. This suggestion contradicts the results obtained in figure 4.16 as an additive effect of insulin secretion was not observed when the INS-1 cells were treated with glibenclamide combined with plant treatment. Perhaps the effect of plant A and glibenclamide may cause β cell membrane desensitization even under acute conditions. It is also possible that the constituents of the plant A extract could have an antagonizing effects on glibenclamide.

There was no significant difference in insulin secretion when 100 μM diazoxide was compared to 100 μM diazoxide combined with 0.025 mg/mL plant A ($p<0.54$). In addition no significant difference in insulin secretion was observed when 100 μM diazoxide was compared 100 μM diazoxide with 0.0125 mg/mL plant A ($p<0.6$). No significant difference was observed when 100 μM diazoxide combined with 0.025 mg/mL plant A was compared to 100 μM diazoxide combined with 0.0125 mg/mL plant A ($p<0.41$).

4.5.2.5 The effect of drug and plant A on total insulin content

The effects of varying drug treatments on insulin content in INS-1 cells are observed in figure 4.16. There is no significant difference between the control (4.42 ± 0.09 ng/mL) and 1 μM glibenclamide (4.59 ± 0.21 ng/mL) on total insulin content. These data show that although glibenclamide dramatically stimulates insulin secretion in INS-1 cells under acute conditions, the insulin content (insulin reserve) is maintained

within a normal range. Chronic exposure of glibenclamide has been implicated in decreasing insulin content in insulin secreting cell lines (Ling *et al*., 2006) and hence depleting insulin stores, since glibenclamide induces an increase of up to 3 fold in insulin secretion in insulin secreting cells under basal conditions as observed in figures 4.12 and 4.15.

100 μM verapamil significantly decreases insulin content by 40.6% to 2.63 ± 0.21 ng/mL. There is a slight increase in insulin content when the cells were treated with 50 μM verapamil to 3.83 ± 0.03 ng/mL. The effect of 0.025 mg/mL plant combined with 50 μM verapamil significantly decreased total insulin content by 62% to 1.68 ± 2.47 ng/mL when compared to the control. The effect of 0.0125 mg/mL plant combined with 50 μM verapamil significantly decreases total insulin content by 48% to 2.31 ± 0.4 ng/mL when compared to the control. Interestingly, the same treatment (0.0125 mg/mL plant A combined with 50 μM verapamil) slightly increased insulin secretion although not significantly (Figure 4.16). If a compound decreases insulin content, the β cells cannot quickly replenish insulin after acute stimulation; hence depletion of insulin stores is possible; since there is no biosynthetic backup to compensate for induced insulin hyper secretion (Bollheimer *et al*., 1998). The reason as to the observed decrease in total insulin content on treatment with 0.0125 mg/mL plant A combined with 50 μM verapamil is unknown, this issue warrants further study.

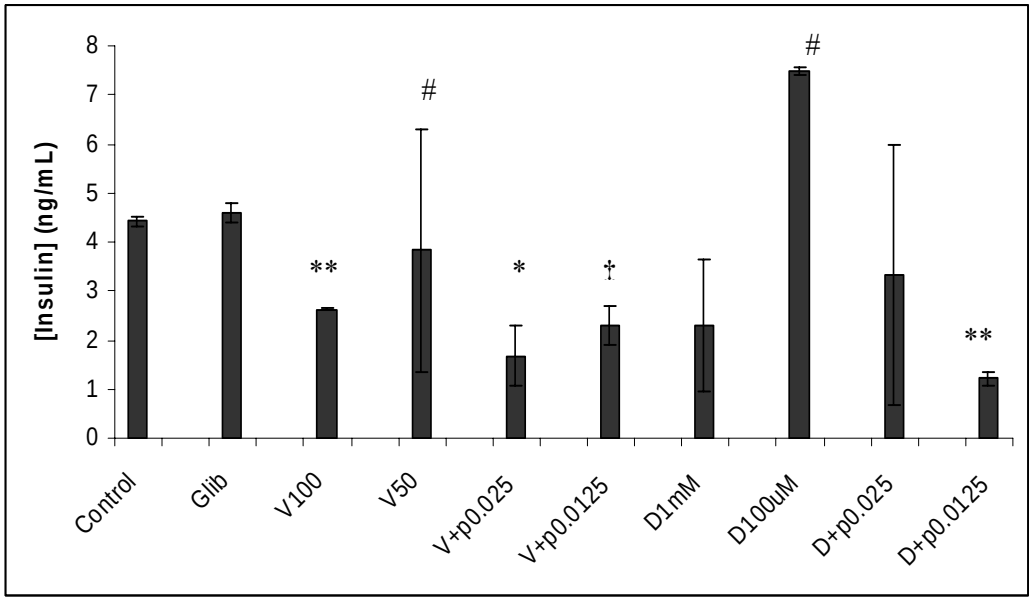

Figure 4.16: **Effect of varying drug concentrations on total insulin content in INS-1 cells. A RIA kit was used to determine insulin concentration using scintillation counting. The control represents INS-1 media. Glib represents 1 µM glibenclamide. V denotes verapamil, D denotes diazoxide. Each value represents means ± SD of a duplicate. #P<0.001, **P<0.005, ‡P,0.02, *P<0.05 when compared to the control.**

There is no significant difference between 1 mM diazoxide (2.29 ± 1.33 ng/mL) and the control. However the effect of 100 µM diazoxide increases total insulin content to 7.47 ± 2.64 ng/mL. Diazoxide has been implicated in maintaining insulin stores in β cells (Gray and Flatt, 1999). The results found in this study are thus consistent with those of Gray and Flatt (1999). In the presence of insulin secretion antagonists (verapamil and diazoxide), there was no insulin secretion, while in the absence of insulin secretion antagonists, there was insulin secretion. The effect of using insulin secretion antagonists prove that insulin secretion was not attributed to β cell damage in the cells (Gray and Flatt, 1999). There was no significant difference in insulin content between the control and effect of 0.025 mg/mL combined with 100 µM diazoxide. Unexpectedly, there was a significant decrease in insulin content when the INS-1 cells were treated with 0.0125 mg/mL plant A combined with 100 µM diazoxide when compared to the control. However there was a decrease in insulin content between the 50 µM diazoxide and plant combinations when compared to the effect of 50 µM diazoxide alone. Interestingly, there was a decrease (but not significant) in total insulin content in the order 100 µM diazoxide combined with 0.0125 mg/mL plant A < 100 µM diazoxide combined with 0.025 mg/mL plant A < 100 µM diazoxide respectively. These data correspond to an increase in insulin

secretion as indicated in figure 4.16 in the order 100 μM diazoxide combined with 0.0125 mg/mL plant A > 100 μM diazoxide combined with 0.025 mg/mL plant A > 50 μM diazoxide respectively. There was no significant difference observed in total insulin content when 100 μM diazoxide was compared to 100 μM diazoxide combined with 0.025 mg/mL plant A ($p<0.2$). A significant difference was observed when 100 μM diazoxide was compared to 100 μM diazoxide combined with 0.0125 mg/mL plant A ($p<0.001$). This suggests that the combined treatment of 100 μM diazoxide combined with 0.0125 mg/mL plant A did not stimulate further insulin transcription in the INS-1 cells and a depletion of insulin stores occurred. Interestingly as observed in figure 4.16, this treatment (100 μM diazoxide combined with 0.0125 mg/mL plant A) induced the most insulin secretion in INS-1 cells when compared to the other tested diazoxide treatments.

4.5.3 DPP IV activity

4.5.3.1 *In vitro* DPP IV activity

On day 10 of CaCo-2 cells past confluence, domes (or hemi-cysts) appeared as shown in figure 4.17. The size of domes increased gradually during culturing.

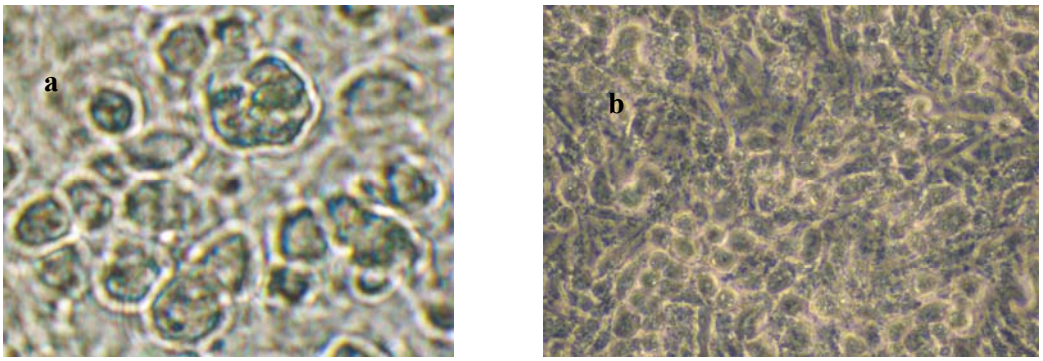

Figure 4.17: CaCo-2 cells observed by phase-contrast light microscopy, a) after 10 days of confluence under X400 magnification, b) after 14 days of confluence just before extracting DPP IV under X200 magnification.

Figure 4.18 shows that 0.25% DMSO had no inhibitory effect ($p<0.5$) on human DPP IV activity when compared to the untreated control. It was vital to test the effect of DMSO on DPP IV activity, as 0.25% DMSO was used to solubilise plant A extract. There was a slight inhibitory, though not significant effect of metformin on direct DPP IV activity ($p<0.5$) when compared to the control, this is approximately a 1.9% decrease in DPP IV activity (see table 5.1). The direct effect of metformin on human DPP IV activity *in vitro* was analyzed in this study. As indicated in figure 4.18 and table 4.1, metformin had no direct effect on DPP IV activity *in vitro*, hence I conclude that metformin has long term indirect effects that occur *in vivo* for metformin to bring about a decrease in DPP IV activity. Recently a study was conducted which showed that metformin and other biguanide compounds significantly increase plasma GLP-1 levels in a dose response manner, in spite of the absence of endogenous DPP IV. Hence they speculated the increase in GLP-1 levels was due to metformin increasing GLP-1 secretion and not an inhibitory effect on DPP IV (Yasuda *et al*., 2002). This is a controversial topic however as some studies have shown that metformin inhibits DPP IV activity *in vitro* (Green *et al*., 2006), while other studies have shown that metformin does not directly affect or decrease human DPP IV activity when they used

20% human serum, porcine kidney DPP IV and recombinant human DPP IV (Hinke *et al*., 2002).

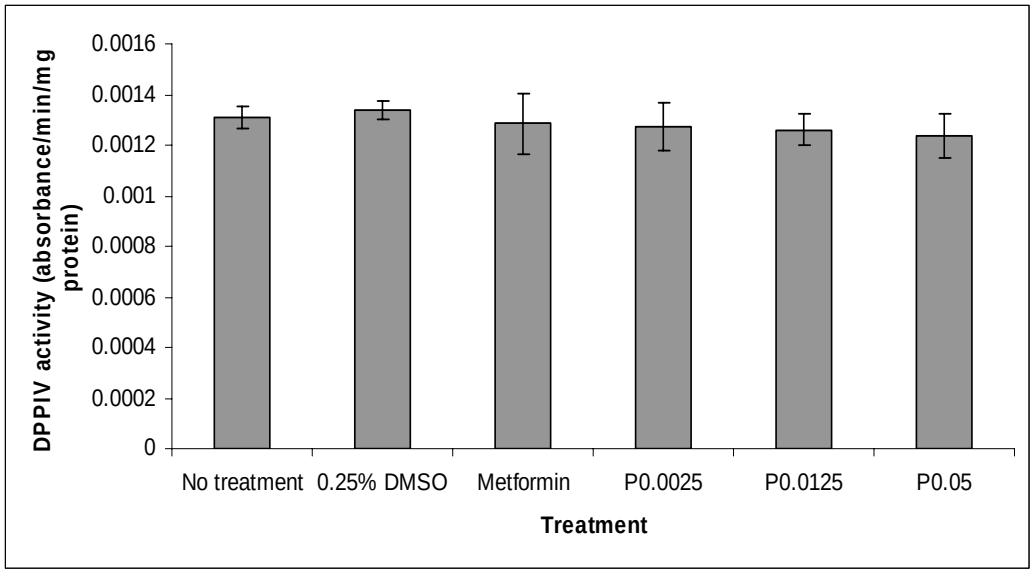

Figure 4.18: Effect of varying treatments on human DPP IV activity, DPP IV was extracted from CaCo-2 cells after 14 days of differentiating CaCo-2 cells past confluence. DPP IV activity is expressed as absorbance/ug protein, each value represents means ± SD, the experiment was performed three independent times (n=3) in duplicates. Plant A is represented in mg/mL ranging from 0.0025 to 0.05 mg/mL. The effect of 5 mM metformin was tested on the DPP IV activity. No treatment represents the effect of assay buffer on DPP IV activity.

Figure 4.18 indicates that *in vitro*, plant A had a slight effect in decreasing human DPP IV activity. Figure 4.18 shows that plant A decreased DPP IV activity in a dose response manner, where 0.0025, 0.0125 and 0.05 mg/mL decreased DPP IV activity by 0.004 %, 0.005% and 0.007% respectively as indicated in Table 4.1. It is evident from the data in figure 4.18 and table 4.1 that metformin and plant A have no direct effect on DPP IV activity. Other researchers have reported that metformin lacks effects on DPP IV activity *in vitro* (Hinke *et al*., 2002). I hypothesize that in order for plant A to inhibit DPP IV activity, plant A needs to be metabolized to bring about this inhibition, *in vivo* studies with a higher number of rats need to be undertaken however to confirm this statement.

Table 4.1: Percentage inhibition of various treatments on human DPP IV activity.

Treatment	% inhibition
No treatment	-
0.25% DMSO	-0.002
5mM metformin	+0.002
[Plant A] (mg/mL)	
0.0025	+0.004
0.0125	+0.005
0.05	+0.007

Values are represented as means ± SD (n=3). The No treatment was regarded as the negative control. The table shows the effect of increasing concentrations of plant A on human DPP IV activity *in vitro* from pooled CaCo-2 cell lysate.

4.5.3.2 *In vivo* DPP IV activity in rat plasma treated with plant A

Metformin is a commonly used oral antidiabetic drug, exclusively for type II diabetics. It is a biguanide implicated in reducing DPP IV activity and hence prolonging GLP-1 activity in type II patients (Green *et al*., 2006). As mentioned earlier GLP-1 is a hormone which is released after meals (postprandially) and stimulates insulin release from the pancreas. DPP IV terminates the activity of GLP-1. Hence inhibition of DPP IV increases circulating GLP-1 levels, thereby insulin release is increased under conditions when it is needed, i.e. after a meal but not during fasting (Michel, 2008). Metformin has been shown to effectively reduce plasma glucose by up to 3.5 mmol/l by decreasing hepatic glucose production and/or improving insulin resistance (Green *et al*., 2006).

Previous *in vivo* studies have shown that metformin lowers DPP IV activity in rat plasma and improving glucose-lowering and insulin releasing effects of GLP-1 administration. In the same study this was also associated with increased circulating concentrations of GLP-1 (Green *et al*., 2006). It has also been reported that prolonged dosing of Zucker diabetic rats with metformin reduced serum DPP IV activity in vivo (Lenhard *et al*., 2004).

The motivation of measuring DPP IV activity in rat plasma is that ingestion of a drug or plant treatment may contribute to the efficacy of the treatment. The limiting factor of using the *in vitro* model is that certain compounds in the plant extract may need to be metabolised in order to be activated or potent, this modification may occur during ingestion, which is not possible in an *in vitro* model. Figure 4.19 shows the effect of

plant A and metformin on DPP IV activity when rat plasma was used as a source. The rat plasma was treated with aprotinin immediately after sampling (and thereafter stored at -80°C) to inhibit trypsin, which would have otherwise degraded DPP IV. The insulin resistant rats (CCH) did not have a significantly higher DPP IV activity when compared to the control ($p<0.8$). The insulin resistant rats (CCH) had significantly higher DPP IV activity when compared to metformin ($p<0.001$) and plant A ($p<0.005$) treated rats. These data indicate that both metformin and plant A decrease DPP IV activity in the insulin resistant state. It is notable that insulin resistant rats treated with metformin had lower DPP IV activity however not significantly ($p<0.9$) lower when compared to the control (CCL) rats on a normal diet. Metformin treated rats were observed to have the lowest DPP IV activity when compared to CCH and Plant A. Plant A had lower DPP IV activity when compared to the control ($p<0.95$) rats and the insulin resistant rats. Variation in DPP IV activity is also noted within a particular group as shown in figure 4.19. Plant A may increase insulin secretion indirectly by lowering DPP IV activity.

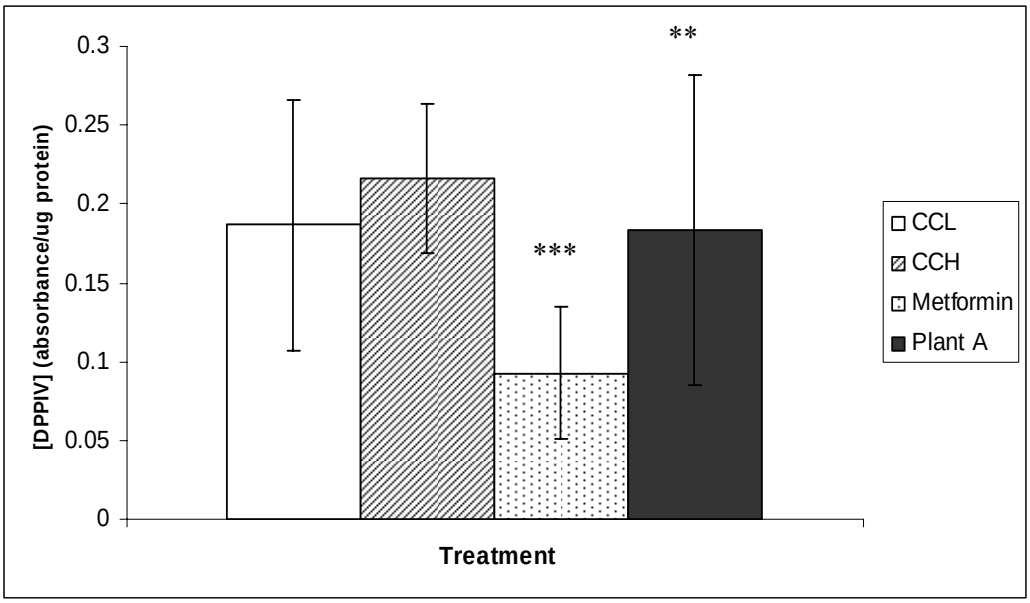

Figure 4.19: The effect of Plant A and metformin on DPP IV activity using rat plasma as a source. DPP IV activity is expressed as absorbance/ug protein, each value represents means ± SD, the experiment was performed three independent times (n=3) in duplicates. Rats were treated with metformin and plant respectively for 28 days. T-test was used for statistical analysis. ***P<0.001, **P<0.005 when compared to the low fat control (CCL).

It has been documented that metformin significantly increases plasma acting GLP-1 levels in obese non-diabetic subjects after oral glucose loading under a euglycemic

hyperinsulinemic clamp protocol. There are two proposed possible mechanisms either (1) metformin inhibits DPP IV which is an enzyme that rapidly degrades GLP-1 after release of the incretin or
(2) metformin increases GLP-1 secretion. There is still controversy about the mechanisms involved (Yasuda, 2002). I propose a third mechanism; that metformin may decrease DPP IV secretion.

I speculate that metformin may not have a direct effect on DPP IV *in vitro* but may have an influence in either a decrease in DPP IV secretion or contribute towards DPP IV degradation or inhibition *in vivo* as indicated in figure 4.19.

4.5.3.3 *In vivo* effect of plant A on IDE concentrations

After liver and kidney, muscle contributes a pivotal role in insulin removal as previously stated (Duckworth *et al*., 1998). Due to the limited liver and kidney samples, IDE activity was determined in muscle and spleen in this study.

Insulin degrading enzyme activity was quantified in relative fluorescence units from muscle (Figure 4.20) and spleen samples (Figure 4.21) respectively using a fluorometer and IDE kit as described in the materials and methods. As shown in figure 4.22 the IDE activity in the muscle samples of insulin resistant rats (46.4 RFU/mg protein) was found to be slightly higher than that of the normal rats (23.5 RFU/mg protein). A few diabetics were described having significantly higher insulin degrading activity of adipose or muscle tissue. Hence increased insulin degradation is implied to cause an impaired response to insulin (Standl and Kolb, 1984). It is also known that increased insulin degradation is accompanied with a state of both insulin deficiency and insulin resistance. The increased (but not significant) IDE levels in the insulin resistant rats (CCH) suggest that there is increased insulin degradation (Standl and Kolb, 1984). Treatment with plant A slightly decreases IDE activity to 28 RFU/mg protein when compared to the insulin resistant (CCH) rats.

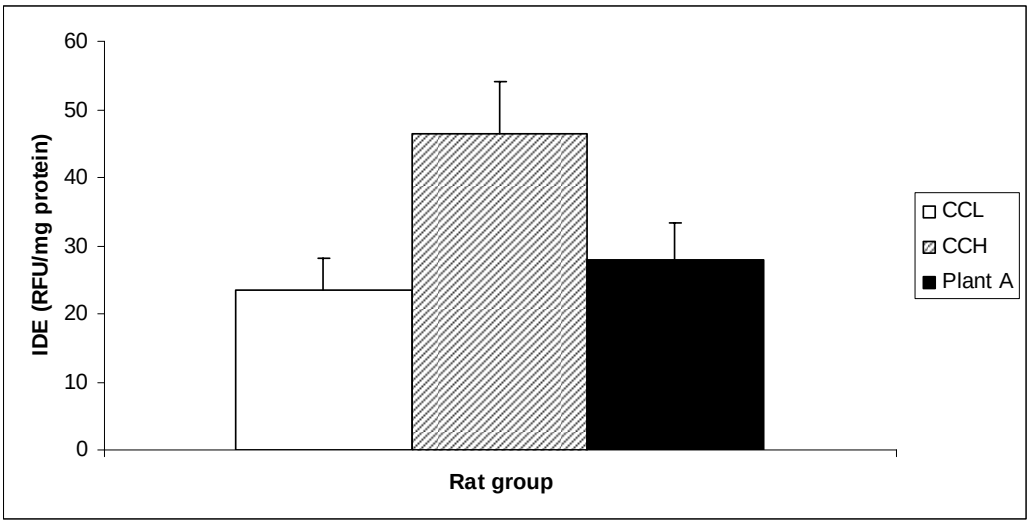

Figure 4.20: Effect of plant A on IDE activity (measured in relative fluorescence units) in muscle samples. Values are represented as means ± SE of a duplicate for 4 rats per group.

Figure 4.21 shows the effect of plant A on IDE activity in spleen samples. There is an increase in IDE activity in the insulin resistant rats (10.1 RFU/mg protein) as compared to the normal rats (3.2 RFU/mg protein). However the increase in IDE activity of the insulin resistant rats is not as dramatic as compared to the normal rats. Data in figure 4.21 show that plant A decreases though not significantly IDE activity in spleen to 9.3 RFU/mg protein compared to the insulin resistant rats. This contrasts the dramatic increase in IDE activity from muscle tissue in the insulin resistant rats when compared to the control rats (Figure 4.23). The data observed in figures 4.20 and 4.21 are in accordance in literature where it is observed that muscle tissue has higher IDE activity when compared to spleen tissue (Duckworth *et al*., 1998). Statistical tests to determine significance could not be carried out with these data as the experiment was only performed once in duplicates, due to a limitation in the number of plates (X1) available in the IDE kit used and the cost of the IDE kit.

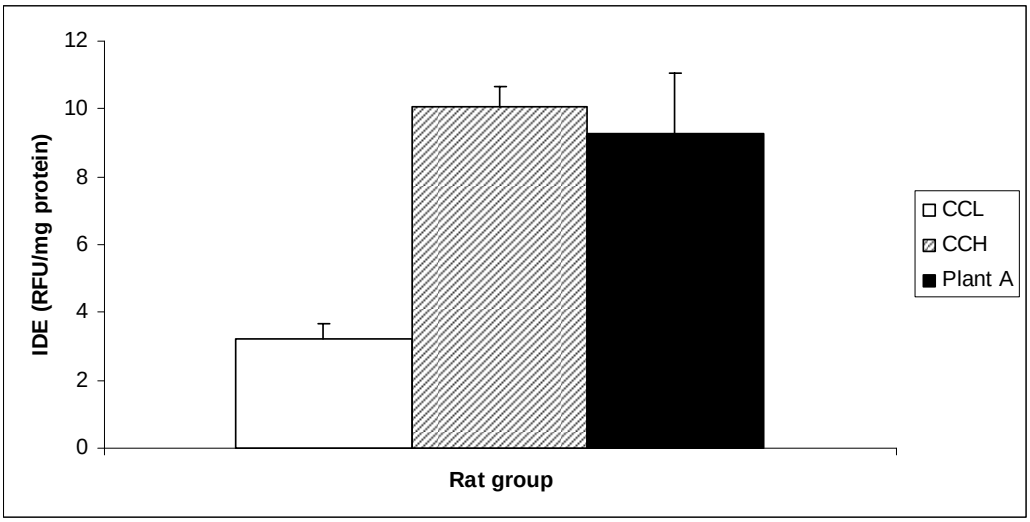

Figure 4.21: Effect of plant A on IDE activity (measured in relative fluorescence units) in spleen samples. Values are represented as means ± SE of a duplicate for 5 rats per group.

It is known that in the even of elevated insulin levels, IDE activity decreases (Duckworth, 1998). This could explain the slight decrease in IDE activity in the muscle and spleen samples of plant A rat when compared to the untreated insulin resistant rats; as the plasma samples obtained from plant A treated rats had markedly elevated insulin levels (Table 1.1 and Figure 4.10). However the statement does not explain the slightly elevated IDE activity in the untreated insulin resistant rats (CCH).

CHAPTER FIVE: ADIPOCYTE GLUCOSE UPTAKE

5.1 INTRODUCTION

GLUT4 is a glucose transporter found in adipose, muscle and brain tissues. The previous study by Karachi (2009) showed a significant increase in glucose uptake in adipose tissue (see table 1.2) from the rats treated with plant A. It was vital to test the influence of plant A on GLUT4 expression in adipose tissue to explain the results obtained by Karachi (2009).

The increased glucose uptake in the adipose tissue of the plant A treated rats is a sign of improved insulin resistance. As a means to ameliorate insulin resistance, GLUT4 mRNA expression would have been increased on plant A treatment and hence the motivation of measuring GLUT4 mRNA expression in adipose tissue. Alternatively, plant A treatment may improve glucose utilization and this necessitated determining the effect of plant A on 3T3-L1 adipocytes.

Glucokinase is involved in blood glucose homoeostasis by phosphorylating excess glucose postprandially. Glucokinase plays a central role in glucose metabolism, while the adipose tissue also plays a vital role in glucose metabolism and storage especially during the postprandial state. During insulin resistance glucose metabolism is impaired. It was vital to test the effect of plant A on glucokinase expression to determine whether plant A may elevate GK expression as a means to reversing insulin resistance.

Gene expression studies are vital when genes that are expressed under certain conditions are to be compared. Northern blotting and reverse transcription PCR (RT-PCR) are some of the techniques that can be employed to evaluate gene expression (Hong *et al*., 2008). A Northern blot allows the identification of specific mRNA sequences of defined lengths by hybridisation with a labelled gene probe; after separation of RNA by agarose gel electrophoresis (Walker and Wilson, 2005). Quantitative real-time PCR (qPCR) is a technique used for the simultaneous quantification and amplification of a target DNA or cDNA molecule. The qPCR technique has become popular in gene expression studies as it offers an opportunity to quantitatively analyze gene expression data (Hong *et al*., 2008). The advantage of

qPCR over northern blot is that qPCR requires less amounts of starting material as compared to the latter which requires large amounts of starting material (RNA) for identification. In addition it is harder to quantify mRNA sequences using the northern blot technique.

qPCR was introduced more than a decade ago and it has become the standard method for quantifying nucleic acid sequences. The method offers many advantages such as ease of use and high sensitivity, specificity with accuracy which has resulted in a rapidly expanding number of applications with increasing throughput of samples to be analyzed (Hellemans *et al*., 2007).

qBase software was used to analyze the qPCR results obtained using the BioRad iCycler. qBase is defined as a flexible and open source program used for managing and analysing qPCR data. qBase uses a proven, advanced and universally applicable relative quantification model (Hellemans *et al*., 2007).

5.1.1 Insulin signalling pathways and glucose uptake

The binding of insulin to the insulin receptor elicits autophosphorylation of the insulin receptor, leading to the binding of assorted scaffold proteins, including the IRS proteins, as well as Src homologue and collagen homologue (SHC) and B type cyclins (Clb). Phosphorylation of these scaffold proteins by the insulin receptor, engages several diverse signalling pathways. IRS family members are involved in the control of metabolic fuel homeostasis (Panunti *et al*., 2004). IRS-1 is the main mediator of insulin-stimulated glucose uptake and activation of anabolic pathways in muscle and adipose tissue. IRS-2 is the main director of anabolic effects in the liver (Figure 5.1).

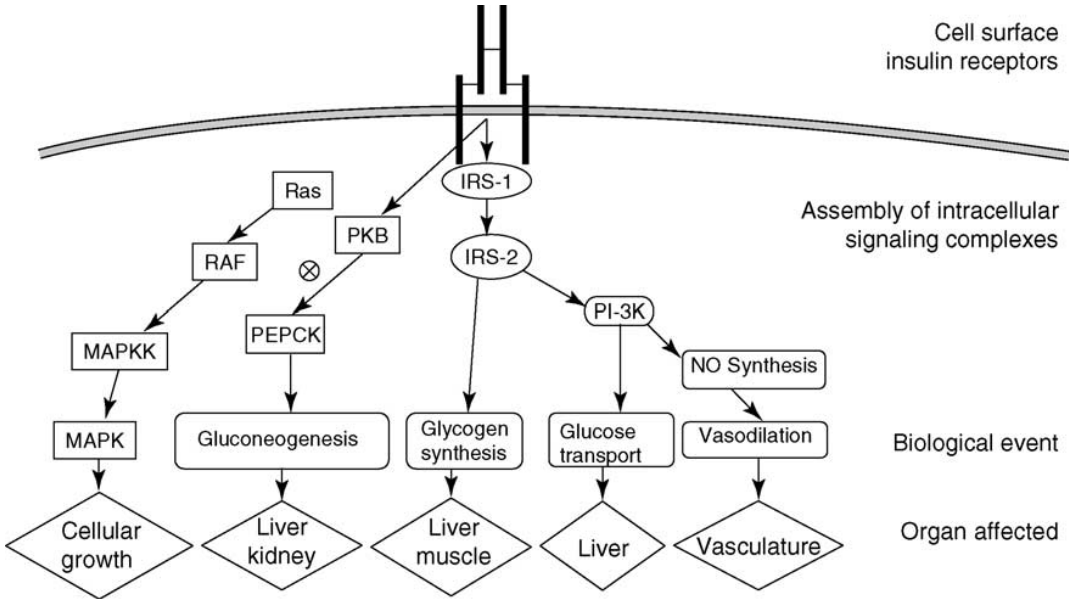

Figure 5.1: **Intracellular pathways involved in insulin signalling and its effects on target organs . IRS: insulin receptor substrate, MAPK: mitogen proliferating kinase, PEPCK: phosphoenolpyruvate carboxykinase , PI-3K: phosphoinositide-3-kinase, PKB: protein kinase B (Panunti *et al*., 2004).**

When IRS-1 and IRS-2 are phosphorylated, they associate with p85 regulatory subunit of PI-3K. p110 (PI-3K's catalytic subunit) is recruited to the plasma membrane by this association, resulting in the conversion of (PtdIns(4,5)P_2) to (PtdIns(3,4,5)P_3). (PtdIns(3,4,5)P_3) helps additional signalling events by binding to PDK1, PDK2 and PKB (or AKT). Co-localization of PDKs and PKB helps activation of PKB by phosphorylation at Thr308 (PDK1) and Ser473 (PDK2), leading to phosphorylation of downstream targets such as GSK3 and the AS160 Rab GTPase-activating protein, which interacts with the small GTPase RAB10 to help translocation of GLUT4-containing vesicles to the cell surface. These actions of insulin encourage glucose uptake and storage under anabolic conditions (Muoio and Newgard, 2008).

In diabetes, there are defects in IRS-1 and PI-3K. Insulin lacks a stimulatory effect on insulin receptor (IR) and IRS-1 tyrosine phosphorylation. There is a reduction in the association of the p85 subunit of PI-3K with IRS-1 correlating with the impairment of glycogen synthase activity and insulin stimulated glucose disposal in diabetic patients. In addition, insulin fails to increase the association of the p85 subunit with IRS-2 in muscle tissue, indicating a combined malfunctioning in IRS-1 and IRS-2 (Panunti *et al*., 2004).

5.2 MATERIALS AND METHODS

5.2.1 GLUT4 and GK RNA quantification

5.2.1.1 RNA extraction, quantity and quality

5.2.1.1 a) Principle

RNA is easily degraded in tissue samples, so all samples were immediately placed in RNAlater (Ambion Inc, USA) to preserve the RNA. RNA must first be extracted from samples using the phenol, chloroform guanidium thiocyanate method, quantification and quality analysis of RNA must then be performed, before the RNA can be used for other downstream analysis.

The Aurum total RNA fatty and fibrous tissue kit was used as it is best for fatty or fibrous tissues and samples that are rich in RNases. With this kit more than 100 μg of total RNA can be isolated from various sample types. Total RNA samples isolated using this kit are suitable for use in many downstream applications e.g. RT-PCR, real time RT-PCR, microarray analysis, northern blots and *in vitro* translation (Aurum™ Total RNA Fatty and Fibrous Tissue kit Instruction Manual).

Samples are first lysed using the PureZOL RNA isolation reagent. Chloroform is then added to achieve separation of the organic and aqueous phases. The aqueous phase contains RNA, which is recovered and mixed with ethanol. Most proteins and DNA are discarded with the organic phase. The sample is then passed through a silica membrane in the Aurum RNA binding mini column, where nucleic acids are bound. The membrane selectively binds to mRNA and larger rRNAs. Small RNA molecules less than 200 nucleotides e.g. 5.8S rRNA, 5S rRNA and tRNA (comprising 15-20% of total RNA) are removed. Any remaining proteins and cellular debris are removed through wash steps. Contaminating genomic DNA is removed by an on-column DNAse I digest step. The RNA is then eluted and is ready for use in downstream applications without any further manipulation (Aurum™ Total RNA Fatty and Fibrous Tissue kit Instruction Manual).

It is vital to determine the quantity of RNA so as to know how much (volume of RNA) must be used to reverse transcribe to DNA. The determination of the quality of RNA is equally vital so as to avoid working with denatured RNA samples. An Agilent BioAnalyzer is used to determine these parameters. The quality of RNA is given a

RIN number (scaled from 1 – 10) with the higher the RIN number representing the better the quality of RNA.

5.2.2.1 b) RNA extraction from samples

The Agilent RNA Nano kits contain chips and reagents designed for analysis of RNA fragments. Each RNA chip consists of an interconnected set of microchannels that is used for separation of nucleic acid fragments based on their size as they are driven through the microchannels electrophoretically. These Agilent RNA kits are specifically designed for use with an Agilent 2100 BioAnalyzer.

Total RNA was isolated from rat samples from approximately 150 mg of rat testicular adipose tissue stored at -20°C in RNAlater (Ambion Inc, USA) using the Aurum total RNA fatty and fibrous tissue kit (BioRad, USA) according to the manufacturer's instructions. Briefly, equipment was sprayed with RNaseZap (Ambion Inc, USA) while plastic ware was autoclaved to destroy any RNAses present. Approximately 150 mg of adipose tissue was added to 1 ml PureZOL with a stainless steel bead in a cryopreservation tube, while working on ice. The samples were then homogenized for 2 min at 30 1/s using a shaker (Reutsh, Germany). The homogenized soluble samples were transferred to a fresh tube then incubated for 5 min at room temperature. 0.2 ml chloroform was added to the samples and the samples were shaken vigorously as above and incubated for 5 min at room temperature, centrifuged at 12 000 x g for 15 min at 4°C. The aqueous phase was then carefully transferred to a new 2 ml tube. An equal volume of approximately 600 µl of 70% ethanol (Analar grade) in RNAse-free water was added to the tube containing the aqueous sample. The lysate was thoroughly mixed by pipetting up and down.

An RNA binding column was inserted into a 2 ml capless tube. 700 µl of lysate was transferred to the binding column and centrifuged for 30 secs at 12000 x g and the filtered solution was discarded. The remaining lysate was added and centrifuged as before. The solution again was discarded leaving RNA bound to the column. 700 µl of low stringency wash buffer was added to the column. The column was again centrifuged for 30 seconds at 12000 x g. 80 µl of reconstituted DNAse I (5µl DNAse I with 75µl DNAse dilution solution) was then added to remove any contaminating

DNA in the lysate. The lysate was incubated for 15 min at RT. 700 µl high stringency wash buffer was added to the tube, to wash off the DNAse I and degraded DNA which was again centrifuged for 2 min at 12 000 x g. 700 µl low stringency solution was added to the tube and centrifuged for 30 seconds at 12000 x g. The RNA binding column was then transferred into a 1.5 ml capped tube. 40 µl of elution solution at 70°C was added to the centre of the membrane stack and incubated for 1 minute then centrifuged for 2 min at 12000 x g (Aurum^{TM} Total RNA Fatty and Fibrous Tissue kit Instruction Manual). The RNA was stored at -80°C until required. The quantity and quality of RNA was determined using the Agilent RNA 2100 BioAnalyzer (Agilent, Germany) with an Agilent RNA 6000 Nano kit, following the manufacturer's instructions.

5.2.1.2 Reverse transcription

Figure 5.2 shows the reverse transcription reaction. Reverse transcriptase is an RNA-dependent DNA polymerase which catalyzes the synthesis of a complementary DNA strand from mRNA template via reverse transcription and using a mixture of four dinucleotide phosphates (dNTPs). A short oligonucleotide primer must also be present for the reaction to occur. The primers provide a free 3'-hydroxyl group which is used as the starting point for the reverse transcriptase. An important requirement is that high quality undegraded mRNA must be used (Walker and Wilson,2005) the integrity of which can be checked by using the Agilent BioAnalyzer as will be explained later on in this chapter.

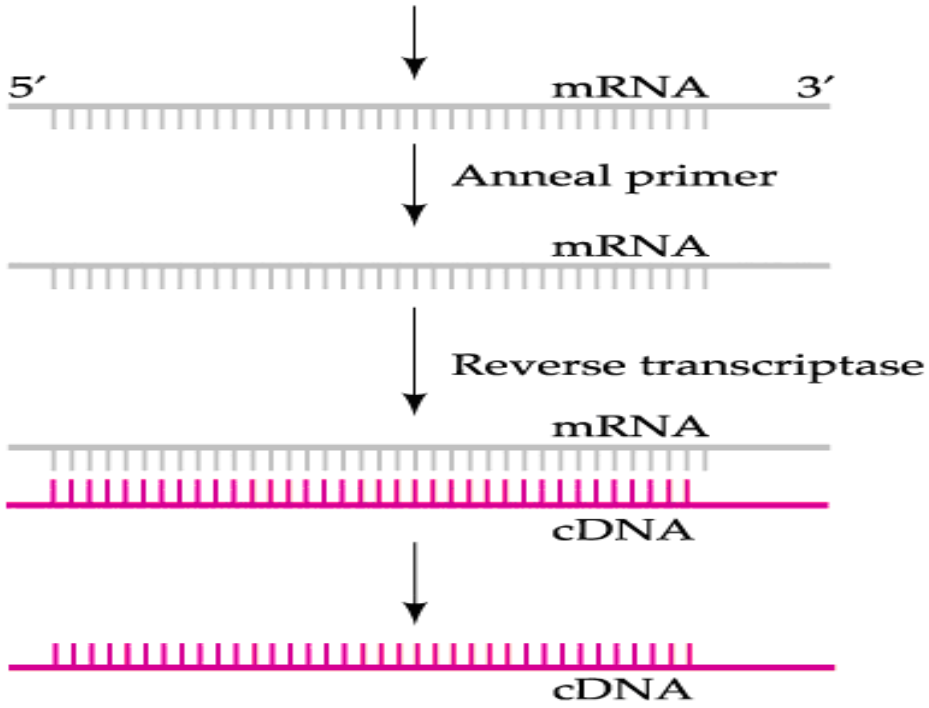

Figure 5.2: Modified figure of reverse transcription reaction (www.8e.devbio.com/article.php).

The reverse transcription reaction mixture per reaction is indicated in table 5.1.

Table 5.1: Reverse transcription reaction components

5x iScript Reaction Mix	4 µl
iScript Reverse transcriptase	1 µl
Nuclease-free H_20	
RNA template	
TOTAL VOLUME	**20 µl**

1 µg of each RNA sample was utilized to synthesize cDNA using the reverse transcription BioRad iScript cDNA synthesis kit (BioRad, USA) according to the manufacturer's instructions. The volume of RNA template added depended on the quantity of RNA obtained from the Agilent BioAnalyzer results. The volume of RNA used was calculated such that 1 µg of RNA is converted to 1 µg of DNA. The total volume of RNA and water was 15 µl. The total volume for the reverse transcription reaction containing reaction mix, reverse transcriptase, nuclease-free water and RNA was 20 µl. It was assumed that 1 µg RNA will yield 1 µg DNA. The reaction mixture

was incubated for 5 minutes at 25°C for RNA unfolding, 30 minutes at 42°C for the reverse transcription reaction to occur and finally incubation for 5 minutes at 85°C to stop the reaction by degrading the enzyme. Thereafter the samples were frozen at -80°C until use for PCR.

5.2.3 qPCR

Polymerase chain reaction (PCR) is a technique that allows the amplification of a cDNA product up to several million times. PCR is divided into 3 steps as indicated in figure 5.2, these steps are denaturation which occurs at high temperatures (94°C - 96°C)-where double stranded DNA is denatured into single stranded DNA; annealing-where primers hybridize to the single stranded DNA, occurring at lower temperatures of 37-65°C and the last step is elongation where the polymerase extends in 3' direction. This process is repeated 20 – 40 times (cycles). In real time PCR, the accumulation of amplified product can be detected and measured as the reaction progresses. In the reaction, a fluorescent molecule is included that binds to double stranded DNA and thus reports an increase in the amount of DNA by a proportional increase in fluorescent signal. Specialized thermal cyclers equipped with fluorescence detection modules are used to monitor the fluorescence in each cycle as amplification occurs. The measured fluorescence reflects the amount of amplified product in each cycle. In quantitative real-time PCR (qPCR) the real-time PCR results are represented as the number of copies of DNA or the absolute quantity of DNA if a standard curve of the amplified sequence is included. Relative quantitation in real time PCR measures the relative expression changes of a sequence. There are several advantages that real time PCR has over conventional PCR such as (1) one can determine the starting template copy number with accuracy and high sensitivity (2) qPCR can be evaluated without gel electrophoresis, resulting in a shorter experiment time and higher throughput (3) reduced contamination and (4) post amplification manipulation is eliminated when performing real time PCR because reactions are run and data evaluated in a closed-tube system (BioRad, USA).

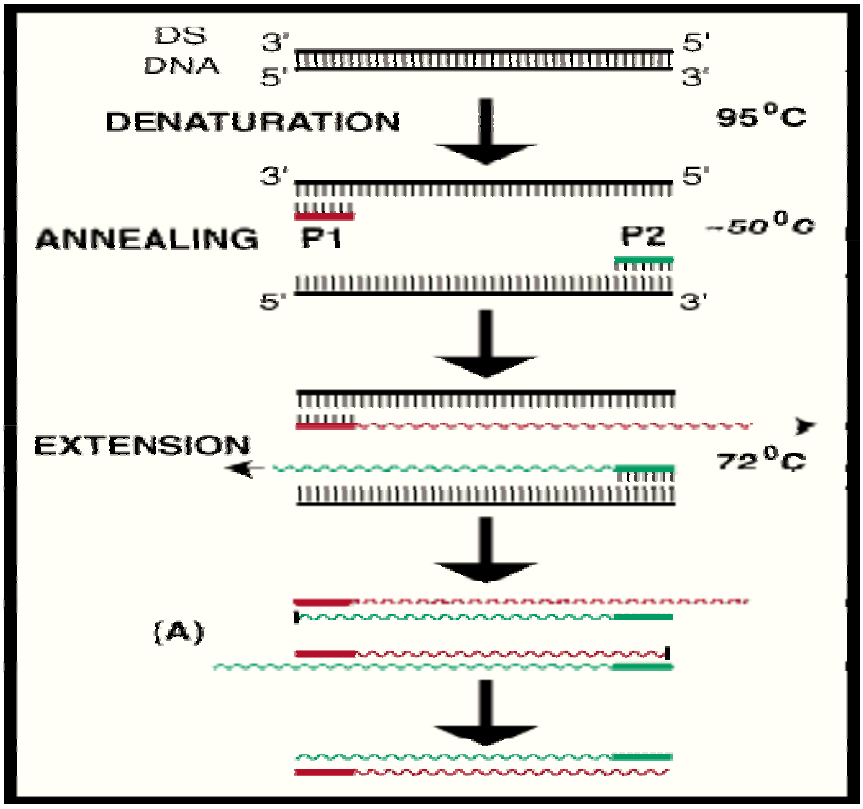

Figure 5.3: PCR reaction (www.flmnh.ufl.edu).

All primers were obtained in lyophilized form. For the GLUT4, glucokinase and TBP primers a 100 µM stock concentration was made of each primer in TE buffer, from this stock a 6.25 times dilution was made of each primer to end up with a final concentration of 16 µM of each primer, thereafter the forward primer is diluted in the reverse primer in a 2 times dilution to produce a primer mix concentration at 8 µM each. 1 µl of this primer mix was used in a 20 µl reaction. Hence the final concentration of each primer in the reaction was 400 nM. The primer sequences are shown in table 5.2.

Table 5.2: Primer sequences used for RT-PCR.

Primer	Sequence
GLUT4	5' ATT GCT TCT GGC TAT CAC 3' 3' AAC TTC CGT TTC TCA TCC 5'
Glucokinase	5' GCA GTG GAG CGT GAA GAC 3' 3'GGA AGG AGA AGG TGA AGC C 5'
TATA bp	5' AGT CCA ATG ATG GCT TAC GG 3' 3' TTG CTA CTG CCT GCT GTT G 5'

The GLUT4 primers were designed by Ursula Gorniak (BioRad, SA) using Beacon Design software. The TBP primers were designed by Dr. Gill Dealtry, Department of Biochemistry and Microbiology, NMMU and synthesised by Inqaba Biotech. Calnexin primers were purchased from PrimerDesign Ltd. UK, information regarding the primer sequence was not given. The GLUT4 primer pair was initially screened to obtain the ideal annealing temperature for the reaction, using a gradient PCR protocol, with the optimum annealing temperature seen as that producing the most specific PCR product with the lowest C_t.

The PCR reaction mixture is comprised of the following as indicated in table 5.3.

Table 5.3: PCR reaction mixture components

2 X IQ SYBR Green Supermix (170-8880)	10 µl
Forward primer (400 nM-final concentration)	0.5 µl
Reverse primer (400 nM final concentration)	0.5 µl
Sterile H_20	4 µl
DNA template	5 µl
TOTAL VOLUME	**20 µl**

Reactions were run on a Real time iCycler IQ system (BioRad, USA). The cycling conditions for GLUT4 PCR comprised of 3 min polymerase activation at 95°C and 40

cycles at 95°C for 30 sec and 72°C for 30 sec and a melt curve was obtained by increasing the set point temperature after cycle 2 by 1°C. The cycling conditions for TBP and Can X PCR comprised of 3 min polymerase activation at 95°C and 40 cycles at 95°C for 30 sec and 60°C for 30 sec. Each assay included (in duplicate): no template control and 250ng of test cDNA.

5.2.4 3T3-L1 cell culturing

3T3-L1 fibroblasts were maintained in Dulbecco's modified Eagle's medium (DMEM; Gemini, USA) and supplemented with 10% FBS. Passage numbers between 24 and 32 were used for the experiments. Cells were seeded at a density of 3 x 10^4 cells/well into 48 well plates when conducting glucose uptake, cytotoxicity and cell density experiments.

5.2.4.1 Cytotoxicity studies with plant A on 3T3-L1 preadipocytes

Cells were seeded at a density of 3 x 10^4 cells/well in a 48 well microtiter plate for 24 hours. The control wells were treated with 2.5% DMSO made up in the stated 3T3-L1 media. Another set of wells contained cells treated with 3T3 media only. Each assigned well was treated with its respective plant A concentration and incubated for 48 hours. Thereafter, all media/treatment was removed from the wells and 500 µl of 5 mg/ml MTT was added to all wells and incubated at 37°C for 3 hours, all the MTT was aspirated. 500 µl DMSO was added to the wells and 200 µl of this was transferred to a 96 well microtiter plate and the absorbance was read at 540 nm (Freshney, 1994). The experiment was conducted in triplicate. The reason for not reading the 48 well plates directly is because the particular plates that were purchased could not fit into the microtiter plate reader.

5.2.4.2 Differentiation of 3T3-L1 preadipocytes

3T3-L1 cells were seeded into 48 well plates at a density of 3 x 10^4 cells/well. Conversion of preadipocytes was induced after 48 hours using rosiglitazone (Velebit *et al*., 2008). A final concentration of 10 µM rosiglitazone (Glaxo Smith Kline, South Africa) in DMEM with 10% FBS was added to designated wells from a 4 mg/mL stock prepared in absolute ethanol. Control cells were not treated with rosiglitazone. Thereafter designated cells were treated with rosiglitazone after every 3 days until day

10, where glucose uptake studies, MTT and oil-red-o (ORO) staining were conducted on the cells.

5.2.4.3 *In vitro* glucose utilization studies in differentiated 3T3-L1 adipocytes

Adipocytes have a purpose of storing energy as a reserve when there is not sufficient energy (Nelson and Cox, 2005).

The principle of the glucose assay is that glucose is converted by glucose oxidase into gluconic acid and hydrogen peroxide, which in the presence of peroxidase oxidizes the chromogen (4-aminoantipyine/ phenol) to a compound that is red in colour (Sera-Pak Plus). A reaction mixture is made containing phosphate buffer, phenol, 4-aminoantipyrine, peroxidise, EDTA and glucose oxidase. Addition of the sample to the reaction mixture initiates the reaction, the reaction proceeds for 2-3 minutes to allow the lag phase to pass. For another 1-2 minutes the formation of the oxidised chromogen is followed at 510 nm in a spectrophotometer. A blank value must be measured to compensate for background activity. The background activity is caused by phosphatase, which contaminates glucose oxidase (Gierow and Jergh, 1988).

10 µl of medium containing 8 mM glucose RPMI was added to a 96 well plate, before adding various treatments. Differentiated 3T3-L1 cells were divided into three experimental groups (1) control cells (8 mM glucose RPMI media), (2) varying plant concentrations (made up in 8 mM glucose RPMI media and 0.25% DMSO) and (3) 1 µM insulin (made up in 8 mM glucose RPMI media) from a 1 mM stock solution. These treatments were added to the designated wells and incubated at 37°C for 180 min, after which, 10 µl from each well was transferred to a 96 well plate; this is referred to as the spent medium. 200 µl of prepared glucose oxidase reagent (see Annexure B) was added to the medium that was not utilized (8 mM glucose RPMI), the spent medium, and the blank (10 µl water), the 96 well plate was incubated at 37°C for 15 min before reading at 492 nm. Glucose utilization was calculated as follows; absorbance units of 8 mM glucose RPMI – absorbance units of spent media after 180 min. A glucose standard curve was set up (see Annexure B) so as to convert the absorbance units read into glucose concentrations.

5.2.4.4 ORO staining

Oil red O (ORO) staining was carried out as described elsewhere (Kuri-Harcuch and Green, 1978). Briefly wells containing differentiated cells (the cells in the 48 well plates) were washed with PBSA twice and fixed with 500 µl 10% formaldehyde overnight. The ORO stock solution was made by dissolving 0.5 g ORO in 100 ml isopropanol using the gentle heat of a water bath. A working solution (4 ml double distilled water in 6 ml ORO stock solution) of 500 µl ORO was added to the wells (to stain the lipid droplets) for 15 min at 37°C. The wells were then thoroughly washed with water to remove excess stain. 500 µl Isopropanol was added to the wells to extract ORO, from this 200 µl was transferred to a 96 well plate and the absorbance was read at 520 nm.

5.3 RESULTS AND DISCUSSION

5.3.1 The effect of Plant A on GLUT4 RNA expression in rat testicular adipose tissue

Analysis of RNA concentration and quality is performed after the isolation of RNA from tissue, the integrity and quantity of RNA must be determined so as to calculate the volume of RNA to use to synthesize cDNA. Thereafter expression studies on the cDNA can be conducted using qPCR. The Agilent BioAnalyzer is used to determine RNA quantity and quality as previously stated.

Figure 5.4 shows the electropherogram traces and analysis of the agarose separations obtained from some representative samples when using the Agilent BioAnalyzer. The quantity of RNA is given in ng/mL. A sample with a RIN value of 6 and above is considered to have high integrity RNA. As shown in figure 5.4 and table 5.4 all the sample RIN values were above 6 except for sample CCL6 with no RIN value, this sample was not used in any subsequent analysis.

Also indicated in figure 5.4 and table 5.4 is that the RNA amount and quality for samples of a particular cohort slightly differed from time to time. This is attributed to sample handling as well as the amount of adipose tissue used for the analysis which differs in RNA amount and quality.

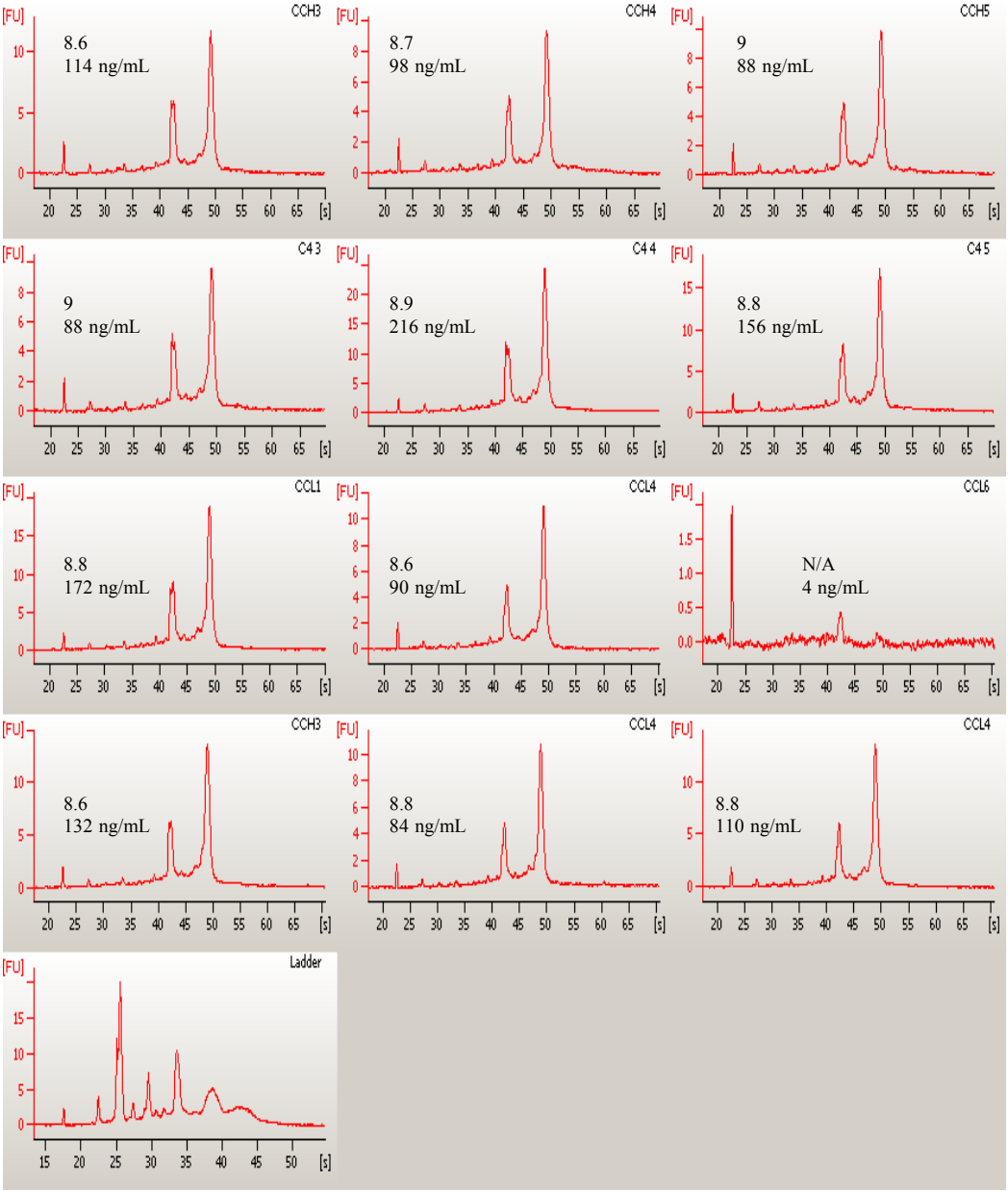

Figure 5.4: An electropherogram showing the RIN and quantity of RNA from rat adipose tissue samples obtained from the Agilent BioAnalyzer. The ladder concentration is 150 ng/µl. CCL represents low fat control samples. CCH represents high fat control samples. C4 represents the plant A treated samples.

Table 5.4: RNA quantity and quality analysis from rat adipose tissue samples using Agilent BioAnalyzer.

Sample	[RNA] (ng/µl)	RIN
COH2	94	8.7
COH3	192	8.4
COH5	152	9.1
COH6	128	8.9
COH7	148	9.0
COL2	158	9.1
COL4	174	9.0
COL5	176	9.1
COL6	94	8.7
COL7	394	8.5
CCH3	114	8.6
CCH4	98	8.7
CCH5	88	9.0
CCH6	760	8.6
CCH7	444	8.6
CCL1	172	8.8
CCL2	806	8.6
CCL4	90	8.6
CCL5	862	8.7
CCL6	4	N/A
C4:1	592	8.3
C4:2	730	8.6
C4:3	88	9.0
C4:4	216	8.9
C4:5	156	8.8

Figure 5.5 shows an electropherogram from the Agilent BioAnalyzer. This technique is used to separate RNA according to size. Electrophoresis provides a quick method for checking the integrity of RNA after extraction before deciding any downstream processing of the RNA (Walker and Wilson, 2005). Ribosomal RNAs (18S and 28S) are well resolved as observed in figure 5.5 in lanes 2 to 8 and lanes 10 to 12. High

integrity RNA samples will have intact 18S and 28 S ribosomal RNAs. Degradation of a sample is observed as a smear (Walker and Wilson, 2005) as observed in lane 9 sample CCL6. The analysis provided by the BioAnalyzer extends this technique; in terms of great sensitivity (measuring down to ng/µl), providing high accuracy and requiring little starting material and indicating quality with a RIN value.

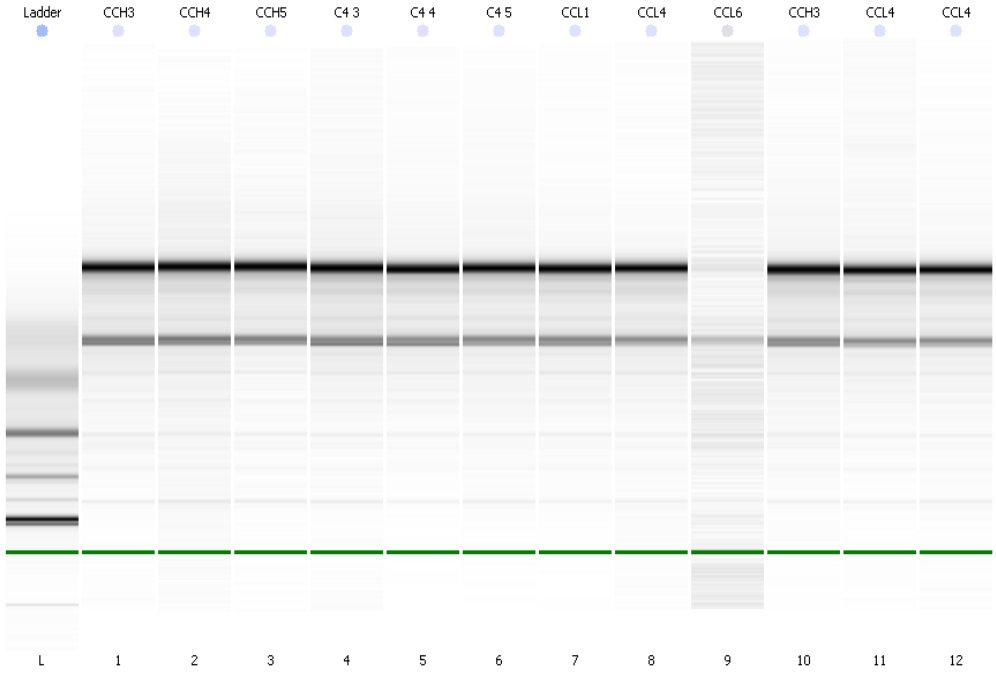

Figure 5.5: An image of a gel separation showing different RNA samples that were run on Agilent BioAnalyzer. Lane 0 shows the RNA marker, while lanes 1 to 12 show different samples labelled at the top of the gel. The two distinct bands in the sample lanes are 18S and 28S RNA. Lane 9 shows that the RNA in CCL6 shows was degraded.

5.3.1.1 qPCR analysis

The DNA-binding dye used in the qPCR study was SYBR Green, which binds non-specifically to double-stranded DNA (dsDNA). SYBR Green fluoresces little when unbound but exhibits fluorescence when bound to dsDNA. The overall fluorescent signal from a reaction is proportional to the dsDNA present. This fluorescent signal increases as the target is amplified. The biggest limitation of DNA-binding dyes is lack of specificity, as DNA-binding dyes bind to any dsDNA (BioRad, USA). The cycle threshold also known as C_t (shown in figure 5.6a, 5.7a and 5.8a) is defined as the number of PCR cycles required to reach the fluorescence threshold in each sample, after PCR (de Kok *et al*., 2005). C_t may alternatively be defined as the cycle

number by which 'enough amplified product accumulates to yield a detectable fluorescence signal' (BioRad, USA). The C_t value is measured in the exponential phase when reagents are not limited thus real-time PCR can be used to accurately calculate the initial amount of template present in the reaction or measure the relative differences in starting amount. The C_t of a reaction is determined by the amount of template present at the beginning of the amplification reaction (BioRad, USA). For any given sample, the lower the expression the higher the C_t value, because more PCR cycles are needed to attain the fluorescence threshold (de Kok *et al*., 2005). In contrast, the higher the expression in a sample, the lower the C_t value, because less PCR cycles are needed to attain the fluorescence threshold. This is because if a large amount of template is present at the start of a reaction, few amplification cycles will be required to accumulate enough product to yield a fluorescent signal above background (BioRad, USA). The orange horizontal line in figures 5.6a, 5.7a and 5.8a is the threshold line. In figures 5.6a, 5.7a and 5.8a, the horizontal lines below the threshold line indicate the negative control, which is water, with no template, hence no expression and hence no PCR cycles or C_t. Figure 5.6a shows that threshold cycles of approximately between 20 and 22 were obtained indicating that the samples had similar amounts of template.

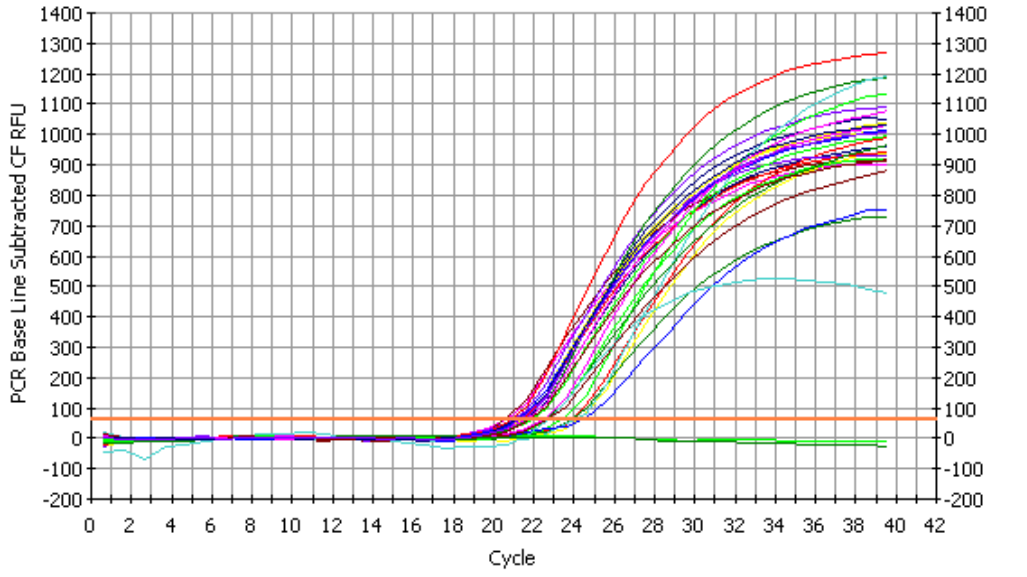

Figure 5.6 a: Amplification plot for CanX PCR.

Melt curve analysis is used in identifying different reaction products and discerning between nonspecific products and specific ones. Once the amplification reaction is completed, a melt curve is generated (as observed in figures 5.5b, 5.6b and 5.7b) by increasing the temperature in small increments and observing the fluorescent signal at each step. During denaturation of the dsDNA, the fluorescence decreases. 'The negative first derivative of the change in fluorescence is plotted as a function of temperature' (BioRad, USA). The characteristic peak at the amplicon's melting temperature (T_m) observed in figure 5.6b, 5.7b and 5.8b identifies it from other products for example primer-dimers, which melt at different temperatures (BioRad, USA).

Figure 5.6b shows a melt peak with a T_m of 83°C, which represents the specific products of the samples used in the CanX PCR reaction.

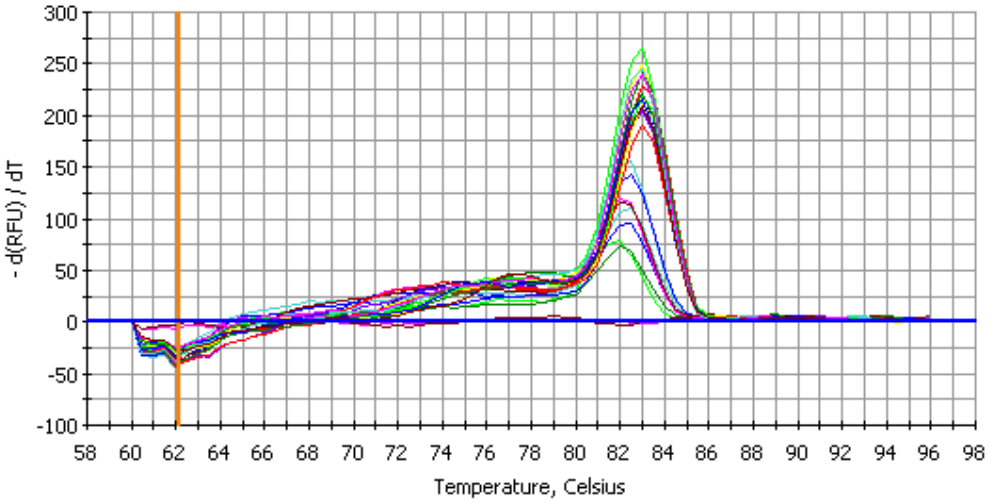

Figure 5.6b: Melt curve plot for CanX PCR. The distinct peaks indicate the Tm value of one PCR product. The melt peak has a T_m of 83°C.

The brown line in figure 5.9a just below the negative control (blue line with C_t of 35.9 and 36.9, see table 5.5) shows one of the replicates of CCH7 with no template or DNA, which as shown in table 5.5 has no C_t value. Figure 5.7a shows that threshold cycles of approximately between 20 and 28 were obtained indicating that the samples had varying amounts of template.

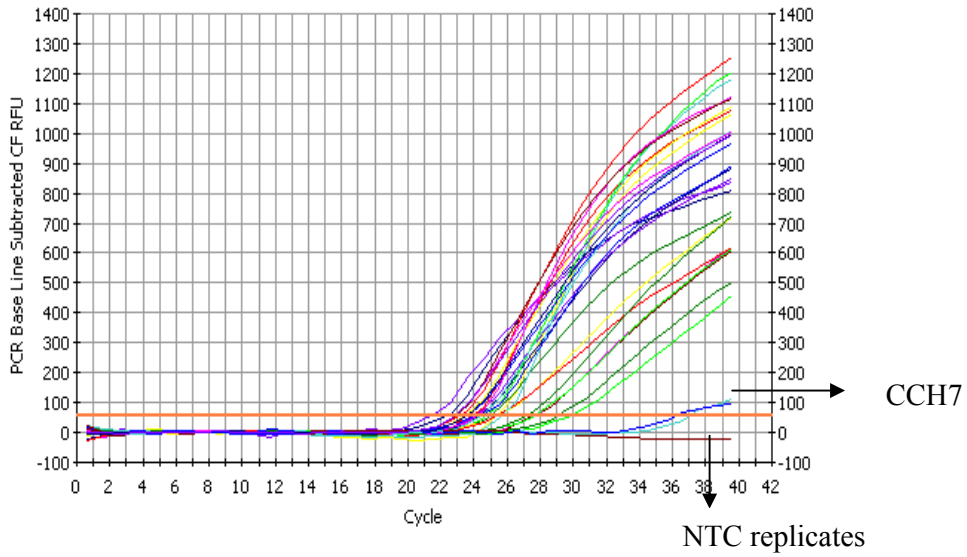

Figure 5.7a: Amplification plot for TBP PCR. NTC represents no template control replicates which have water as the negative control.

Figure 5.7b shows a melt peak with a T_m of 85°C, which represents the specific products of the samples used in the TBP PCR reaction.

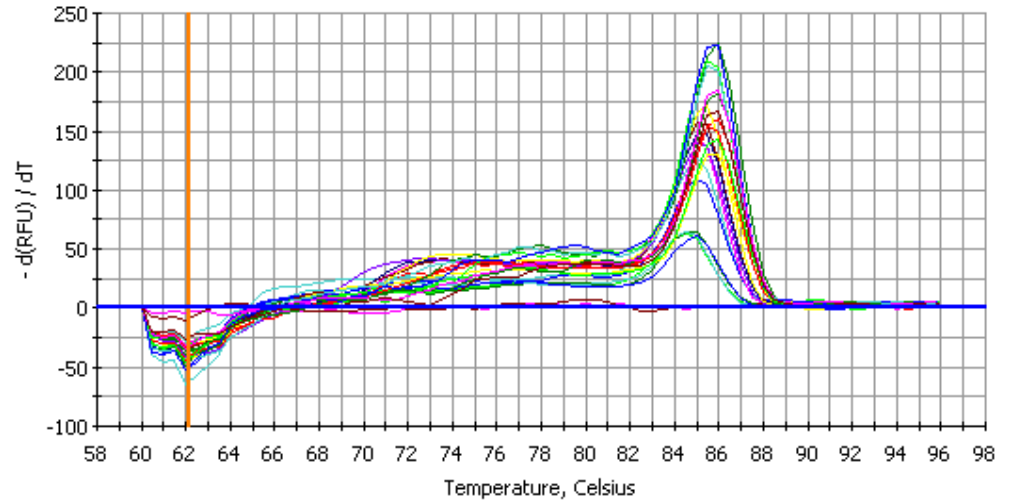

Figure 5.7b: Melt curve plot for TBP PCR. The distinct peaks indicate the Tm value of one PCR product. The melt peak has a T_m of 85°C.

Figure 5.8a shows threshold cycles of approximately between 20 and 24 were obtained indicating that the samples had varying amounts of template.

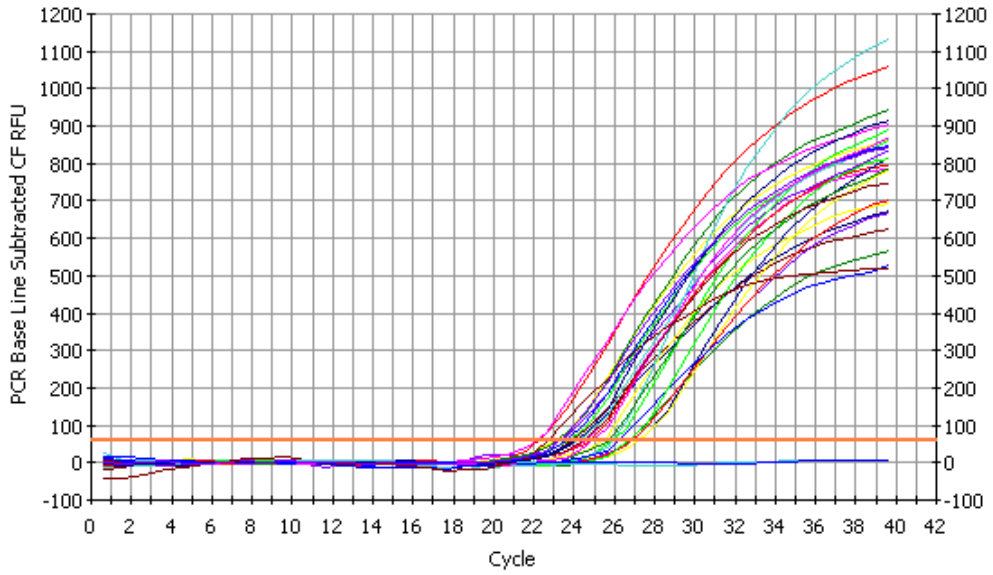

Figure 5.8a: Amplification plot for GLUT4 PCR.

Figure 5.8b shows a melt peak with a T_m of 90°C, which represents the specific products of the samples used in the GLUT4 PCR reaction.

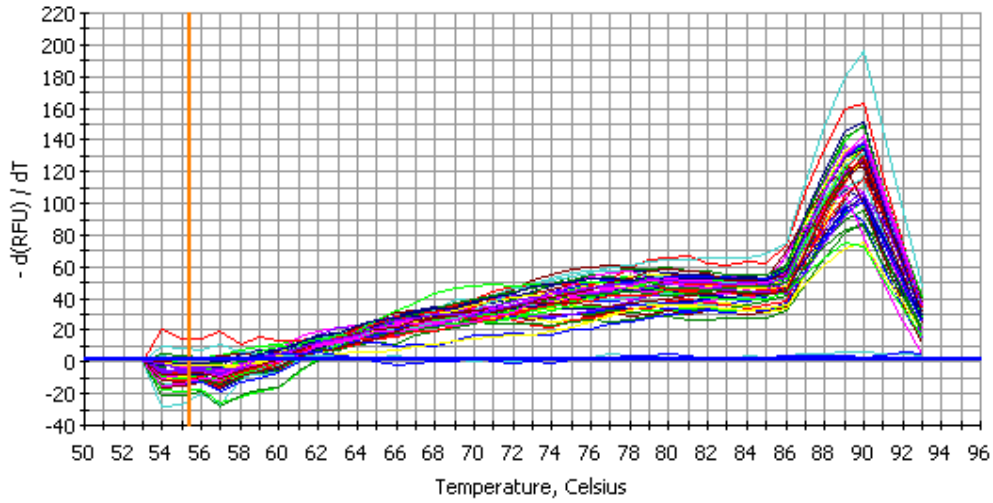

Figure 5.8 b: Amplification plot for GLUT4 PCR. The distinct peaks indicate the Tm value of one PCR product. The melt peak has a T_m of 90°C.

Table 5.5: PCR quantification of CanX, TBP and Glut4 showing the cycle threshold of samples.

Sample	C_t (CanX)	C_t (TBP)	C_t (Glut4)
COL2	23	23.9	26
COL2	23.2	24.5	26.1
COL4	20.1	22.2	24.9
COL4	19.9	21.9	24.8
COL5	21.5	21.5	26.2
COL5	21	22.3	24.5
COL6	19.4	21.4	29.3
COL6	19.9	21.8	28.9
COL7	21.7	22.4	23.6
COL7	21.4	22.7	21.9
COH2	20.1	23.6	28.1
COH2	19.9	24.4	27.6
COH3	24.8	26.6	25.2
COH3	25.3	26.3	24.9
COH5	19.1	21.8	21.8
COH5	19.9	22	21.7
COH6	20	21	22.5
COH6	19.9	21.2	22.3
COH7	22.9	28.8	31.8
COH7	22.3	28.2	30.9
CCL1	20.6	27.5	24.2
CCL1	20.4	27.4	23.6
CCL2	21.2	24.1	26.9
CCL2	21.3	23.8	26.6
CCL4	21.3	25.1	26.9
CCL4	21.1	25.1	26.6
CCL5	22.6	29.6	26.4
CCL5	22.5	28.8	25.3
CCH3	21.5	22.1	23.7
CCH3	20.9	21.2	22.9
CCH4	21	23.2	22.7
CCH4	20.8	22.9	22
CCH5	21.8	27.6	23.3
CCH5	21.5	26.9	22.8
CCH6	22.7	24.2	23.9
CCH6	21	23.3	23.2
CCH7	22.4	24	24.7
CCH7	22.6	N/A	24.1
PLANT1	24.1	25.3	25
PLANT1	23.8	23.6	24.5
PLANT2	23.3	24.5	25.6
PLANT2	23.8	24.8	26.5
PLANT3	23.9	25.6	25.7
PLANT3	24.2	23.9	26
PLANT4	21.6	22.8	21.8
PLANT4	21.7	22.7	22.5
PLANT5	21	23.3	23.8
PLANT5	21.2	22.7	23
WATER	N/A	36.9	N/A
WATER	N/A	35.9	N/A

Duplicate C_t values per sample were obtained after PCR. N/A indicates no reaction occurred hence no C_t value.

Analysis of raw C_t data is shown in table 5.5 for the samples with each gene. The software programs provided along with the various qPCR instruments permit straightforward extraction of threshold cycle values from the recorded fluorescence measurements (Figures 5.6 to 5.8). These programs usually do not process raw data into meaningful results, such as normalized and calibrated relative quantities. The major analysis tools all have one or more of the following problems; (i) intrinsic limitations: dedication for one instrument (ii) cumbersome data import (iii) a limited number of samples and genes can be processed (iv) forced number of replicates (v) normalization using only one reference gene (vi) lack of data quality controls (such as negative controls, reference gene expression stability, replicate variability), inability to calibrate multiple runs, limited result visualization options, lack of experimental archive and closed software architecture (Hellemans *et al*., 2007). However, qBase is the best available software at present.

Treatment with plant A increases glucose uptake in the adipose tissue (Karachi, 2009), plant A may increase GLUT4 expression, translocation and activation.

Initially, 5 different cohorts of rats were included in the qBase analysis from the RT-PCR generated results. The different groups were COL (5 samples), COH (5 samples), CCL (4 samples), CCH (5 samples) and Plant A treated (5 samples) rats. Only 4 samples of CCL were included as the RNA from adipose tissue in sample CCL6 was degraded (Figure 5.5 and table 5.4).

COL: denotes rats on a normal diet; lean control that were not insulin resistant and sacrificed at12 weeks. COH: denotes rats that were fed a HF diet that were insulin resistant and sacrificed at 12 weeks. The COL and COH were used to confirm if the rats on a high fat diet were insulin resistant. The groups COL and COH were sacrificed 4 weeks before the CCL, CCH and Plant A treated rats. Variable results were found with COL and COH, as shown in figure 5.9 and table 5.5, it was decided not to incorporate these as part of the controls for Plant A treated rats. Hence it was decided that CCL and CCH should be the low and high fat controls respectively for plant A treated rats as these three groups were sacrificed after the same duration of treatment i.e. 16 weeks. As shown in figure 5.9 there was a lot of variation (intra-

group variation) within a particular group of rats, hence GLUT4 expression differed from rat to rat as well as from group to group.

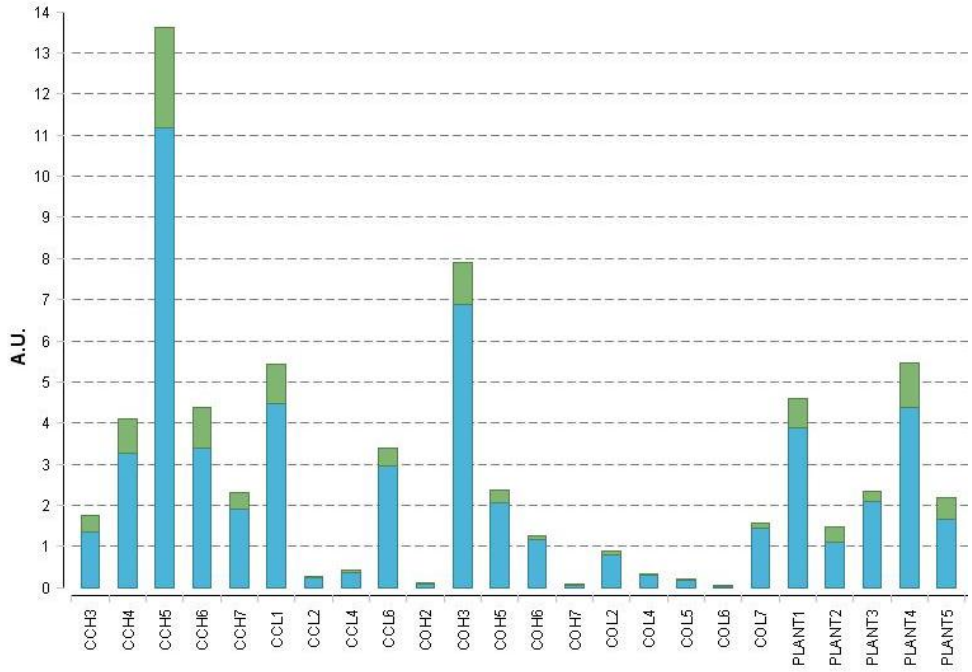

Figure 5.9: Single histogram of GLUT4 expression generated by qBase showing COL (low fat controls sacrificed after 12 weeks on a normal diet), COH (high fat controls sacrificed after 12 weeks on a high fat diet), CCL (low fat controls sacrificed after 16 weeks), CCH (high fat controls sacrificed after 16 weeks) and Plant A (sacrificed after 16 weeks; 12 weeks of high fat with 4 weeks of plant treatment) samples.

The data were further analyzed our data using qBase without the COH and COL and only incorporating CCL, CCH and Plant A. Figure 5.10 is a histogram showing this analysis excluding COH and COL. Rats CCH4 and Plant 2 were excluded from GLUT4 expression analysis (i) as a means to reduce variation within the groups and (ii) also to have the same number of rats in each group, since there are only 4 rat samples in the CCL group.

As indicated in figure 5.10, the CCL samples had lower GLUT4 expression compared to the CCH and plant A samples. GLUT4 expression in rat CCL1 was unusually high compared to the other rats of the CCL cohort. GLUT4 expression within the CCH group was fairly constant, with GLUT4 expression in CCH5 slightly higher than the other rats of the cohort. Great variation was observed in GLUT4 expression within the Plant A treated rats of the group.

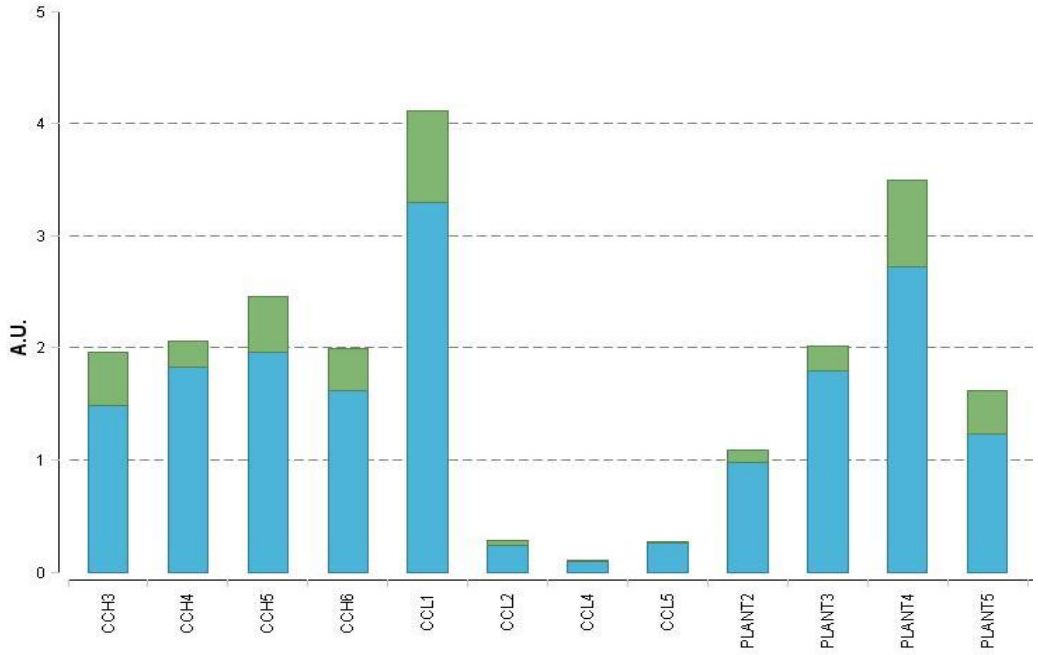

Figure 5.10: Single histogram of GLUT4 expression analysis generated by qBase showing individuals samples of CCL, CCH and Plant A.

Internal control genes are used to normalize mRNA fraction. The internal control is known as a housekeeping (HSK) or reference gene (Vandesompele *et al*., 2007). It is assumed that references genes (CanX and TBP in this study case) are expressed stably across all tested samples and can be used as using reference genes for the normalization of relative quantities (Hellemans *et al*., 2007). However literature shows that housekeeping gene expression can vary considerably (Vandesompele *et al*., 2002). Hellemans and colleagues stated that 'when using only one reference gene, its stability cannot be evaluated.' They further motivate that the use of multiple genes is paramount as it produces more reliable data and allows an evaluation of the stability of these genes (Hellemans *et al*., 2007).

Dealtry *et al*., 2006, tested TBP and CanX as potential HSK genes in adipose tissue, from rats fed diets containing differing amounts of fat to induce insulin resistance, they established that TBP and CanX could be used as HSK genes for rat adipose tissue. However they did not examine their use as HSK genes in plant A treated rats.

Ideally, a HSK gene should exhibit the same expression level across all samples after normalization (Vandesompele *et al*., 2002). The coefficient of variation (CV)

indicates how stably the gene is expressed. M denotes the gene stability (Hellemans *et al*., 2007). M and CV values of 1.903 and 78% respectively were obtained from the data generated in figure 5.10 and table 5.5, M and CV values lower than 0.5 and 25% respectively, are typically observed for stably expressed reference genes in relatively homogenous sample groups. In more heterogeneous groups, the mean M and CV values can increase to 1 and 50% respectively (Hellemans *et al*., 2007). In this study the GLUT4 expression sample groups were very heterogeneous or variable. The problem lies in the HSK genes chosen. I suggest that HSK genes stably expressed in plant A treated samples should have been identified before attempting to quantify GLUT4 expression in these samples. Another suggestion is that a larger group of rats in each cohort should have been reared to get a more accurate representation of GLUT4 expression or alternatively more HSK genes should have been incorporated. A third problem could be due to the fact that qPCR calculation models could be improved (Hellemans *et al*., 2007). Furthermore assessment of statistical significance requires a standardized data set, because variation in data from multiple replicates might not result in statistically significant differences, although the biological effect is clearly distinguishable in each of the individual replicates (Willems *et al*., 2008). Willems and colleagues have recently described a data standardization procedure that can be applied to data sets that show high variation between biological replicates, which enables proper statistical analysis, so that relevant conclusions can be drawn (Willems *et al*., 2008).

Figure 5.11 shows the relative GLUT4 expression from the means of the groups CCL, CCH and Plant A, generated from figure 5.9. Hence figure 5.11 is a representation of the mean relative GLUT4 expression taken from each sample (Figure 5.10) within a particular group. It is also indicated in figure 5.11 that there is no significant difference in GLUT4 expression between CCL, CCH ($p<0.38$) and Plant A ($p<0.44$), although there is a trend of increased expression in the CCH and plant A treated groups. The figure shows that CCL (normal-low fat control) had the lowest average GLUT4 expression compared to CCH (insulin resistant rats on a high fat diet) and Plant A (plant A treated rats). CCH had the highest GLUT4 expression compared to CCL and plant A. The data shown in figure 5.11 indicating an increase in GLUT4 expression in the insulin resistant rats was unexpected. The increase in GLUT4 expression in the insulin resistant rat adipose tissues vastly contrasts those of literature

which state that GLUT4 expression is decreased in the DM2 and insulin resistant states (Kim *et al*., 2007). In the insulin resistant and DM2 states, GLUT4 is not translocated to the membrane in order to transport glucose into the cell (Gnudi *et al*., 1996).

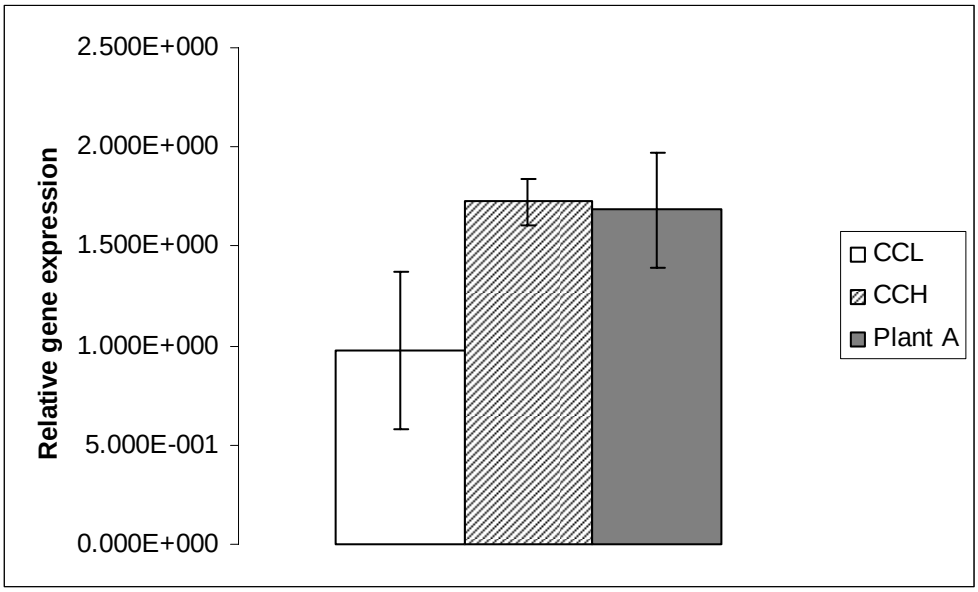

Figure 5.11: Relative GLUT4 expression in CCL, CCH and Plant A. Values are represented as a means ± SD (n=4). For statistical analysis the t-test was used.

Impaired insulin-stimulated glucose transport into muscle and adipose tissue could be due to defects in the intracellular signalling mechanisms of insulin, leading to altered glucose-transporter translocation, fusion with the plasma membrane, or activation. On the other hand, reduced insulin-stimulated glucose transport could be due to a decrease in the expression of glucose transporters. Evidence suggests that both these mechanisms may contribute to insulin resistance in obesity and diabetes in animal models and in human subjects (Gnudi *et al*., 1996).

It is unknown as to why there was an increase in mRNA GLUT4 expression in the untreated insulin resistant rats (CCH) when compared to the non-insulin resistant rats (CCL), as insulin resistance induces a decrease in mRNA GLUT4 expression (Panunti *et al*., 2004). Plant A may not affect GLUT4 expression when compared to the untreated control; CCL (Figure 5.10) or translocation into the membrane.

It is possible plant A may activate GLUT1 expression and activity. Hence inducing increased glucose uptake in adipose tissue of the plant A treated rats. This results in improved insulin resistance following GLUT1 translocation to the membrane and therefore increased GLUT-1 facilitated glucose transportation. However further studies need to be conducted to determine the effect of plant A on GLUT1 expression. Studies using berberine (alkaloid compound from medicinal plants) increased GLUT1 expression and activity, hence increasing glucose uptake (Kim *et al*., 2007).

5.3.2. The effect of Plant A on glucokinase RNA expression in rat testicular adipose tissue

Figure 5.12a and 5.12b show the amplification plot and melt curve analysis of the glucokinase primer product respectively in adipose tissue. As observed in figure 5.12b, no reaction occurred, as there is no distinct peak of an amplicon, and the C_t was above 30. This attempt was repeated 3 times even with a temperature gradient to determine the most suitable annealing temperature for the glucokinase reverse and forward primers. The gradient feature of the iCycler allows the testing of a range of annealing temperatures simultaneously (BioRad, USA). Annealing temperatures are vital to optimize the PCR reactions. I conclude that the designed glucokinase primers were not effective. The glucokinase primers were designed using Beacon Design software, however it was difficult to design these specific primers and this compromised primer design.

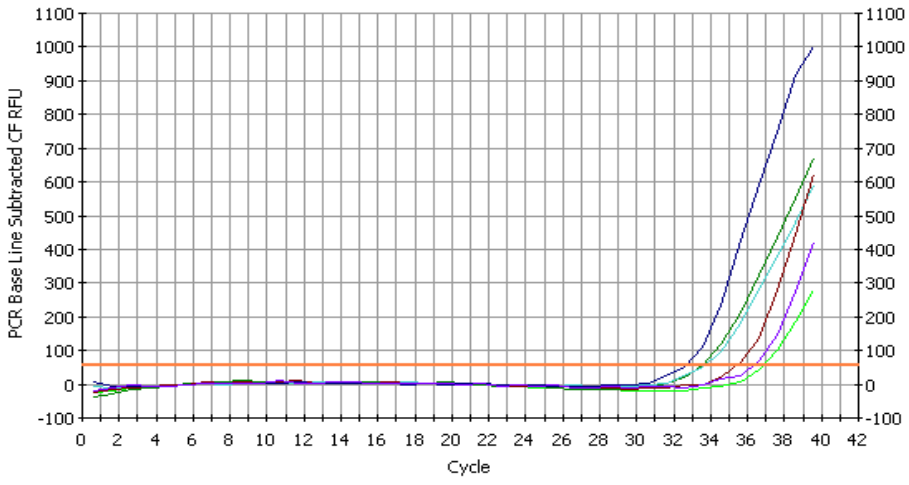

Figure 5.12 a: Amplification plot cycle for glucokinase.

Figure 5.11b shows no melt peak in the Glucokinase PCR reaction.

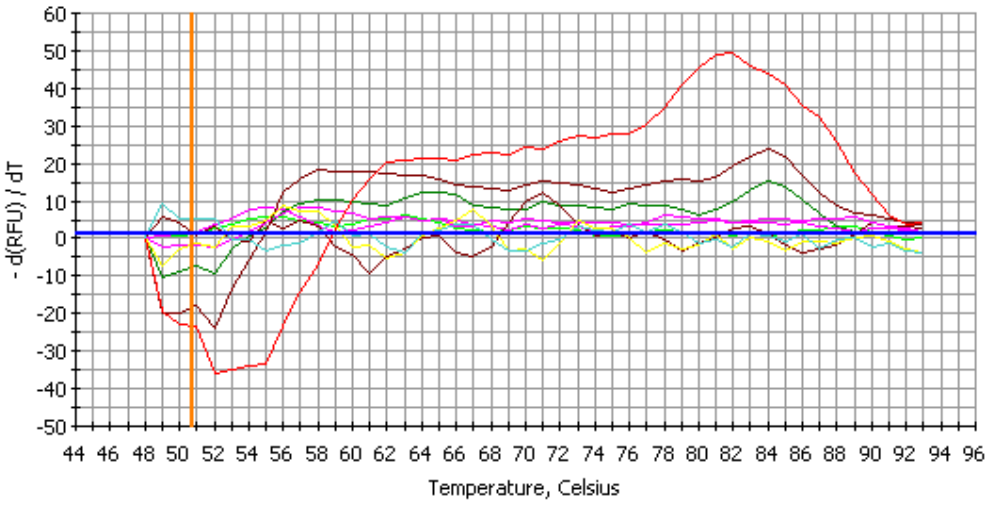

Figure 5.12 b: Melt curve for glucokinase.

5.3.3 Differentiation of 3T3-L1 cells

The differentiation of 3T3-L1 (a preadipocyte cell line) was monitored by observing morphological changes and performing ORO staining procedures. The first batch of cells that was removed from cryopreservation did not differentiate and the phenomenon of extensive 'lifting' or 'peeling' of the cells was observed as shown in figure 5.13.

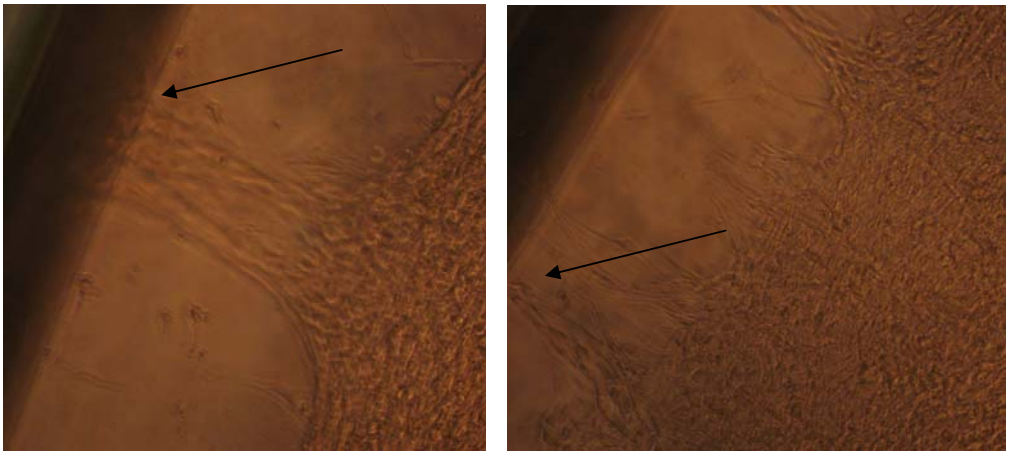

Figure 5.13: Lifting of 3T3-L1 cells after 4 days of treatment with differentiation media (IBMX, DEX and insulin) under X200 magnification. Arrows show 3T3-L1 cells lifting.

Initially, several attempts were made to differentiate the cells with an IBMX, DEX, and insulin cocktail mix as previously described (Toscani *et al*., 1990). Attempts were

made to coat the plates with collagen before seeding for differentiation experiment but with little improvement in ameliorating lifting. Cells were observed to survive 2 more days after treatment with differentiation media before lifting when the plates were treated with collagen as compared the non-collagen treated plates. This was not sufficient time for the cells to differentiate, as they usually require 7 days of differentiation (Toscani *et al*., 1990). Different methods were tested for 8 weeks in an attempt to prevent lifting and promote subsequent differentiation in 3T3-L1; in addition more lifting was observed with higher passage numbers. It was concluded that the cells from this batch had already mutated. The lifting phenomenon with 3T3-LI cells has been encountered by many researchers in the past (Tomlinson *et al*., 2006, www.protocol-online.org). Lifting in 3T3-L1 cells may be attributed to the differentiation media (IBMX, DEX and insulin mix) used to differentiate the cells, perhaps one of the components induced lifting in 3T3-L1 cells, however this warrants further studies to be undertaken.

Another batch of 3T3-L1 cells were removed from cryopreservation. These cells displayed minimal lifting. It was then decided to use rosiglitazone (a PPARγ-agonist) as an agent to differentiate the 3T3-L1 preadipocytes into adipocytes.

5.3.3.1 Morphological changes in differentiated 3T3-L1

The reason for differentiating 3T3-L1 preadipocytes into adipocytes is because 3T3-L1 preadipocytes do not have insulin mediated glucose uptake. This is because 3T3-L1 preadipocytes do not have sufficient numbers of insulin receptors and those present have low affinity for insulin, therefore an increase in the insulin binding capacity and an increase in receptor number only occur during differentiation of 3T3-L1 cells (Reed and Lane, 1980). In addition, there is expression of GLUT4 only in differentiated adipocytes (Ueyama *et al*., 1999), as stated previously GLUT4 transports glucose in response to insulin. It is known that the 3T3-L1 cell line is among the most characterized and reliable model for studying the conversion of preadipocytes to adipocytes (Ntambi and Kim, 2000). The ORO dye was used in the adipocyte differentiation studies. 'Morphological analysis of lipid accumulation has been shown to correlate with the differentiation state of the cell' (Toscani *et al*., 1990). Figure 5.14 shows the morphological changes that occur from a 3T3-L1 preadipocyte to a differentiated 3T3-L1 preadipocyte. Differentiated 3T3-L1

preadipocytes have most of the ultra structural characteristics of adipocytes from animal tissue (Ntambi and Kim, 2000). As observed in figure 5.14 c to f, differentiated 3T3-L1 preadipocyte develop fat droplets as in adipose tissue.

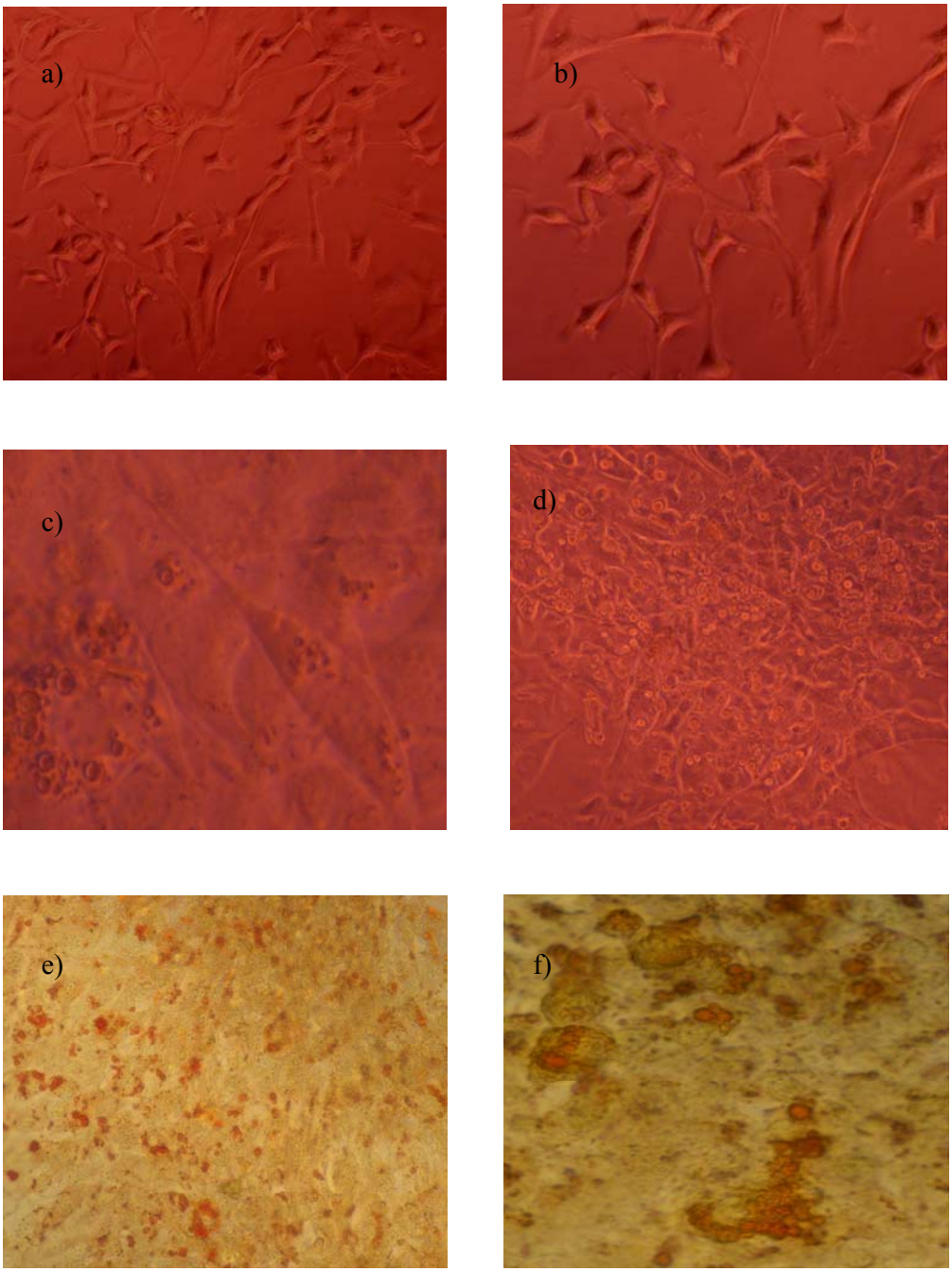

Figure 5.14: Morphological changes in 3T3-L1 adipocytes after 10 days of 10 µm rosiglitazone treatment under 400X magnification using a Zeiss microscope (a) and b) untreated cells, (c) to (f) cells treated with rosiglitazone, (c) and (d) no ORO staining, (e) ORO staining of lipid droplets under X200 magnification and (f) ORO staining of lipid droplets under X400 magnification.

Figure 5.14 e and f indicate the accumulation of high concentrations of intracellular lipid as detected microscopically using a lipid specific fat soluble dye Oil Red O. Figure 5.14 g shows that rosiglitazone significantly induced differentiation (detected by accumulation of lipid droplets) in treated cells (0.19 ± 0.06 absorbance units) compared to the untreated cells (0.04 ± 0.03 absorbance units). Rosiglitazone is a thiazolidinedione (TZD). Thiazolidinediones are a class of oral insulin-sensitizing drugs used in DM2 treatment (Juvet *et al*., 2003). These drugs are high-affinity ligands for peroxisomes proliferator activated receptors. It is thought that the glucose-lowering ability of TZD occurs by activating PPARγ (Velebit *et al*., 2008). The mechanism of action of TZDs is in adipose tissue since PPARγ is abundantly expressed in adipose tissue. PPARγ agonists control adipocyte differentiation, while PPARγ activation improves insulin resistance. Rosiglitazone is a PPARγ agonist and our results in figure 5.14 c to 5.14 g indicate that this drug induces differentiation in 3T3-L1, Velebit and colleagues also found that rosiglitazone induced differentiation in 3T3-L1 (Velebit *et al*., 2008). TZDs upregulate lipid biosynthesis and glucose transport in adipocytes (Liu *et al*., 2001).

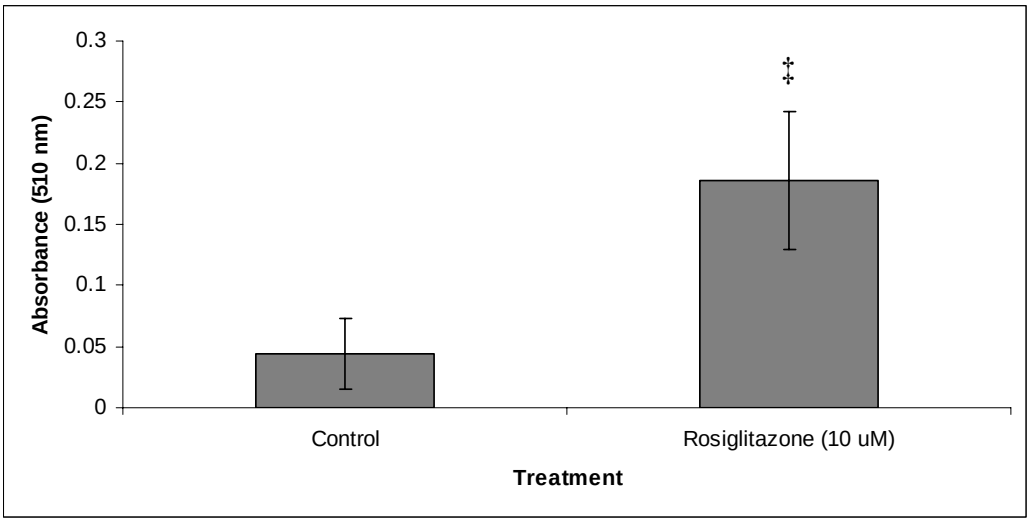

Figure 5.14 g: Quantification of adipocyte differentiation using ORO staining at 520 nm. Sub confluent, actively proliferating 3T3-L1 cells were treated with either 10 µM rosiglitazone or 3T3-L1 media only. At 10 days after treatment, the cultures were fixed with formaldehyde and stained with Oil Red O. The absorbance was read at 520 nm. ‡ P<0.02 when compared to the control.

5.3.3.2 Cytotoxicity studies of plant A on differentiated 3T3-L1 adipocytes

Figure 5.15 shows the effect of varying concentrations of plant A (from 0.0025 mg/mL to 1mg/mL) on 3T3-L1 adipocytes. It is notable from figure 5.15 that 0.2 mg/mL of plant A was toxic to the 3T3-L1 pre-adipocytes, as less than 80% of the cells survived.

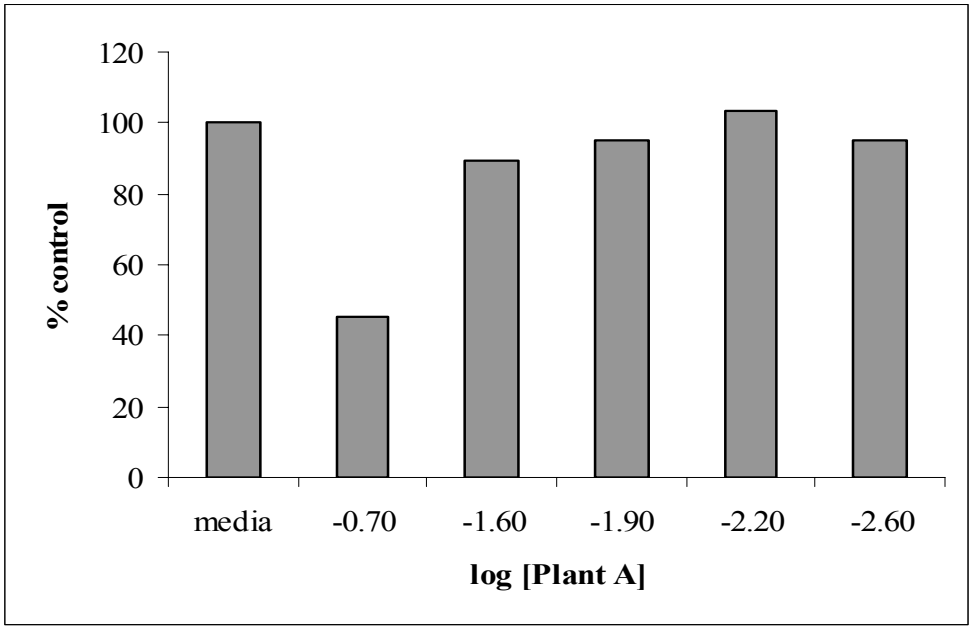

Figure 5.15: Cytotoxicity results of plant A extract on 3T3-L1. Cells were seeded in a 48 well plate at a density of 3 x 10^4 cells/well and incubated for a 24-h period. The cells were treated with plant A extract and incubated for a 48-h period. Plant A concentrations ranged between 0.0025 and 0.2 mg/ml. Data points represent the mean ± SD (n=3) from a single experiment.

5.3.3.3 The effect of plant A on glucose utilization in differentiated 3T3-L1 adipocytes

The acute effect of plant A and insulin on glucose utilization in differentiated 3T3 adipocyte is indicated in figure 5.16. Figure 5.16 shows that 1 μM insulin slightly but not significantly increased glucose utilization as compared to the control wells containing cells treated with RPMI media with 8 mM glucose. Insulin was used as a positive control as it increases glucose uptake in adipose tissue and differentiated 3T3-L1 adipocytes. There is only one set of the experiments that insulin significantly increased glucose utilization. In the presence of insulin, GLUT4 is translocated from subcellular membranes to the PM of adipocytes. Insulin increases the mobilization of cell surface GLUT1 by 5 fold and GLUT4 by 15-20 fold. Translocation of glucose

transporters to the PM precedes glucose transport (Yang *et al*., 1992). It is through translocation to the PM that the glucose transported is activated and this is how insulin stimulates glucose transport in adipocytes (Vogt *et al*., 1991). In addition, insulin modulates the activity of the glucose transportation so as to activate glucose uptake (Vogt *et al*., 1992).

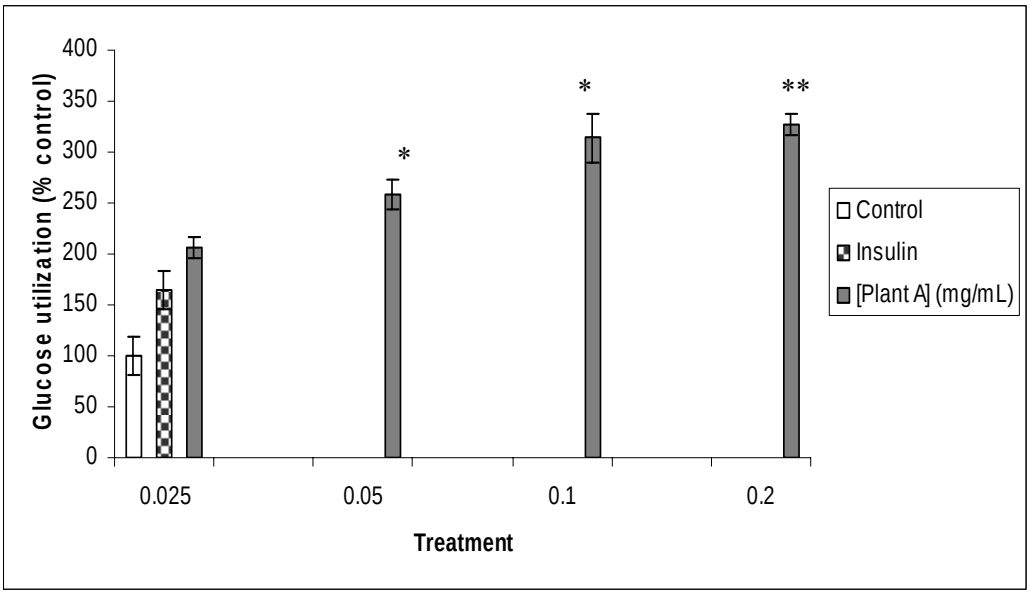

Figure 5.16: The acute effect of plant A on glucose utilization in rosiglitazone differentiated 3T3-L1 preadipocytes after 180 min. Experiments were conducted after 10 days of differentiation with 10 µM rosiglitazone. The negative control was when RPMI media containing 8 mM glucose was used to treat the cells. 1 µM insulin was used as a positive control. Plant extract concentrations of 0.025, 0.05, 0.1 and 0.2 mg/mL were used to treat the cells. Data are represented as means ± SE (n=3). ** P < 0.01, * P<0.05 when compared to the control.

0.025 mg/mL of plant A caused the differentiated 3T3-L1 preadipocytes to increase glucose utilization as compared to the negative control and insulin. There was a significant increase ($p<0.05$) in glucose uptake when the 3T3-L1 cells were treated with 0.05 mg/mL of plant A. 0.1 mg/mL plant A treatment induced the cells to significantly ($p<0.05$) increase glucose utilization. The highest concentration of 0.2 mg/mL plant A induced the 3T3-L1 cells to significantly increase glucose utilization ($p<0.01$). Plant A induced glucose utilization in the 3T3-L1 in a dose response manner; the highest plant A concentration used induced the most glucose utilization within the differentiated 3T3-L1 preadipocytes. The results in this study correlate with those of Karachi, (2009) as indicated in table 1.2 who found that adipose tissue from rats treated with plant A had increased glucose utilization. The increased glucose utilization in 3T3-L1 cells on plant A treatment could be attributed to the speculated

increase in GLUT1 expression and hence increased GLUT1 activity induced by plant A. The increase in GLUT1 expression and hence activity may be the mechanism by which plant A increases glucose transport. Plant A induced high C peptide levels in rat plasma samples (Figure 4.10). The increased glucose utilization could be attributed to C-peptide levels as C-peptide has been implicated in increasing glucose utilization (Willhem *et al*., 2008).

CHAPTER SIX: CONCLUSIONS AND RECOMMENDATIONS

There was an increase in G6Pase activity (catalytic subunit) in the insulin resistant rats. It was concluded that one cannot use G6Pase as a marker for insulin resistance if an intact G6Pase system is not obtained. Samples that have undergone freeze and thaw cycles are also not recommended for use when attempting to measure G6Pase activity, freeze and thaw cycles were likely to have occurred during analysis of samples for different experiments. It is speculated that the detergents used to measure G6Pase activity may change the conformation of the G6Pase system or disrupt its integrity. Overall, G6Pase activity can only be used as an insulin resistant marker when intact microsomes are isolated.

The use of GK as an alternative marker for insulin resistance was not established in this study since the insulin resistant rats (CCH) did not have significantly lower GK activity.

INS-1 cells secrete insulin in a glucose dependent way (Hugl and Merger, 2007). In this study, INS-1 cells did not produce insulin with response to increasing glucose concentrations. More insulin was produced by INS-1 cells when exposed to 2.5 mM glucose than when exposed to 20 mM glucose. The batch of INS-1 cells may have limited glucose responsiveness capacity during acute challenge. I also suggest routine checks to verify the effect of stimulatory concentrations of glucose on plasma membrane potential as a means to combat the effect of loss of glucose responsiveness or notice the limitation as performed by Fulceri *et al*.(2000). I suggest that a new batch of INS-1 cells be purchased for acute and chronic challenge studies. Other cell lines such as the BRIN-BD11; insulin secreting clonal rat cell line (Hannan *et al*., 2006) produced from electrofusion of RINmF5 (Gray *et al*., 2000) or RINmF5; rat pancreatic insulin secreting immortal cell line (Gray *et al*., 2000) may also be utilized in future to achieve testing the effect of plant A and other potential anti-diabetic plants on insulin secretion under varying glucose concentrations in insulin secreting cells.

1 mM diazoxide decreased insulin secretion by INS-1 cells more than 100 μM verapamil. 100 μM diazoxide combined with 0.0125 mg/mL plant A may influence

the closing of K_{ATP} as a mode of stimulating insulin secretion. Interestingly, additive effects by plant A combined with glibenclamide on insulin secretion by INS-1 cells were not observed. The effect of verapamil and plant A combinations did not increase insulin secretion, suggesting that plant A does not induce insulin secretion via opening the Ca^{2+} voltage channels. The effect of verapamil, diazoxide and glibenclamide combined with plant A should be repeated with more varied concentrations.

The lower plant A concentrations induced an increase in insulin secretion by the INS-1 cells at basal conditions although not significantly when compared to the control. The most insulin was secreted by INS-1 cells at basal conditions when the cells were exposed to 0.0125 mg/mL plant A. 0.1 mg/mL plant A stimulated less insulin secretion by the INS-1 cells at basal conditions when compared to the control. It is possible that the higher plant concentrations stimulate insulin secretion in response to prevailing glucose concentrations, thus, the higher the glucose concentration the more insulin is secreted by the INS-1 cells in the presence of plant A. It would have been beneficial to determine the effect of plant A at high glucose concentrations (15 – 20 mM) and low glucose concentrations (2- 4 mM). However, due to a morphological change in the INS-1 cells and lack of response to glucose, these experiments could not be conducted. This effect could be determined in further studies. The ideal plant would induce insulin secretion in β cells with response to high prevailing glucose concentrations and not stimulate insulin secretion at low glucose concentrations.

A decrease in glucose stimulated insulin secretion on acute treatment of INS-1 cells with high glucose levels (15 mM and 20 mM glucose) was observed as shown in figure 3.12, however interestingly a decrease in insulin content at 15 mM and 20 mM glucose on acute treatment with these high glucose levels was not observed. I conclude that changes in gene expression need to occur for insulin content to be decreased in β cells when exposed to high glucose levels which would require chronic treatment as opposed to acute treatment. Further studies on the effect of glucose and plant A on INS-1 expression of exocytosis proteins should be conducted. Prolonged β cell exposure to high glucose concentrations causing glucotoxicity impairs gene transcription of insulin and results in decreased insulin synthesis and eventually secretion (Panunti *et al*., 2004).

In all the insulin secretion studies it would have been best to represent the insulin secretion in terms of protein or cells/well for a better quantitative representation of insulin concentrations obtained from the studies. This was realised later on by the investigator.

The effect of plant A on INS-1 β cell proliferation should be conducted in future studies, one can determine the presence of proliferation markers such as Ki-67, which is a nuclear antigen associated with cell proliferation, its presence is found in the active cycle and absent in resting cells. Thus an increase in expression of Ki-67 is a reflection of cell proliferation (Honegger *et al*., 2003).

There was no significant difference in GLUT4 expression in plant A treated adipose tissue when compared to the non-insulin resistant rats (CCL) and the insulin resistant rats. In the absence of insulin, plant A (0.05 mg/mL, 0.1 mg/mL and 0.2 mg/mL) induced a significant increase in glucose uptake by 3T3-L1 cells when compared to the untreated control. Further studies should incorporate the effect of plant A in the presence of insulin on 3T3-L1 glucose utilization (Kim *et al*., 2007). This study would elucidate whether plant A has insulin like (if there is no synergistic effect on glucose utilization when 3T3-L1 cells are treated with plant A combined with insulin treatment) or plant A has insulin-sensitizing effect (if there is an additive effect in glucose utilization when 3T3-L1 cells are treated with plant A combined with insulin treatment). Plant A may improve insulin sensitivity or ameliorate insulin resistance or has insulin-like effects in adipose tissue, although the mechanism of action still needs to be elucidated in further studies with the plant.

In vitro studies using human DPP IV indicated that plant A did not decrease human DPP IV activity. I conclude that plant A may be an indirect inhibitor of DPP IV, perhaps by lowering gene expression and hence lowering DPP IV concentration within the body. Further *in vitro* DPP IV studies should incorporate the use of a known DPP IV inhibitor as a control such as vildagliptin instead of using metformin. In rat *in vivo* studies, plant A decreased DPP IV activity when compared to the normal and insulin resistant rats. It is concluded that plant A increases insulin secretion by lowering DPP IV activity and hence increasing the half-life of GLP-1, which eventually promotes insulin secretion from β cells. It is suggested that further studies

should incorporate a larger cohort of rats to get a better representation of DPP IV activity within a group.

This study showed that plant A increased insulin secretion in the presence of an insulin secretory inhibitor (diazoxide). Thereby, indicating that plant A stimulates insulin secretion by targeting the closure of the K_{ATP} channel. It is inconclusive whether plant A increases insulin secretion at higher glucose concentrations and further studies need to be conducted on glucose responsive insulin secreting cell lines. *In vitro* studies showed that plant A did not have an effect on human DPP IV activity, however *in vivo* studies showed that plant A decreased rat DPP IV activity. These data suggest that plant A is implicated in increasing insulin secretion by indirectly inhibiting DPP IV. In this investigation, plant A treatment was observed to decrease IDE levels and hence decrease insulin degradation, however for more conclusive and statistical significant data, the experiment needed to be performed more than once and with more replicates per sample, due to cost and reagent limitation, this was not possible.

REFERENCES

Agius L. 2008. Glucokinase and molecular aspects of liver glycogen metabolism. *Biochem J*, 414:1–18.

Agius L. 2009. Targeting hepatic glucokinase in type II diabetes. *Diabetes*, 58:18-20.

Ahren B, Gudbjartsson T, Al Amin AN, Martensson H, Myrsen-Axcrona U, Karlsson S, Mulder H, Sundler F. 1999. Islet perturbations in rats fed a high-fat diet. *Pancreas* 18: 75–83.

Amano J and Oshima M. 1999. Expression of the H type 1 blood group antigen during enterocytic differentiation of Caco-2cells. *The journal of Biological Chemistry*, 274: 21209-21216.

Andrews C and Shultz J. 1995. Protein quantitation using the quantify protein assay system. *Promega Notes Magazine*, 52:20-23.

Arion, WJ, Canfield WK, Ramos FC, Su ML, Burger HJ, Hermmerie H, Schubert G, Below P, Herling AW. 1998. Chlorogenic acid analogue S 3483: a potent competitive inhibitor of the hepatic and renal glucose-6-phosphatase systems. *Arch. Biochem.Biophys*, 351:279-285.

Bollheimer LC, Skelly RH, Chester MW, McGarry JD, Rhodes CJ. 1998. Chronic exposure to free fatty acid reduces pancreatic β cell insulin content by increasing basal insulin secretion that is not compensated for by a corresponding increase in proinsulin biosynthesis translation. *J. Clin. Invest*, 101:1094-1101.

Brennan CL, Hoenig M, Ferguson DC. 2004. GLUT4 but not GLUT1 expression decreases early in the development of feline development. *Domestic Animal Endocrinology*, 26:291-301.

Buettner R, Parhofer KG, M Woenckhaus M, Wrede CE, Kunz-Schughart LA, J Schölmerich J, Bollheimer LC. 2006. Defining high-fat-diet rat models: metabolic and molecular effects of different fat types. *Journal of Molecular Endocrinology*, 36: 485–501.

Burchell A and Clottes E. 1998. Three thiol Groups are important for the activity of the liver microsomal Glucose-6-Phosphatase system. *The American society for Biochemistry and Molecular Biology*, 273:19391-19397.

Carantoni M, Abbasi F, Warmerdam F, Klebanov M, Wang P, Chen YDI, Salman Azhar S, Reaven GM. 1998. Relationship between insulin resistance and partially oxidized LDL in healthy nondiabetic volunteers. *Arterioscler Thromb Vasc Biol*., 18:762-767.

Castelhano AL, Dong H, Fyfe MFC, Gardner LS, Kamikozawa Y, Kurabayashi S, Nawano M, Ohashi R, Procter MJ, Qui L, Rasamison CM, Schofield KL, Shah VK, Ueta K, Williams GM, Witter D, Yasuda K. 2005. Glucokinase-activating ureas. *Bioorganic & Medicinal chemistry letters*, 15:1501-1504.

Chen X, Scholl TO, Leskiw MJ, Donaldson MR, Stein TP. 2003. Association of glutathione peroxidase activvity with insulin resistance and dietary fat intake during normal pregnancy. *The Journal of Endocrinology and Metabolism*, 88:5963-5968.

Cheon HG, Kim SS, Kim KR, Rhee SD, Yang SD, Ahn JH ,Park SD, Lee JM,Jung WH, Lee HS, Kim HY. 2005. Inhibition of dipeptidyl peptidase IV by novel inhibitors with pyrazolidine scaffold. *Biochemical Pharmacology*, 70:22–29.

Clore, J N, Stillman, J, Sugerman, H. 2000. Glucose-6-Phosphatase flux *in vitro* is increased in Type 2 Diabetes. *Diabetes*, 49:969-973.

Clottes, E and Burchell. 1998. Three Thiol groups are important for the activity of the liver microsomal glucose-6-phosphatase system. *The Journal of biological chemistry*, 273:19391-19397.

Cogan, E B, Birrell, G B, Griffith, O H. 1999. A robotics-based automated assay for inorganic and organic phosphates. *Analytical biochemistry*, 271:29-35.

Collier, J J and Scott, D K. 2004. Sweet changes; Glucose Homeostasis can be altered by manipulating genes controlling hepatic glucose metabolism. *Molecular Endocrinology*, 18:1051-1063.

de Kok JB, Roelofs RW, Giesendorf BA, Pennings JL, Waas ET, Feuth T, Swinkels DW, Span PN. 2005. Normalization of gene expression measurements in tumour tissues: comparison of 13 endogenous control genes. *Laboratory Investigation*, 85:154-159.

Deacon CF and Holst JJ. 2006. Dipeptidyl peptidase IV inhibitors: A promising new therapeutic approach for the management of type 2 diabetes. *The International Journal of Biochemistry & Cell Biology* ,38: 831–844.

Dealtry G, Coetzee C, Louw J, Roux S. 2006. Comparison of PPARγ and mRNA expression in different fat pads of male and female rats on a diabetes inducing diet. *Diabetic Medicine*, 23:477.

Diabetes Voice. 2007. *International Diabetes Federation 5th edition*, 52:1-48.

Dubois M, Vacher P, Roger B, Huyghe D, Vandewalle B, Kerr-Conte J, Pattou F, Moustaid-Moussa N, Lang J. 2007. Glucotoxicity inhibits late steps of insulin exocytosis. *Endocrinology*, 148:1605-1614.

Duckworth WC, Bennet RG, Hamel FG. 1998. Insulin degradation: progress and potential. *The Endocrine Society*, 5:608-624.

Farris W, Mansourian S, Leissring MA, Eckman EA, Bertram L, Eckman CB, Tanzi RE, Selkoe DJ. 2004. Partial Loss-of-Function Mutations in Insulin-Degrading Enzyme that Induce Diabetes also Impair Degradation of Amyloid ß-Protein. *American Journal of Pathology,* 164:1425-1434.

Freshney RI. 1994, Cultured of animal cells 3rd edition. *Wiley-Liss, Inc* 11-14.

Fulceri R, Kardon T, Banhegyi G, Pralong WF, Gamberucci A, Marcolongo P, Benedetii A. 2000. Glucose-6-phosphatase in the insulin secreting cell line INS-1. *Biochemical and Biophysical Research communications*, 375:103-107.

Gibbon, C. 2005. South African Medical Formulary (SAMF). 7th Edition. Pinelands .

Gierow, P and Jergh, B. 1998. Spectrophotometric method for Glucose-6-Phosphate Phosphatase. *Analytical Biochemistry*, 327:114-118.

Gnudi L, Shepherd PR, Kahn B. 1996. Over-expression of GLUT4 selectively in adipose tissue in transgenic mice: implications for nutrient partitioning. *Proceedings of the Nutrition Society*, 55:191-199.

Göpel, SO, Kanno T, Barg S, Weng XG., Gromada J, Rorsman, P. 2000. Regulation of glucagon release in mouse α-cells by K_{ATP} channels and inactivation of TTX-sensitive Na^+ channels. *The Journal of Physiology*, 528:509-520.

Gould GW and Holman GD. 1993. The glucose transporter family: structure, function and tissue-specific expression. *Biochem J*, 295: 329-341.

Gray AM, Abdel-Wahab YHA, Flat PR. 2000. The traditional plant treatment, *Sambucus nigra*, exhibits insulin like and insulin releasing actions *in vitro*. *Journal of Nutrition*, 130:15-20.

Gray AM, Flatt PR. 1999. Insulin-secreting activity of the traditional antidiabetic plant Viscum album (mistletoe). *Journal of Endocrinology*, 160:409-414.

Green BD, Irwin N, Duffy NA, Gault VA, Harte FPM, Flatt PR. 2006. Inhibition of dipeptidyl peptidase-IV activity by metformin enhances the antidiabetic effects of glucagon like peptide-1. *European Journal of Pharmacology*, 547:192-199.

Gu HF, Efendic, S, Nordman, S, Ostenson, CG, Brismar, K, Brookes, AJ, Prince, JA. 2004. Quantitative Trait Loci Near the Insulin-Degrading Enzyme (*IDE*) Gene Contribute to Variation in Plasma Insulin Levels. *Diabetes*, 53:2137- 2142.

Hannan JMA, Marenah L, Ali L, Rokeya B, Flatt PR, Abdel-Wahab YHA. 2006. Ocimum sanctum leaf extracts stimulate insulin secretion from perfused pancreas isolated islets and clonal pancreatic β-cells. *Journal of Endocrinology*, 189:127-13.

Hřebíček J, Janout V, Malinčíková J, Horáková D, Čížek L. 2002. Detection of Insulin Resistance by Simple Quantitative Insulin Sensitivity Check Index QUICKI for Epidemiological Assessment and Prevention. *The Journal of Clinical Endocrinology & Metabolism*, 87:144-147.

Hellemans J, Mortier G, De Paupe A, Speleman F, Vandesompele J. 2007. qBase relative quantification framework and software for management and automated analysis of real-time quantitative PCR data. *Genome Biology*, 8:R19.

Henquin, JC. 2000. Triggering and amplifying pathways of regulation of insulin secretion by glucose, *Diabetes*, 49: 1751-1760.

Henriksson M, Johansson J, Moede T, Liebiger I, Shafqat J, Berggren PO, Jornvall H. 2006. Proinsulin C-peptide and insulin: Limited pattern similarities of interest in inter-peptide interactions but no C-peptide effect on insulin and IGF-1 receptor signalling' *Cellular and Molecular Life Sciences*, 63:3055-3060.

Hill CE and Brunskill NJ. 2008, Intracellular signalling by C-peptide. *Exp Diabetes Res*, 2008.

Hinke SA, Kuhn-Wache K, Hoffmann T, Pederson RA, McIntosh CH, Demuth HU. 2002. Metformin effects on dipeptidylpeptidase IV degradation of glucagon-like peptide-1. *Biochem. Biophs. Res. Commun*, 291:1302-1308.

Holst-Hansen C, Brűnner Nils N. 1998. Cell Biology: A laboratory Handbook. 2nd edition.

Honegger J, Prettin C, Feuerhake F, Manfred P, Schutle-Monting J, Reincke M. 2003. Expression of Ki-67 antigen in nonfunctioning pituitary adenomas: correlation with growth velocity and invasiveness. *Journal of Neurosurgery*, 99:674-679.

Hong SY, Seo PJ, MS, Xiang F, Park CM. 2005. Exploring valid reference genes for gene expression studies in *Brachypodium distachyon* by real-time PCR. *BMC Plant Biology*, 8:112.

Hugl SB and Merger M. 2007. Prolactin stimulates proliferations of the glucose-dependent beta-cell line INS-1 via different IRS-proteins. *Journal of Pancreas*, 8:739-752.

Huotari M, Palgi J, Otonkoski T. 1998. Growth factor mediated proliferation and differentiation of insulin producing INS-1 and RINm5F cells: identification of betacellulin as a novel β-cell mitogen. *Endocrinology*, 139:1494-1499.

Janjic D, Maechler P, Sekine N, Bartley C, Annen AS, Wollheim CB. 1999. Free radical modulation of insulin release in INS-1 cells exposed to Alloxan. *Biochemical Pharmacology*, 57:639-649.

Juvet LK, Andressen SM, Schuster GU, Dalen KT, Tobin KAR, Holling K, Haugen F, Jancinto S, Ulven SM, Bamberg K, Gustafsson JA, Nebb HI. 2003. On the role of liver X receptors in lipid accumulation in adipocytes. *Molecular endocrinology*, 17:172-182.

Kaleem M, Medha P, Ahmed QU, Asif M, Bano B. 2008. Beneficial effects of Annona squamosa extract in streptozotocin induced diabetic rats. *Singapore Med J*, 49:800-804

Karachi JK 2009, 'Efficacy of a Kenyan medicinal plant extract in the treatment of diabetes', Master's dissertation, Department of Biochemistry & Microbiology, *Nelson Mandela Metropolitan University*.

Katz S, Nambi SS, Mather K, Baron AD, Follmann DD, Sullivan G, Quon MJ. 2000. Quantitative insulin sensitivity check index: a simple accurate method for assessing insulin sensitivity in humans. *The Journal of endocrinology and metabolism*, 85:2402-2410.

Khan, AH and Pessin, JE. 2002. Insulin regulation of glucose uptake: a complex interplay of intracellular signalling pathways. *Diabetologia*, 45:1475-1483.

Kim B, Carlson OD, Jang HJ, Elahi D, Berry C, Egan JM. 2005. Peptide YY Is Secreted after Oral Glucose Administration in a Gender-Specific Manner. *The Journal of Clinical Endocrinology & Metabolism*, 90:6665-6671.

Kim SH, Shen EJ, Kim ED, Bayaraa T, Frost SC, Hyun CK. 2007. Berberine activates GLUT-1 mediated glucose uptake in 3T3-L1 adipocytes. *Biol. Pharm. Bull*, 30:2120-2125.

Kjems LL, Christiansen E, Volund A, Bergman RA, Madsbad S. 2000. Validation of methods for measurement of insulin secretion in humans *in vivo*. *Diabetes*, 49:580-588.

Krentz AJ and Friedmann PS. 2006. Type 2 diabetes, psoriasis and thiazolidinediones. *Int J Clin Pract* 60:362-363.

Kuri-Harcuch W, and Green H. 1978. Interruption of the adipose conversion of 3T3 cells by biotin deficiency: differentiation without triglyceride accumulation. *Cell*, 14: 53-59.

Lam TKT, van de Werve G, Giacca A. 2003. Free fatty acids increase basal hepatic glucose production and induce hepatic insulin resistance at different sites. *Am J Physiol Endocrinol Metab*, 284:E281-E290.

Lauritzen HPMM, Ploug T, Ai H, Donsmark M, Prats C, Galbo H. 2008. Denervation and high-fat diet reduce insulin signalling in t-tubules in skeletal muscle of living mice. *Diabetes*, 57:13-23.

Lenhard JM, Croom DK, Minnick DT. 2004. Reduced serum dipeptidyl-IV after metformin and Pioglitazone treatments. *Biochem. Biophys. Res. Commun*, 324:92-97.

Lewis, GF Carpentier, A Adeli, K Giacca, A. 2002**.** Disordered Fat Storage and Mobilization in the Pathogenesis of Insulin Resistance and Type 2 Diabetes. *Endocrine Reviews,* 23 (2): 201-229.

Li L, El-Kholy W, Rhodes CJ, Brubaker PL. 2005. Glucagon like peptide-1 protects beta cells from cytokine-induced apoptosis and necrosis: role of protein kinase B. *Diabetologia*, 48:1339-1349.

Liang Y, Najafi H, Matschinsky FM. 1990. Glucose regulates glucokinase activity in cultured islets from rat pancreas. *J. Biol. Chem*, 265: 16863-16866.

Linco Reasearch. 2008. Rat Insulin RIA Kit.

Ling Z, Wang Q, Stange G, Veld PI, Pipeleers D. 2006. Glibenclamide treatment recruits β-cell subpopulation into elevated and sustained basal insulin synthetic activity. *Diabetes*, 55:78-85.

Lingohr MK, Buettner R & Rhodes CJ. 2002. Pancreatic beta-cell growth and survival – a role in obesity-linked type 2 diabetes? *Trends in Molecular Medicine* 8: 375–384.

Liu F, Kim JK, Li Y, Liu X, Li J, Chen X. 2001. An extract of *Lagerstroemia* speciosa L. has insulin like glucose uptake stimulatory and adipocyte differentiation inhibitory activities in 3T3-L1 cells. *The Journal of Nutrition*, 2242-2247.

Lyall, H, Grant, A, Scott, H M, Burchell, A. 1992. Regulation of the hepatic microsomal glucose-6-phosphatase enzyme. *A. Biochem. Soc. Trans,* 20:271S.

Maedler K and Donath M Y. 2004. β cells in type 2 diabetes: a loss of function and mass. *Hormone Research*, 62:67-73.

Mannucci E, Ognibene A, Cremasco F, Bardini G, Mencucci A, Pierazzuoli E, Ciani S, Messeri G, Rotella CM. 2001. Effect of metformin on glucagon-like peptide 1 (GLP-1) and leptin levels in obese nondiabetic subjects. *Diabetes Care*, 24: 489-494.

Masek J and Fabry P. 1959. High-fat diet and the development of obesity in albino rats. *Experientia*, 15: 444–445.

Matschinsky FM and Collins H W. 1997. Essential biochemical design features of the fuel-sensing system in pancreatic beta-cells. *Chem Biol*, 4:249-257.

Matschinsky FM, Magnuson MA, Zelent D, Jetton TL, Doliba N, Han Y, Taub R, Grimsby J. 2006. The network of glucokinase-expressing cells in glucose homeostasis and the potential of glucokinase activators for diabetes therapy. *Diabetes*, 55:1–12.

Matschinsky FM. 1996. A lesson in metabolic regulation inspired by the glucokinase glucose sensor paradigm. *Diabetes,* 45:223–242.

Matschinsky FM. 2002. Regulation of pancreatic β-cell glucokinase: from basics to therapeutics. *Diabetes*, 51: S394-S404.

McIntosh CHS, Demuth HU, Kim HJ, Pospisilik JA, Pederson RA. 2006. Applications of dipeptidyl peptidase IV inhibitors in diabetes mellitus. *The International Journal of Biochemistry and Cell Biology*, 38: 860-872.

Mentlein R, Gallwitz B, Schmidt WE. 1993. Dipeptidyl-peptidase IV hydrolyses gastric inhibitory polypeptide, glucagon-like peptide-1(7–36) amide, peptide histidine methionine and is responsible for their degradation in human serum. *Eur J Biochem* 214:829–35.

Michel MC, Fliers E, Van Noorden CJF. 2008. Dipeptidyl peptidase IV inhibitors in diabetes: more than inhibition of a glucagon like peptide -1 metabolism? *Naunyn-Schmiedeberg's Arch Pharmacol*, 377:205–207.

Minassian C, Tarpin S, Mithieux G. 1998. Role of Glucose-6-phosphatase, glucokinase and glucose-6-phosphate in liver and its correction by metformin. *Biochemical Pharmacology*, 55:1213–1219.

Minassian C, Tarpin S, Mithieux G. 1998. Role of glucose-6-phosphatase, glucokinase, and glucose-6-phosphate in liver in insulin resistance and its correction by metformin. *Biochem-Pharmacol*, 55:1213-1219.

Mithieux G, Rajas F, Gautier-Stein A. 2004. A novel role for Glucose-6-Phosphatase in the small intestine in the control of glucose homeostasis. *The Journal of Biological Chemistry*, 279:44231-44234.

Moller DE. 2001. New drug targets for type 2 diabetes and the metabolic syndrome. *Nature*, 414:821-827.

Moore C and Cooper G. 1991. Co-secretion of amylin and insulin from cultured islet beta-cells: modulation by nutrient secretagogues, islet hormones and hypoglycemic agents. *Biochem Biophys Res Commun* 179: 1–9.

Morrissey J. 2006. Lecture 5: Diabetes integration of metabolism 1:1-9.

Mueckler M. 2001. Insulin resistance and the disruption of Glut4 trafficking in skeletal muscle. *J. Clin. Invest.* 107:1211-1213.

Mukiama TK. 2005. Medicinal plants of Kenya. Kenya Agricultural Research Institute.

Muniappan L and Ozcan S. 2007. Induction of insulin secretion in engineered liver cells by nitric oxide. *BMC Physiology*, 7:1-9.

Muoio DM and Newgard CB. 2008. Molecular and metabolic mechanisms of insulin resistance and β-cell failure in type 2 diabetes. *Nature Reviews molecular cell biology*.

Nelson DL and Cox MM. 2005. Lehninger principles of biochemistry. 5th edition. WH Freeman Company.

Ntambi JM and Kim YC. 2000. Adipocyte differentiation and gene expression. *American Society for Nutritional Sciences*, 3122S-3126S

O'Brien M. 2006. DPP IV-Glo protease assay: a more sensitive method for measuring Gly-Pro cleaving activity in serum. *Promega Corporation Cell Notes*, 16: 9-11.

Oakes ND, Cooney GJ, Camilleri S, Chisholm DJ, Kraegen EW. 1997. Mechanisms of liver and muscle insulin resistance induced by chronic high-fat feeding. *Diabetes*, 46: 1768–1774.

Palgrave KC. 1981. Trees of Southern Africa. C Struik Publishers, Cape Town: 210.

Panserat S, Médale F, Blin C, Brèque J, Vachot C, Plagnes-Juan E, Gomes E, Krishnamoorthy R, Kaushik S. 2000. Hepatic glucokinase is induced by dietary carbohydrates in rainbow trout, gilthead seabream and common carp. *Am J Physiol Regulatory Integrative Comp Physiol*, 278:1164-1170.

Panunti B, Jawa AA, Fonseca VA. 2004. Mechanisms and therapeutic targets in type 2 diabetes mellitus. *Drug discovery today: Disease mechanisms*, 1:151-157.

Perfetti R, Ahmad A. 2000. Novel Sulfonylurea and Non-sulfonylurea Drugs to Promote the Secretion of Insulin. *Trends in Endocrinology and Metabolism*, 11:218-233.

Perseghin G, Caumo A, Caloni M, Testolin G, Luzi L. 2001. Incorporation of the fasting plasma FFA concentration into QUICKI improves its association with insulin sensitivity in nonobese individuals. *J Clin Endocrinol Metab*, 86:4776–4781.

Pirola L, Johnston AM, Van Obberghen E. 2004. Modulation of insulin action. *Diabetologia*, 47:170-184.

Plummer DT. 1978. An introduction to practical biochemistry. 2nd edition. *McGraw-Hill Book Company Limited*.

Postic C, Shiota M, Magnuson MA. 2001. Cell specific role of glucokinase in glucose metabolism. *Journal of Endocrinology*, 195-217.

Rabasa-Lhoret R, Bastard JP, Jan V, Ducluzeau PH, Andreelli F, Guebre F, Bruzeau J, Louche-Pellissier C, MaÎtrepierre C, Peyrat J, Chagné J, Vidal H, Martine Laville M. 2003. Modified Quantitative Insulin Sensitivity Check Index Is Better Correlated to Hyperinsulinemic Glucose Clamp than Other Fasting-Based Index of Insulin Sensitivity in Different Insulin-Resistant States. *The Journal of Clinical Endocrinology & Metabolism*, 88:10 4917-4923.

Rea S and James DE. 1997.The biogenesis and trafficking of GLUT4 storage vesicles. *Diabetes* 46:1667-1677.

Real-Time PCR Applications. Guide Bio-Rad Laboratories, Inc.

Reed BC and Lane MD. 1980. Insulin receptor and adipocyte turnover in differentiating 3T3-L1 preadipocytes. *Proc. Natl. Acad. Sci*, 77:285-289.

Ren J, Jin P, Wang E, Liu E, Harlan DL, Li X, Stroncek DF. 2007. Pancreatic islet cell therapy for type 1 diabetes: understanding the effects of glucose stimulation on islets in order to produce better islets for transplantation. *Journal of translation medicine*, 5:1-15.

Routh VH, McArdle, JJ. Sanders NM, Song Z, Wang R. 2007. Glucose sensing neurons. *Springer-Verlag Berlin Heidelberg,* :206-228

Saltiel AR, Kahn CR. 2001. Insulin signalling and the regulation of glucose and lipid metabolism. *Nature* 414:799-806.

Savage DB, Petersen KF, Shulman GI. 2005. Mechanisms of insulin resistance in humans and possible links with inflammation. *Hypertension*, 45:828-833.

Simon JE, Koroch AR, Acquaye D, Jefthas E, Juliani E, Govindasamay E. 2007. Medicinal crops of Africa. *Issues in new crops and new uses*, 322-331.

Smith PK, Krohn, RI, Hermanson, GT, Mallia AK, Gartner FH, Provenzano MD, Fujimoto EK, Goeke NM, Olson BJ, Klenk DC. 1985. Measurement of protein using bicinchoninic acid. *Anal. Biochem*. 150: 76 – 85.

Standl E and Kolb HJ. 1984. Insulin degrading enzyme activity and insulin binding of erythroxytes in normal subjects and type 2 (non-insulin-dependent) diabetic patients. *Diabetologia*, 27:17-22.

Terauchi Y, Takamoto I, Kubota N, Matsui J, Suzuki R, Komeda K, Hara A, Toyoda Y, Miwa I, Aizawa S, Tsutsumi S, Tsubamoto Y, Hashimoto S, Eto K, Nakamura A, Noda M, Tobe K, Aburatani H, Nagai R, Kadowaki T. 2007. Glucokinase and IRS-2 are required for compensatory β cell hyperplasia in response to high fat diet induced insulin resistance. *J. Clin. Invest.* 117: 246-257.

Tice, LW and Barnett, R J. 1962. The fine structural localization of glucose-6-phosphatase in rat liver. *J. Histochem. Cytochem*, 10:754-762.

Tomlinson JJ, Boudreau A, Wu D, Atlas E, Hache RJG. 2006. Modulation of Early Human Preadipocyte Differentiation by Glucocorticoids. *Endocrinology*, 147:5284–5293.

Toscani A, Soprano DR, Sorprano KJ 1990,'Sodium butyrate in combination with insulin or dexamethasone can terminally differentiate actively proliferating Swiss 3T3 cells into adipocytes', *The Journal of Biochemical Chemistry*, 265:5722-5730.

Ueyama A, Yaworsky KL, Wang Q, Ebina Y, Klip A. 1999. GLUT-4myc ectopic expression in L6 myoblasts generates a GLUT-4 specific pool conferring insulin sensitivity. *Am. J. Physiol.Endocrinol.Metab.* 277:E572-E578.

Van Cauter E, Mestrez F, Sturis J, Polonsky KS. 1992. Estimation of insulin secretion rates from C-peptide levels. Comparison of individual and standard kinetic parameters for C-peptide clearance. *Diabetes*, 41:368-377.

Van Schaftingen E, Gerin I. 2002. The glucose-6-phostase system. *Biochem. J*, 362:513-532.

Vandesompele J, De Preter K, Pattyn F, Poppe B, Van Roy N, De Paupe A, Speleman F .2002. Accurate normalization of real-time quantitative RT-PCR data by geometric averaging of multiple internal control genes. *Genome Biology*, 3.

Vats RK, Kumar V, Kothari A, Mital A, Ramachandran U. 2005. Emerging targets for diabetes. *Current science* 88(2):241-249.

Velebit J, Kovacic PB, Prebil M, Chowdhury HH, Grilc S, Kreft M, Jensen J, Isenovic ER, Zorec R. 2008. Rosiglitazone modulates insulin-induced plasma membrane area changes in single 3T3-L1 adipocytes. *J Membrane Biol*, 223:141-149.

Vogt B, Mushack J, Seffer E, Haring HU. 1991. The translocation of the glucose transporter sub-types GLUT1 and GLUT4 in isolated fat cells is differently regulated by phorbol esters. *Biochem. J*, 275:597-600.

Waeber G, Thompson N, Nicod P, Bonny C. 1996. Transcriptional Activation of the GLUT2 Gene by the IPF-l/STFl/IDX-1 Homeobox Factor. *Molecular Endocrinology*, 10: 1327-1334.

Wahren J, Ekberg K, Johansson J, Pramanik A, Johannson BL, Rigler R, Jornvall H. 2000. Role of C-peptide in human physiology. *Am J Physiol Endocrinol Metab*, 278: E759–E768.

Walker K and Wilson J. 2005. Principles and Techniques of biochemistry and molecular biology. 6th edition, Cambridge university press.

Wang X, Cahill CM, Pineyro MA, Zhou J, Doyle ME, Egan JM. 1999. Glucagon-like peptide-1 regulates the beta cell transcription factor, PDX-1, in insulinoma cells. *Endocrinology* 140:4904–4908.

Weyer C, Borgadus C, Mott DM, Pratley RE. 1999. The natural history of insulin secretory dysfunction and insulin resistance in the pathogenesis of diabetes mellitus 2. *J. Clin. Invest*, 104:787-794.

Wilhelm B, Kann P, Pfützner A. 2008. Influence of C-Peptide on Glucose Utilisation. *Experimental Diabetes Research*, 2008: 1-3.

Willems E, Leyns L, Vandesompele J. 2008.Standardization of real-time PCR gene expression data from independent biological replicates. *Analytical Biochemistry*, 379:127-129.

Wilson G. 2006. An optimization for *in vitro* antidiabetic screening, Master's dissertation, Department of Biochemistry and Microbiology, *Nelson Mandela Metropolitan University*.

Yang J, Clark AE, Harrison R, Kozka IJ, Holman GD. 1992. Trafficking of glucose transporters in 3T3-L1 cells. *Biochem. J*, 281:809-817.

Yasuda N, Inoue T, Nagakura T, Yamazaki K, Kira K, Saeki T, Tanaka I. 2002. Enhanced secretion of glucagon-like peptide 1 by biguanide compounds. *Biochemical and Biophysical Research Communications*, 298:779-784.

Yeom SY, Kim GH, Kim CH, Jung HD, Kim SY, Park JY, Pak YK, Rhee DK, Kuang SQ, Xu J, Han DJ, Song DK, Lee JW, Lee KU, Kim SW. 2006. Regulation of Insulin Secretion and ß-Cell Mass by Activating Signal Cointegrator 2. *Molecular and Cellular Biology*, 26:4553-4563.

Yoon JC, Puigserver P, Chen G, Donovan J, Wu Z, Rhee J, Adelmant G, Stafford J, Zhou L, Yang Y, Wang X, Liu S, Shang W, Yuan G, Li F, Tang J, Chen M, Chen J. 2007. Berberine stimulates glucose transport through a mechanism distinct from insulin. *Metabolism*, 56:405-417.

Zierath JR, Galuska D, Johansson BL, Henriksson HW. 1991. Effect of human C-peptide on glucose transport in vitro incubated human skeletal muscle. *Diabetologia*, 34:899-901.

Zor T and Selinger T. 1996. Linearization of Bradford assay increases its sensitivity: theoretical and experimental studies. *Analytical Biochemistry*, 236:302-308.

http:// www.pdb.org date retrieved 19.02. 2008

http://www.medbio.info/orn/Time%203.4/Secretion_of_insulin_glucagon.htm date retrieved 08.04.2008
http://www.milleniumindicators.un.org/unSD/mdg/Host date retrieved 12.02.2008
http://www.eatlas.idf.org/Cost_of _diabetes date retrieved 12.02.2008
http://www.who.org date retrieved 12.02.2008
http://www.worlddiabetesfoundation.org/composite_33.htm date retrieved 12.02.2008
http://www.sigma.com retrieved 15.03.2008
http://www.biodiversityexplorer.org/.../enb04732.jpg
http://8e.devbio.com/article.php?ch=4&id=32 date retrieved 11.12.2008
http://www.flmnh.ufl.edu/cowries/PCR.gif date retrieved 20.12.2008
http://www.protocol-online.org/biology-forums/posts/39416 date retrieved 20.12.2008

ANNEXURE A

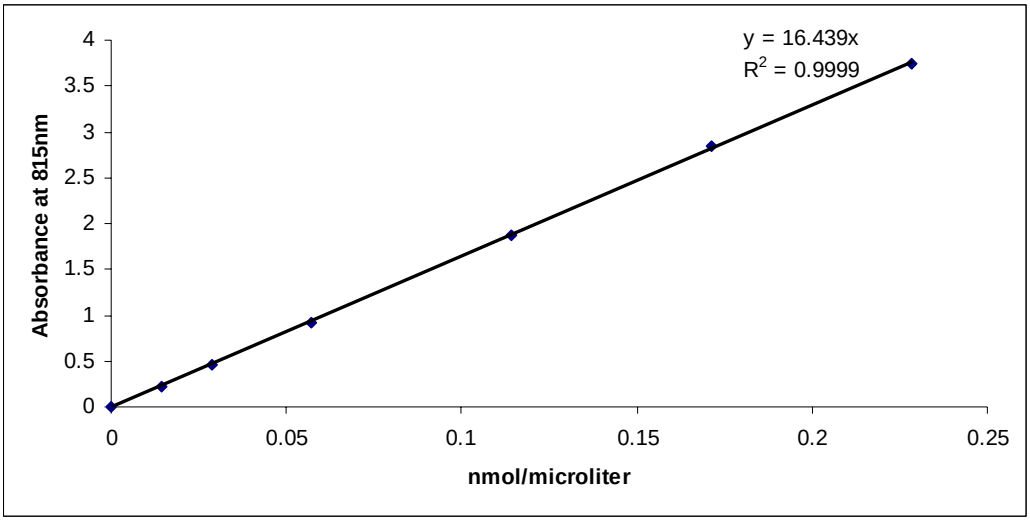

Figure A.1:Phosphate standard curve used to calculate [phosphate] in G6Pase activity study. The equation obtained from linear regression is shown on each graph, along with the r2 value.

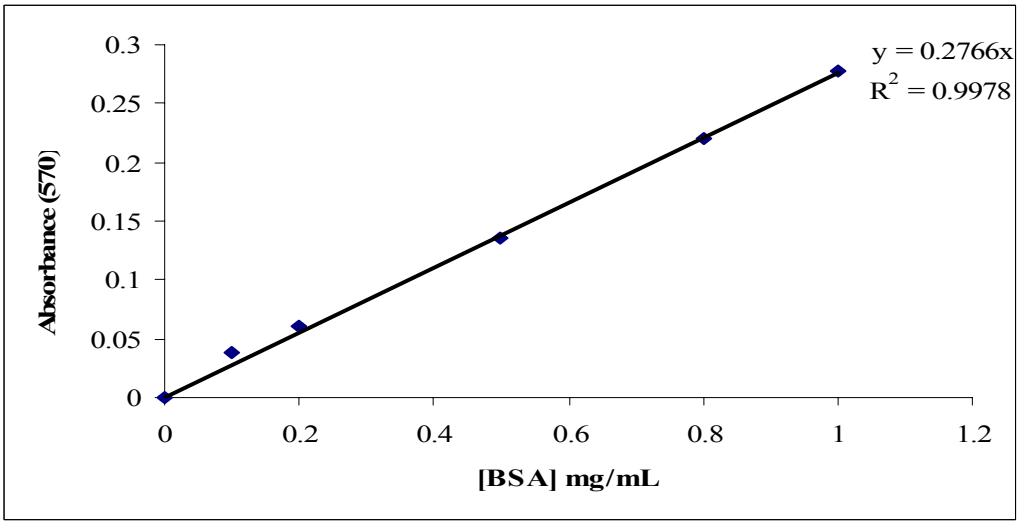

Figure A.2: Protein standard curve using the BCA assay used in the calculation of protein content in the G6Pase activity study. The equation obtained from linear regression is shown on each graph, along with the r2 value.

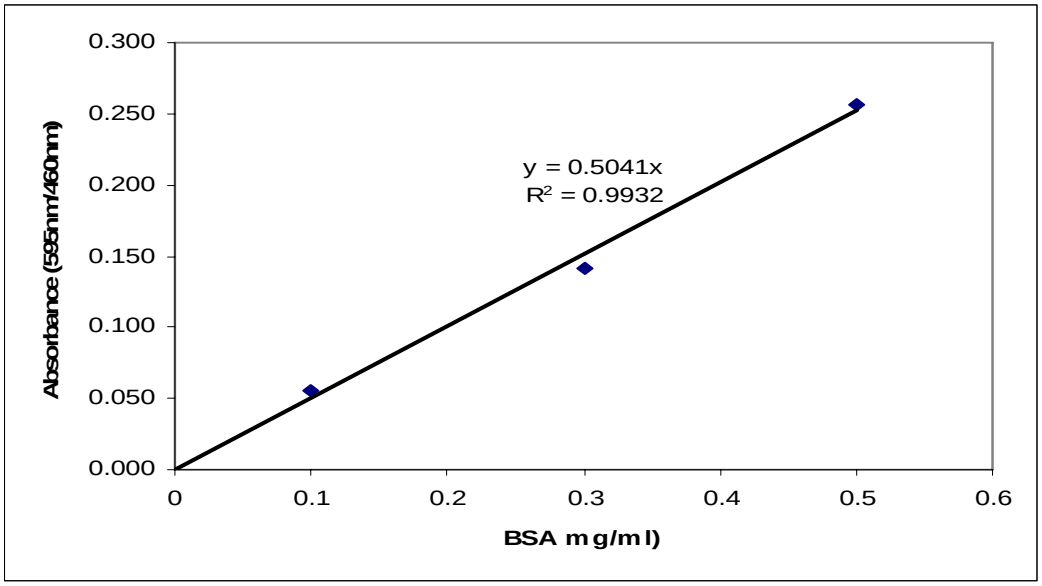

Figure A.3: Protein standard curve using the Bradford assay used in the calculation of GK activity. The equation obtained from linear regression is shown on each graph, along with the r2 value.

ANNEXURE B

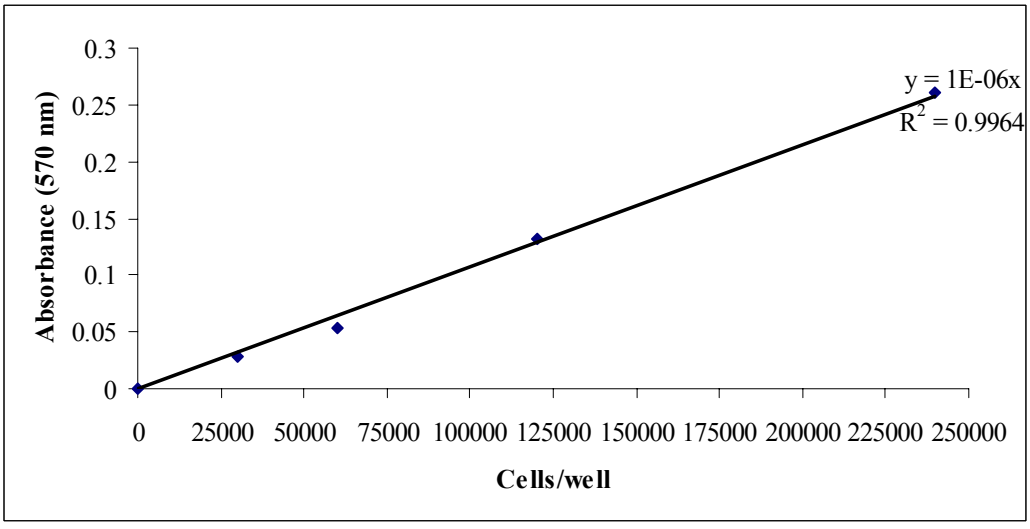

Figure B.1: **Standard curve of INS-1 cells quantifying the number of cells/well using the MTT assay. The equation obtained from linear regression is shown on each graph, along with the r2 value.**

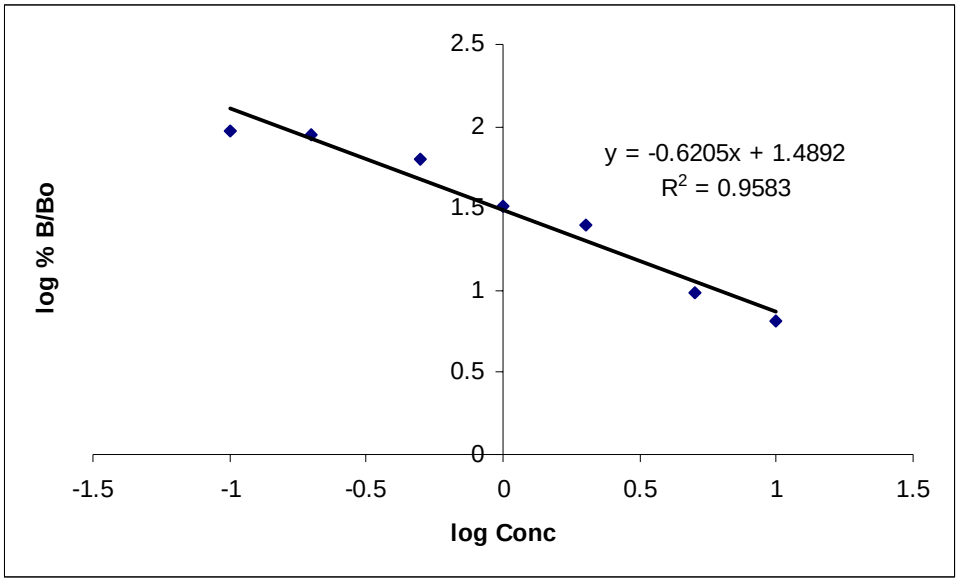

Figure B.2: Standard curve obtained used to calculate insulin concentration. The equation obtained from linear regression is shown on each graph, along with the r2 value.

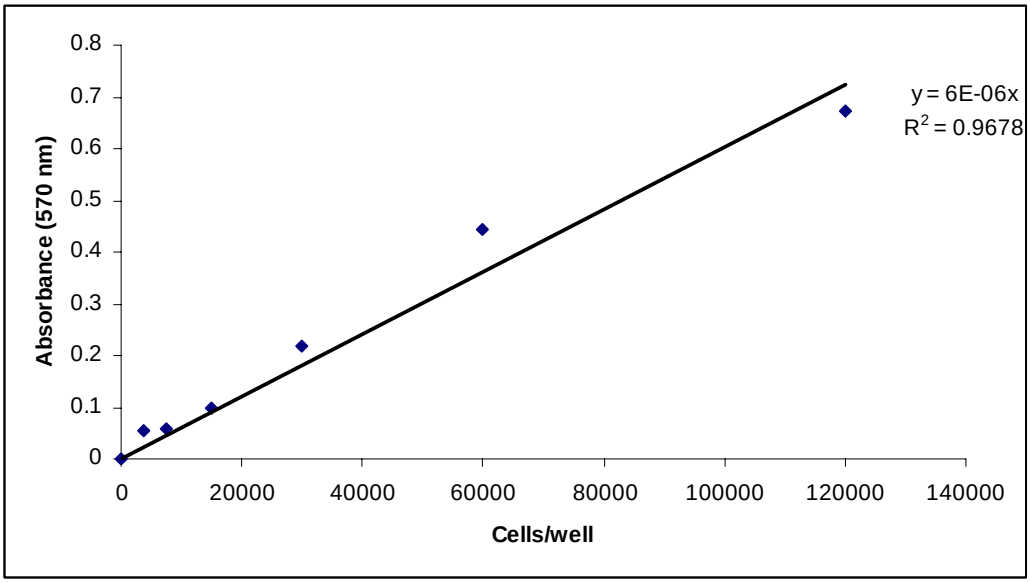

Figure B. 3: Standard curve of 3T3-L1 cells quantifying the number of cells/ well using the MTT assay used in the calculation of 3T3-L1/plant A cytotoxicity study. The equation obtained from linear regression is shown on each graph, along with the r2 value.

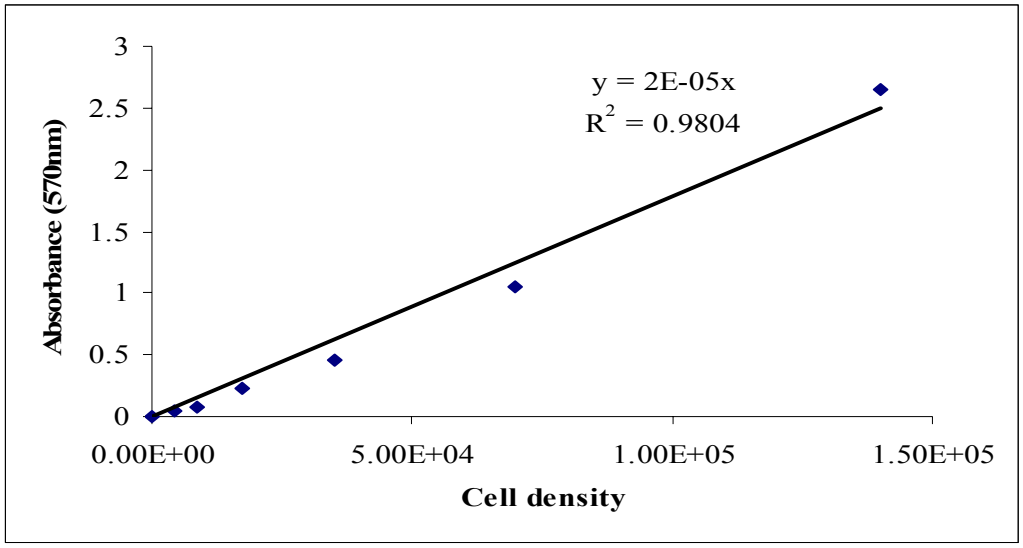

Figure B. 4 : Cell density standard curve of 3T3-L1 cells used in the calculation of the glucose uptake study. The equation obtained from linear regression is shown on each graph, along with the r2 value.

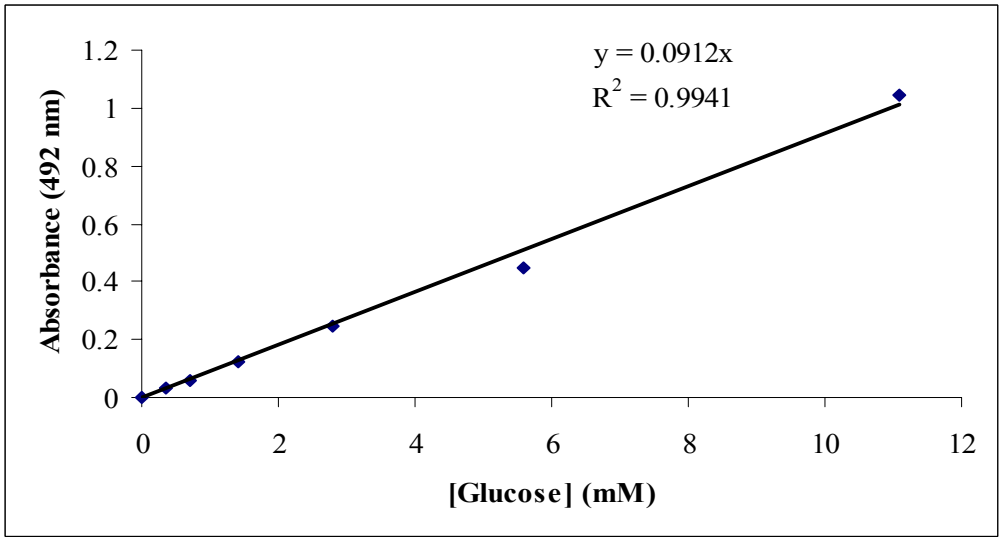

Figure B. 5 : Glucose standard curve used in the calculation of the glucose uptake study. The equation obtained from linear regression is shown on each graph, along with the r2 value.

Glucose oxidase reagent.

Solution A:

Add the following reagents to 100 ml of phosphate buffer (7g NaH_2PO_4 in 100 ml water);

0.028 g phenol (SIGMA, USA)

0.008 g 4-aminoantipyrine (Fluka, USA)

0.074 g EDTA (Fluka, USA)

65 µl glucose oxidase (SIGMA, USA)

0.001 g peroxidise (SIGMA, USA)

Solution B:

Dissolve 18 g NaH_2PO_4 in 400 ml water

Add 10 ml solution A to 40 ml solution B and dilute with water to a final volume of 1.3 L and use for the glucose utilization study.

ANNEXURE C

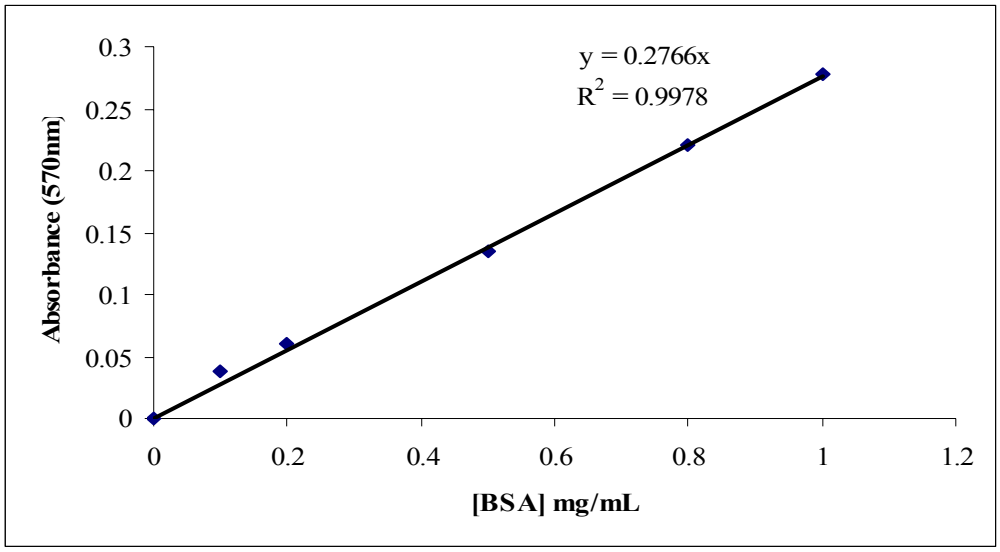

Figure C. 1: Protein standard curve used for the quantification of DPP IV activity for both the rat plasma samples and the enzyme extract from CaCo-2 cells. The equation obtained from linear regression is shown on each graph, along with the r2 value.